Manual of diagnostic ultrasound

vol. 2

During the last decades , use of ultrasonography became increasingly common in medical practice and hospitals around the world, and a large number of scientific publications reported the benefit and even the superiority of ultrasonography over commonly used X-ray techniques, resulting in significant changes in diagnostic imaging procedures.

With increasing use of ultrasonography in medical settings, the need for education and training became essential. WHO took up this challenge and in 1995 published its first training manual in ultrasonography. Soon, however, rapid developments and improvements in equipment and indications for the extension of medical ultrasonography into therapy indicated the need for a totally new ultrasonography manual.

The manual (consisting of two volumes) has been written by an international group of experts of the World Federation for Ultrasound in Medicine and Biology (WFUMB), well-known for their publications regarding the clinical use of ultrasound and with substantial experience in the teaching of ultrasonography in both developed and developing countries. The contributors (more than fifty for the two volumes) belong to five different continents, to guarantee that manual content represents all clinical, cultural and epidemiological contexts

This new publication, which covers modern diagnostic and therapeutic ultrasonography extensively, will certainly benefit and inspire medical professionals in improving 'health for all' in both developed and emerging countries.

ISBN 978 92 4 154854 0

Vol. 2

Manual of diagnostic ultrasound

Manual of diagnostic ultrasound

volume 2

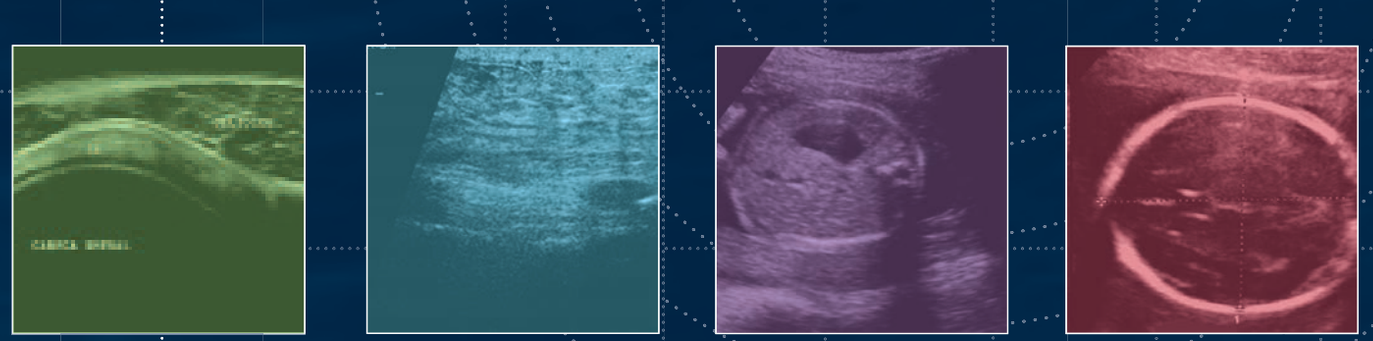

Second edition

WHO

World Health Organization

Manual of diagnostic ultrasound

volume 2

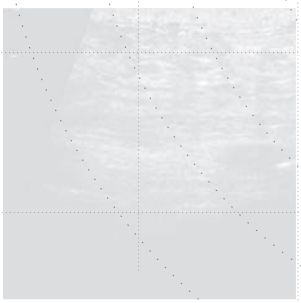
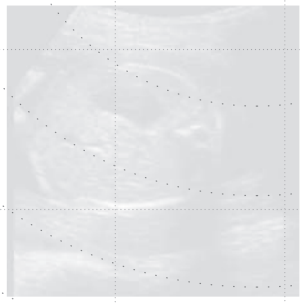
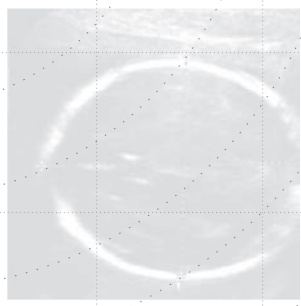

Second edition

World Health Organization

WHO Library Cataloguing-in-Publication Data

Manual of diagnostic ultrasound. Vol. 2 – 2nd ed. / edited by Elisabetta Buscarini, Harald Lutz and Paoletta Mirk.

1.Diagnostic imaging. 2.Ultrasonography. 3.Pediatrics - instrumentation. 4.Handbooks. I.Buscarini, Elisabetta. II.Lutz, Harald. III.Mirk, P. IV.World Health Organization. V.World Federation for Ultrasound in Medicine and Biology.

ISBN 978 92 4 154854 0 (NLM classification: WN 208)

Production editor: Melanie Lauckner
Design & layout: Sophie Guetaneh Aguettant and Cristina Ortiz

Printed in Slovenia

Contents

Acknowledgements

The Editors **Elisabetta Buscarini, Harald Lutz** and **Paoletta Mirk** wish to thank all members of the Board of the World Federation for Ultrasound in Medicine and Biology for their support and encouragement during preparation of this manual.
The Editors also express their gratitude to and appreciation of those listed below, who supported preparation of the manuscript by contributing as co-authors and by providing illustrations and competent advice.

Domenico Arduini: Department of Obstetrics and Gynecology, University of Roma Tor Vergata, Rome, Italy
Stan Barnett: Discipline of Biomedical Science, Faculty of Medicine, University of Sydney, Sydney, Australia
Ibtissem Bellagha: Department of Paediatric Radiology, Tunis Children's Hospital, Tunis, Tunisia
Paolo Belli: Department of Radiological Sciences, Catholic University of the Sacred Heart, Rome, Italy
Leonardo Caforio: Department of Obstetrics and Gynecology, Catholic University of the Sacred Heart, Rome, Italy
Lucia Casarella: Department of Obstetrics and Gynecology, Catholic University of the Sacred Heart, Rome, Italy
Anna Franca Cavaliere: Department of Obstetrics and Gynecology, Catholic University of the Sacred Heart, Rome, Italy
Giovanni Cerri: School of Medicine, University of Sao Paulo, Sao Paulo, Brazil
Maria Cristina Chammas: School of Medicine, University of Sao Paulo, Sao Paulo, Brazil
Ferid Ben Chehida: Department of Radiology, Ibn Zohr Center, Tunis, Tunisia
Melania Costantini: Department of Radiological Sciences, Catholic University of the Sacred Heart, Rome, Italy
Alain Couture: Department of Paediatric Radiology, Arnaud de Villeneuve Hospital, Montpellier, France
Vincenzo D'Addario: Department of Obstetrics, Gynecology and Neonatology, University of Bari, Bari, Italy
Marco De Santis: Department of Obstetrics and Gynecology, Catholic University of the Sacred Heart, Rome, Italy
Josef Deuerling: Department of Internal Medicine, Klinikum Bayreuth, Bayreuth, Germany

Alessandra Di Giovanni: Department of Obstetrics and Gynecology, University of Roma Tor Vergata, Rome, Italy
Alessia Di Legge: Department of Obstetrics and Gynecology, Catholic University of the Sacred Heart, Rome, Italy
Wiem Douira Khomsi: Department of Paediatric Radiology, Tunis Children's Hospital, Tunis El Manar University, Tunis, Tunisia
Caterina Exacoustos: Department of Obstetrics and Gynecology, University of Roma Tor Vergata, Rome, Italy
Hassen A Gharbi: Department of Radiology, Ibn Zohr Center, Tunis, Tunisia
Azza Hammou: National Center for Radio Protection, Tunis, Tunisia
Hela Louati: Department of Paediatric Radiology, Tunis Children's Hospital, Tunis, Tunisia
Lucia Masini: Department of Obstetrics and Gynecology, Catholic University of the Sacred Heart, Rome, Italy
Maria Elena Pietrolucci: Department of Obstetrics and Gynecology, University of Roma Tor Vergata, Rome, Italy
Maurizio Romani: Department of Radiological Sciences, Catholic University of the Sacred Heart, Rome, Italy
Paolo Rosati: Department of Obstetrics and Gynecology, Catholic University of the Sacred Heart, Rome, Italy
Cristina Rossi: Department of Obstetrics, Gynecology and Neonatology, University of Bari, Bari, Italy
Renato A. Sernik: Musculoskeletal Dept. Clinical Radiology, University of Sao Paulo, Sao Paulo, Brazil
Stefania Speca: Department of Radiological Sciences, Catholic University of the Sacred Heart, Rome, Italy
Antonia Carla Testa: Department of Obstetrics and Gynecology, Catholic University of the Sacred Heart, Rome, Italy
Claudia Tomei: Department of Obstetrics and Gynecology, Catholic University of the Sacred Heart, Rome, Italy
Corinne Veyrac: Department of Paediatric Radiology, Arnaud de Villeneuve Hospital, Montpellier, France
Daniela Visconti: Department of Obstetrics and Gynecology, Catholic University of the Sacred Heart, Rome, Italy
Maria Paola Zannella: Department of Obstetrics and Gynecology, Catholic University of the Sacred Heart, Rome, Italy

Chapter 1

Safety of diagnostic ultrasound

1

Safety of diagnostic ultrasound

Ultrasound and the World Health Organization

The World Health Organization (WHO) recognizes ultrasound as an important medical diagnostic imaging technology. Manuals on ultrasound have been published by WHO since 2001, with the purpose of guiding health professionals on the safe and effective use of ultrasound. Among the diagnostic imaging technologies, ultrasound is the safer and least expensive, and technological advances are making it more user friendly and portable. Ultrasound has many uses, both diagnostic and therapeutic. For the purposes of this manual, only diagnostic ultrasound will be considered and further analysed.

Basic physics of ultrasonographic imaging was released in 2005; since then, WHO has addressed the physics, safe use and different applications of ultrasound as an important diagnostic imaging tool. Since it is a nonionizing radiation technology, along with nuclear magnetic resonance imaging, the risks inherent to its use are lower than those presented by other diagnostic imaging technologies using ionizing radiation, such as the radiological technologies (X-rays and computed tomography scanners).

To disseminate policies, programmes and strategies, WHO holds the official collaboration of international nongovernmental organizations. Out of 183 such organizations, at least four deal with topics related to ultrasound:

- ISR: the International Society of Radiology
- ISRRT: the International Society of Radiographers and Radiological Technologists
- IFMBE: the International Federation for Medical and Biological Engineering
- WFUMB: the World Federation for Ultrasound in Medicine and Biology.

It is WFUMB that has authored and edited volumes 1 and 2 of this *Manual of Diagnostic Ultrasound*.

WHO has three collaborating centres working on studies to demonstrate the clinical effectiveness, economic impact and affordability of ultrasound technologies. Today, these studies are being conducted by the following WHO collaborating centres: the National Center for Fetal Medicine, Trondheim University Hospital (Norway), Jefferson Ultrasound Research and Education Institute (USA) and the National Center for Health Technology Excellence (Mexico).

The Diagnostic Imaging and Medical devices unit of the Department of Essential Medicines and Health products of WHO's Health Systems and Innovation cluster, along with WHO's Public Health and Enviroment cluster, are working on the Basic Safety Standards and the Basic Referral Guidelines, which will support and recommend the use of ultrasound for specific diseases and diagnostics.

The WFUMB has been working with WHO for 10 years in the publishing and editing of ultrasound manuals, from the first version to the present one, to increase the safe use of ultrasound for the different pathologies that will be demonstrated in volumes 1 and 2 of this publication.

WHO is now working with the International Commission of Non-Ionizing Radiation to review the safe use of ultrasound for diagnostic and therapeutic applications.

Safety of ultrasound

The use of diagnostic ultrasound is generally accepted as safe, in the absence of plausible, confirmed evidence of adverse outcome in humans. Nevertheless, with rapid technological advances, the possibility of ultrasound-induced adverse effects occurring in the future cannot be ruled out. While there may be no concern with regard to most applications, prudent use is justified. Obstetric applications are of particular concern, as rapidly dividing and differentiating embryonic and fetal tissues are sensitive to physical damage, and perturbation of cell differentiation might have significant biological consequences. Technological advances have resulted in improved diagnostic acuity but have been accompanied by substantially increased levels of acoustic output, and the possible health effects of equivalent levels of exposure have not been studied in humans.

Modern ultrasound equipment combines a range of frequencies in complex scan modes to increase diagnostic accuracy. Misdiagnosis is, however, a real risk to patients, and the clinical benefit of procedures such as Doppler flow embryosonography should be established. Unregulated use of freely available equipment by unaccredited or inadequately trained people increases the risk for misdiagnosis and harm. So-called entertainment or social scanning is frowned upon by professional ultrasound societies and is the subject of a project of the Safety Committee of the World Federation for Ultrasound in Medicine and Biology.

In obstetrics scanning, the amount of ultrasound-induced heating of the fetus correlates with gestational age and increasing mineralization of bone. Because of its particularly high acoustic absorption characteristics, bone is rapidly heated when placed in the path of an ultrasound beam. Significant increases in temperature have been consistently recorded when pulsed Doppler ultrasound beams encounter bone in either transcranial or fetal exposures. The greatest heating is usually associated with the use of pulsed spectral Doppler ultrasound applications, in which a stationary beam of relatively high intensity is directed at a single tissue target. As a result, tissue near bone can be heated by around 5 °C. A responsible, cautious approach

is justified, particularly in the use of Doppler ultrasound in pregnancy; however, there is no risk for adverse heating effects from simple B-mode ultrasound scanning procedures when tissues are insonated for fractions of a second each time a beam passes. Diagnostic ultrasound causes a modest temperature increase in soft embryonic tissue and is unlikely to be a major concern, thermally, during the first trimester.

The World Federation for Ultrasound in Medicine and Biology concluded that the effects of elevated temperatures can be minimized by keeping the time during which the beam passes through any area of tissue as short as possible.

The nonthermal biological effect that has been most thoroughly examined is acoustic inertial cavitation, which involves collapse of bubbles in liquid in a sound field and the sudden release of energy, which can be sufficiently intense to disrupt molecular bonds.

While it is comforting that there is no conclusive evidence of serious adverse health effects caused by antenatal exposure to ultrasound, the scientific database has obvious limitations and inadequacies. The available epidemiological data refer to exposure to ultrasound at levels considerably lower than those from modern ultrasonographic equipment. There are no data on perinatal applications of spectral or colour flow Doppler or of other modern ultrasound procedures, such as harmonic imaging techniques and use of echocontrast agents.

It is important that users of ultrasound for clinical purposes:

- monitor the thermal and mechanical indices and keep them as low as consistent with clinical needs;
- document output display indices as a part of the permanent record of an examination;
- verify the accuracy of the displayed mechanical index, particularly when new hardware or software is introduced;
- examine the adequacy of the mechanical index as a guide to the likelihood of rupture of contrast microbubbles.

It is suggested that manufacturers set the default (switch-on) mechanical index to less than 0.4, except for high mechanical index modes, and that they provide an unambiguous on-screen display of centre frequency (acoustic working frequency). For scientific purposes, it would be helpful if the value of the peak negative acoustic pressure were made available, to allow studies of alternative means of assessing clinical biological responses under particular circumstances.

Conclusion

Ultrasound is a core technology for diagnostics and remains one of the safest. Clinical effectiveness is enhanced when used properly. The following chapters provide information on the best use and applications of diagnostic ultrasound. A responsible, cautious approach to ultrasound is required to maintain safety, particularly in the use of Doppler ultrasound in pregnancy. The output displays on modern ultrasonographic equipment allow users to take greater responsibility in risk–benefit assessments. With new ultrasound applications, continued safety and effectiveness can be assured only if it is used according to recognized guidelines at the lowest exposure necessary to provide essential diagnostic information.

Chapter 2

Obstetrics

2

Obstetrics

First trimester

The first trimester is the gestational period between conception and 13 weeks + 6 days of gestational age. An **embryo** is the product of conception until 10 weeks + 0 days of gestational age; a **fetus** is the product of conception from 10 weeks + 1 day until delivery.

Indications

The indications for ultrasound during the first trimester are:

- vaginal bleeding or pelvic pain;
- a discrepant uterine size for gestational age;
- estimation of gestational age;
- support for an invasive diagnostic procedure (e.g. sampling the chorionic villus);
- prediction of the risk for recurrence of fetal anomalies;
- screening for fetal anomalies and aneuploidies (in selected, high-risk pregnancies);
- routine assessment (screening) of low-risk pregnancies.

The purposes of ultrasound during the first trimester are:

- to visualize the gestational sac inside the uterus and evaluate the number and implant site of sacs;
- to visualize the embryo or fetus, evaluate their number and visualize their cardiac activity;
- to estimate gestational age, by measuring the mean sac diameter or crown–rump length or the biparietal diameter of the head;
- to evaluate the morphology of the uterus and adnexa;
- to provide an early diagnosis of fetal anomalies (in selected cases);
- to screen for aneuploidy (in selected cases).

With these evaluations, it is possible to diagnose during the first trimester:

- a normal (intrauterine) or ectopic (intra- or extrauterine) implant;
- embryo or fetus life or early pregnancy failure (miscarriage, abortion);

- the number of embryos or fetuses (single or multiple pregnancy);
- chorionicity and amnionicity in multiple pregnancies;
- correct gestational age;
- anomalies of the uterus (e.g. malformations, myomas) and adnexa (e.g. cysts, neoplasms);
- morphological fetal abnormalities;
- aneuploidy, by measuring nuchal translucency between 11 and 14 weeks of gestation.

Preparation

For **transabdominal ultrasound**, the woman should have a full bladder. To fill her bladder, the woman should drink 1 l (four glasses) of water 0.5–1 h before the procedure. If the woman cannot drink and transabdominal ultrasound must be used, the bladder can be filled with saline solution through a Foley catheter. For **transvaginal ultrasound**, the woman should have an empty bladder: she must void her bladder immediately before the procedure.

Examination technique

The first trimester scan can be made either transvaginally or transabdominally. If a transabdominal scan does not provide all the necessary information, it should be complemented by a transvaginal scan, and vice versa.

Position and scanning technique

For transabdominal ultrasound, the woman should lie on the examination bed on her back, with extended or flexed legs. After ultrasonographic gel has been applied to the woman's skin, the ultrasonographic probe should be used to examine the pelvis and lower part of the abdomen in horizontal (transverse), vertical (sagittal) and oblique scanning planes (Fig. 2.1a).

For transvaginal ultrasound, the woman must be lying on the examination bed on her back in the gynaecological position, with flexed hips and knees on supports. A clean transvaginal probe placed in an aseptic probe cover (condom) filled with ultrasonographic gel is inserted into the anterior fornix of the vagina. The pelvis should be examined in all planes by smoothly moving and rotating the probe inside the vagina (Fig. 2.1b).

Technical characteristics of ultrasound probes

For transabdominal ultrasound, the probe frequency should be at least 3.5 MHz; for transvaginal ultrasound, the probe frequency should be at least 5.0 MHz.

Fig. 2.1. (a) Transabdominal ultrasound, convex probe. (b) Transvaginal ultrasound, convex probe. P, pelvic bone; B, bladder (full in (a); empty in (b)); U, uterus; star, gestational sac; R, rectum

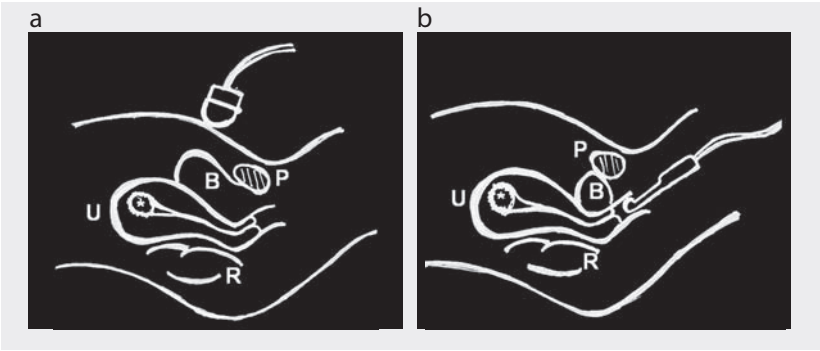

End-points of first-trimester scans

- Establish the presence of a gestational sac inside the uterus.
- Visualize the embryo or fetus.
- Evaluate the number of embryos or fetuses.
- Establish the presence or absence of embryonic or fetal cardiac activity, only with B-mode or M-mode technique up to 10 weeks + 0 days; later, pulse or colour Doppler can be used.
- Estimate gestational age by one of two means.

The mean gestational sac diameter can be measured from 5–6 to 11 weeks but is advisable only if the embryo cannot be assessed. The gestational sac can be visualized from 6 menstrual weeks by transabdominal ultrasound and from 5 weeks by transvaginal ultrasound. It is suggested that the mean sac diameter be measured from the average internal diameter of the gestational sac, calculated by adding the three orthogonal dimensions of the chorionic cavity (anteroposterior, longitudinal and transverse) and dividing by 3, with the calipers inner-to-inner on the sac wall, excluding the surrounding echogenic rim of tissue (Fig. 2.2).

The gestational age, *a*, can be calculated from the mean sac diameter, *d*, with the formula:

$$a = d + 30$$

where *a* is measured in days and *d* in millimetres.

Embryo or fetus size can be measured from the **crown–rump length** or **biparietal diameter**. Crown–rump length can be measured by transvaginal ultrasound when the embryo reaches 2–5 mm (5–6 weeks' menstrual age) and by transabdominal ultrasound at 5–10 mm (6–7 weeks). The conventional crown–rump length

Fig. 2.2. Measurement of diameter of mean gestational sac at 7 weeks' gestational age, using transvaginal ultrasound. (a) Longitudinal and anteroposterior sac diameter. (b) Transverse sac diameter. The yolk sac (arrow) and a subserosal fibroid (F) are also visible

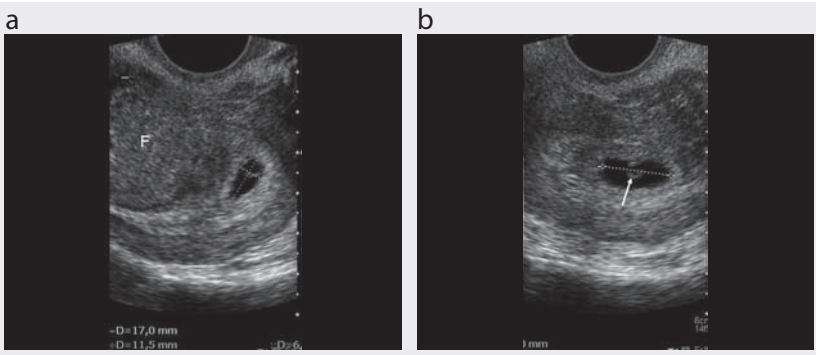

measurement is the maximal straight-line length of the embryo or fetus, obtained along its longitudinal axis; the embryo or fetus must be neither too flexed (curved) nor too extended. The accuracy of crown–rump length for dating pregnancy is ± 3–4 days between 7 and 11 weeks (Fig. 2.3).

Fig. 2.3. Measurement of crown–rump length (calipers) with transvaginal ultrasound, at 8 weeks' gestational age

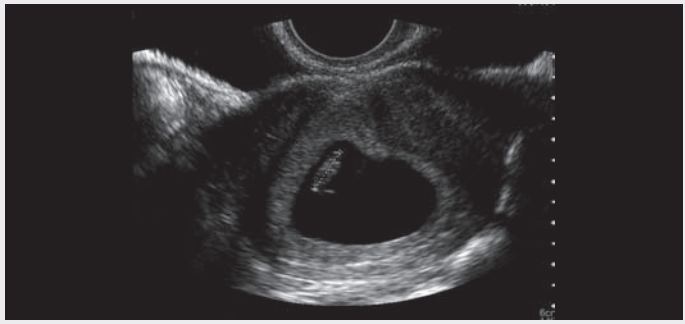

Because normal embryonic growth is almost linear at 1 mm/day, gestational age, *a*, can be estimated with an accuracy of ± 3 days between 43 and 67 days, from the formula:

$$a = l + 42$$

where *a* is measured in days and crown–rump length, *l*, in millimetres.

Towards the end of the first trimester, rapid fetal development and flexion and extension positional changes limit the accuracy of crown–rump length determination, and measurement of the biparietal diameter of the head becomes the preferred biometric for calculating gestational age. The accuracy of measurement of biparietal diameter between 12 and 16 weeks' gestational age is ± 3–4 days. The diameter must be measured in a transverse section of the fetal head at the level of the thalami, the positioning of the calipers depending on the reference curve used (Fig. 2.4).

- Evaluate the morphology of the uterus and adnexa.
- Evaluate chorionicity and amnionicity in twin pregnancies.

Fig. 2.4. Measurement of biparietal diameter, transverse section of fetal head. (a) Transvaginal ultrasound, 11 weeks; the calipers are positioned outer-to-outer on the skull. (b) Transabdominal ultrasound, 13 weeks; the calipers are positioned outer-to-inner on the skull

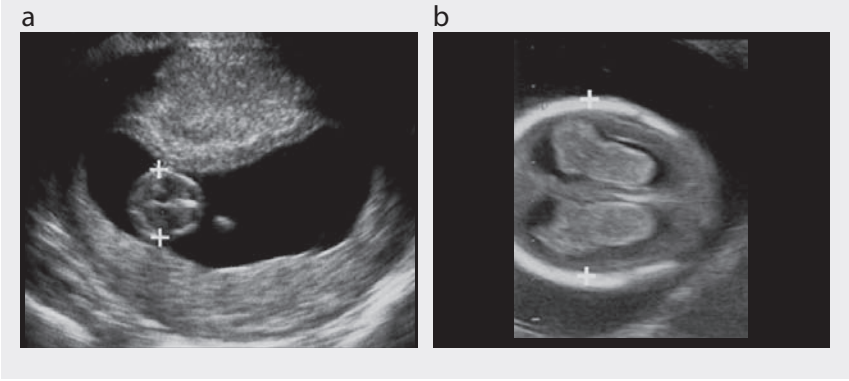

Normal findings

The first sonographic finding to suggest early pregnancy is visualization of the gestational sac. With transabdominal ultrasound, it is possible to visualize the gestational sac at as early as 5 weeks' gestational age; with transvaginal ultrasound, the gestational sac is visible when the mean sac diameter is 2–3 mm, at a gestational age of slightly more than 4 weeks (Fig. 2.5). The sac appears as a small, round fluid collection completely surrounded by an echo-rich rim of tissue, located in a lateral position in the uterine fundus. As the sac implants into the decidualized endometrium, it is possible to visualize the so-called double decidual sac or inter-decidual sign as a second echo-rich ring around the sac, caused by the decidual reaction to sac implantation.

Table 2.1 lists the visible landmarks that can be used for pregnancy dating.

The **yolk sac** is the first anatomical structure to be identified within the gestational sac. With transvaginal ultrasound, it can be seen as early as 5 weeks' gestational

Fig. 2.5. (a) Transverse transvaginal scan of early pregnancy (6 weeks): the round gestational sac (arrow) containing the yolk sac is implanted eccentrically inside the uterine cavity. (b) Three-dimensional reconstruction of the uterine cavity containing the gestational sac (arrow)

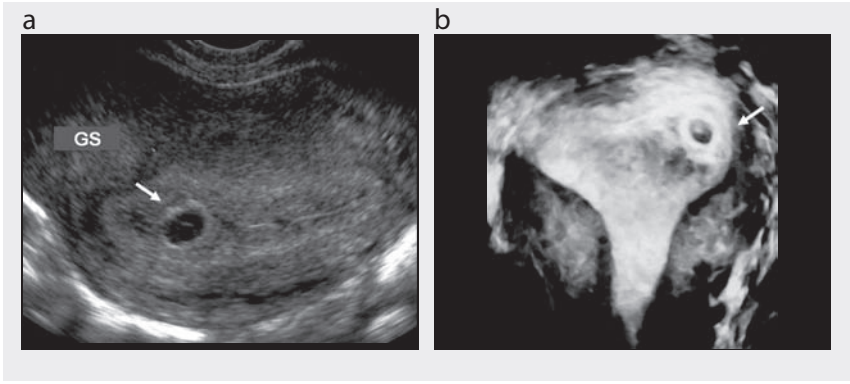

Table 2.1. Guidelines for dating a pregnancy during the first trimester by transvaginal ultrasound

Stage of development	Gestational age (weeks)
Gestational sac (no yolk sac, embryo or heartbeat)	5.0
Gestational sac and yolk sac (no embryo or heartbeat)	5.5
Gestational sac and yolk sac (living embryo too small to be measured, crown–rump length < 5 mm)	6.0
Embryo or fetus ≥ 5 mm in length	Based on crown–rump length[a]

[a] See Table 2.2

age (mean sac diameter, 5 mm), while with transabdominal ultrasound, the yolk sac should be evident by 7 weeks (mean sac diameter, 20 mm). The yolk sac diameter increases steadily between 5 and 10 weeks' gestational age, to a maximum diameter of 5–7 mm, which corresponds to a crown–rump length of 30–45 mm. The yolk sac is spherical, with a well-defined echogenic periphery and a sonolucent centre and is located in the chorionic cavity, outside the amniotic membrane.

Often, the **vitelline duct** is visible. It corresponds to the omphalomesenteric duct, which connects the embryo and the yolk sac; the vitelline vessels can be detected with colour Doppler. By the end of the first trimester, the yolk sac is no longer seen (Fig. 2.6).

Fetal membranes and amniotic cavity: At 6 weeks' gestational age, the amniotic membrane is formed, closely applied to the embryo, but it is not usually identified until 7 weeks because it is very thin. With transvaginal ultrasound, the thin amniotic membrane becomes apparent, surrounding the embryo at 6–7 weeks, with a crown–rump length of 7 mm. The amniotic sac appears as a circular structure inside the coelomic cavity. The diameter of the amniotic sac increases linearly with

Fig. 2.6. (a) Yolk sac (arrow) and easily visible vitelline duct. (b) Yolk sac (arrow) inside the coelomic cavity; the embryo and the amniotic membrane are also visible

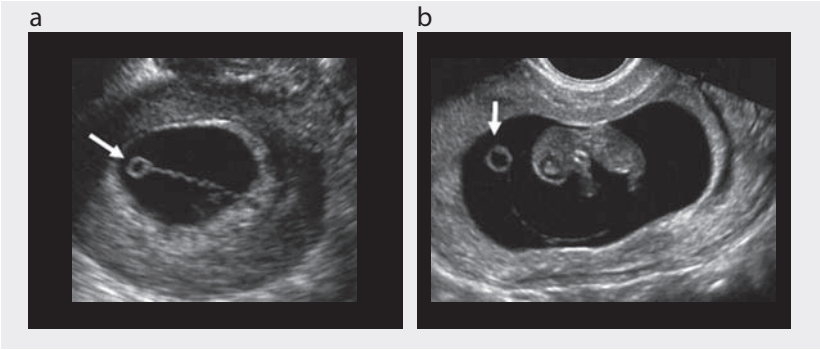

crown–rump length. Because the amniotic cavity enlarges more rapidly than the chorionic cavity, the latter is obliterated as the amniotic membrane reaches the chorion. Apposition begins in the middle of the first trimester but is often incomplete until 12–16 weeks' gestational age (Fig. 2.7).

Fig. 2.7. (a, b) Transvaginal ultrasound, showing the thin amniotic membrane (arrow) dividing the amniotic from the coelomic cavity

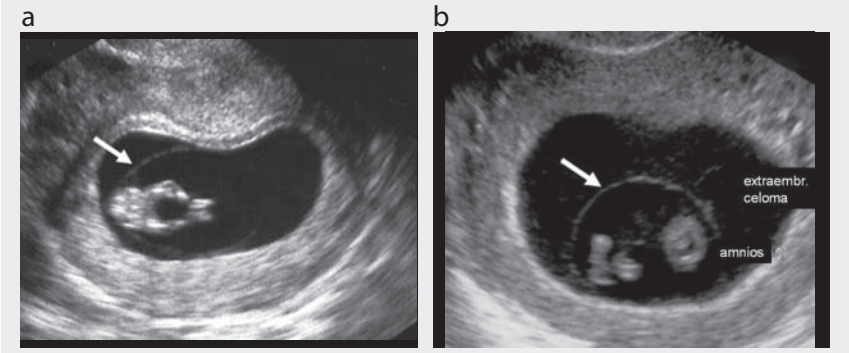

Placenta and umbilical cord: Placental development begins during the 8th week of gestational age. The echo-rich ring surrounding the sac becomes asymmetric, with focal peripheral thickening of the most deeply embedded portion of the sac. At 8 weeks' gestational age, the vitelline and allantoic ducts are visible as a thick structure connecting the embryo to the gestational sac wall. Once the amniotic membrane has developed, the vitelline duct separates from the forming umbilical cord, which then elongates, and its vessels start coiling inside the Wharton jelly (Fig. 2.8).

Embryo and fetus: At 5 weeks' gestational age, the embryonic disc is visible using transvaginal ultrasound as a subtle area of focal thickening (1–2 mm in length)

Fig. 2.8. Umbilical cord and placenta on transvaginal ultrasound. (a) 11 weeks; (b) 9 weeks

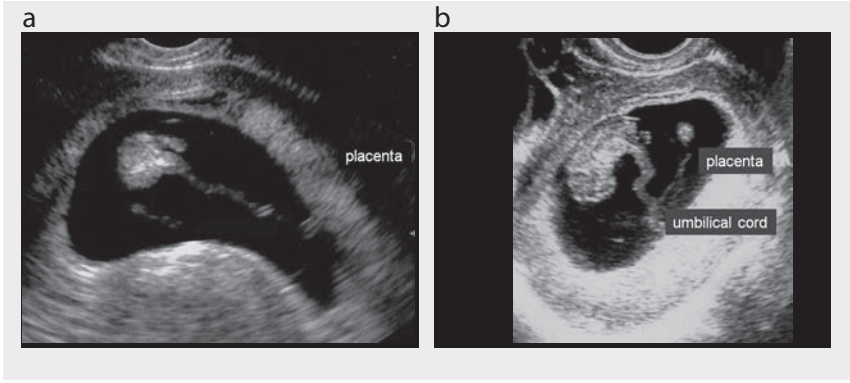

along the periphery of the yolk sac, when the mean diameter of the gestational sac is 5–12 mm. Sonographic observations throughout the embryonic period reveal dramatic changes in anatomical structures between 6 and 10 weeks, with the crown–rump length increasing by 1 mm/day. At 6 weeks, due to the ventral folding of its cranial and caudal ends, the shape of the embryo changes from a flat disc into a C-shaped structure. The rapidly developing brain becomes prominent, and the head size is almost half the total length of the embryo, while the caudal end elongates and curves, generating a tail. At this stage, the amniotic sac develops, and the embryo and the yolk sac diverge progressively. Limb buds appear at 7–8 weeks and evolve, protruding ventrally by 9 weeks. The trunk elongates and straightens, and the midgut herniates into the umbilical cord. At 10 weeks (crown–rump length, 30–35 mm), the embryo has visible hands and feet, and the tail has disappeared. Table 2.2 shows the relations between crown–rump length and gestational age.

The midgut herniation turns into the abdominal cavity at 11–12 weeks' gestational age. Fetal movements can be detected from 7 weeks and increase in complexity at 9 weeks; flexion and extension of the body and limbs are clearly visible by 10–12 weeks. At 10 weeks (72 days from the last menstrual period; 56 days' conceptional age), embryogenesis is almost complete, and the embryo becomes a fetus (Fig. 2.9).

Cardiac activity: Cardiac contractions begin at 5 weeks + 2 days (37 days from the last menstrual period) when the embryonic length is 1.6 mm. The heartbeat can be detected routinely with transvaginal ultrasound at 6 weeks (embryonic length, 4–5 mm; mean sac diameter, 13–18 mm). With transabdominal ultrasound, cardiac activity is evident by 7 weeks (crown–rump length, 8–10 mm; mean sac diameter, 25 mm). Up to 10 weeks' gestational age, cardiac rates can be visualized in B-mode and recorded in M-mode; for safety reasons, pulse or colour Doppler should not be used.

Before 6 weeks, the cardiac rate is relatively slow (100–115 beats per min), although rates of 82 at 5 weeks and 96 beats per min at 6 weeks have been reported. Thereafter, it increases linearly, and by 8 weeks is 144–170 beats per min; after 9 weeks,

Table 2.2. Relations between crown–rump length and gestational age

Crown–rump length (mm)	Mean predicted gestational age (weeks)	Crown–rump length (mm)	Mean predicted gestational age (weeks)
2	5.7	29	9.7–9.9
3	5.9	30	9.9–10.0
4	6.1	31	10.0–10.1
5	6.2–6.3	32	10.1–10.2
6	6.4–6.5	33	10.2–10.3
7	6.6–6.7	34	10.3–10.4
8	6.7–6.9	35	10.4–10.5
9	6.9–7.0	36	10.5–10.6
10	7.1–7.2	37	10.6–10.7
11	7.2–7.4	38	10.7–10.8
12	7.4–7.5	39	10.8–10.9
13	7.5–7.7	40	10.9–11.0
14	7.7–7.9	41	11.0–11.1
15	7.9–8.0	42	11.1–11.2
16	8.0–8.2	43	11.2–11.3
17	8.1–8.3	44	11.2–11.4
18	8.3–8.5	45	11.3–11.4
19	8.4–8.6	46	11.4–11.5
20	8.6–8.7	47	11.5–11.6
21	8.7–8.9	48	11.6–11.7
22	8.9–9.0	49	11.7–11.8
23	9.0–9.1	50	11.7–11.9
24	9.1–9.3	51	11.8–11.9
25	9.2–9.4	52	11.9–12.0
26	9.4–9.5	53	12.0–12.1
27	9.5–9.6	54	12.0–12.2
28	9.6–9.7	55	12.1–12.3

Fig. 2.9. Midgut herniation (arrows) at 12 weeks. (a) Transverse transvaginal ultrasound of fetal abdomen. (b) Longitudinal transvaginal ultrasound of the fetus

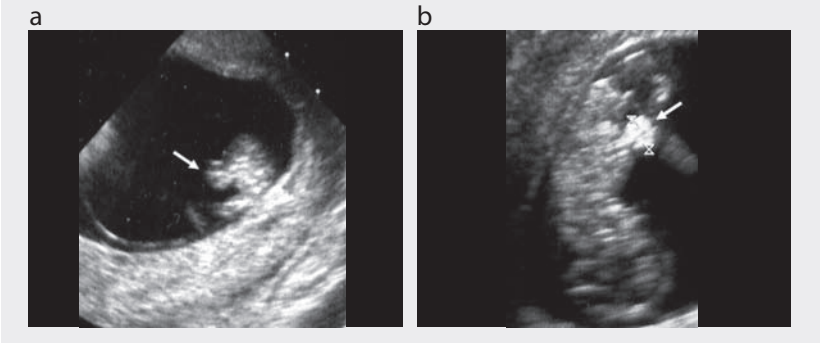

the rate plateaus at 137–150 beats per min. The cardiac rate is stable in early gestation but shows progressively more variation with gestational age.

Embryonic anatomy: With continued technological improvements, imaging of the embryo has progressed beyond identifying cardiac activity and measuring crown–rump length. By 10 weeks' gestational age, the fetal cranium, brain, neck, trunk, heart, bladder, stomach and extremities can be visualized, and gross anomalies can be detected or excluded in the late first trimester (after 12 weeks), mainly with transvaginal ultrasound. Ossification of the skull is reliably seen after 11 weeks, and examination of the four chambers of the heart is possible after 10 weeks (Fig. 2.10).

Fig. 2.10. Anatomical study by transvaginal ultrasound in the first trimester. (a) Inside the fetal head, cerebellum (right) and midline. (b) From the left: cerebellum, fourth ventricle, third ventricle and lateral ventricles. (c) Open fetal hand with fingers

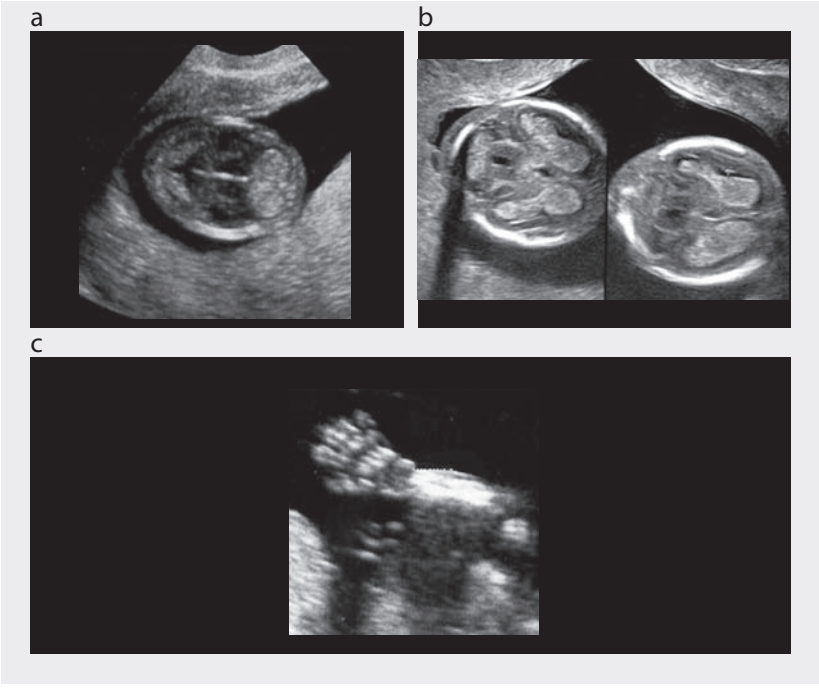

Twin pregnancies, determination of zygosity and chorionicity: Multiple pregnancies can result either from the ovulation and subsequent fertilization of more than one oocyte (to produce polyzygotic or nonidentical twins) or from the splitting of one embryonic mass to form two or more genetically identical fetuses (monozygotic twins). In all polyzygotic multiple pregnancies, each zygote develops its own amnion, chorion and placenta (polychorionic). In monozygotic pregnancies, the twins can share the same placenta (monochorionic), amniotic sac (monoamniotic) or even fetal organs (conjoined). When embryonic splitting occurs, the third day after

fertilization, there is vascular communication of the circulation in the two placentas (monochorionic). Zygosity can be determined only by DNA analysis, but chorionicity can be determined by ultrasound on the basis of the number of placentas, the characteristics of the membrane between the two amniotic sacs and fetal sex.

With transvaginal ultrasound, a multichorionic twin pregnancy, in which each fetus has a different amniotic sac and yolk sac can be easily recognized at 7–9 weeks' gestational age. The chorionic membrane is thick and echo-rich up to 10–11 weeks, and the two yolk sacs are always divided by a membrane. Sonographic examination of the base of the inter-twin membrane allows reliable differentiation of dichorionic and monochorionic pregnancies: in dichorionic twins, the inter-twin membrane is composed of a central layer of chorionic tissue between two layers of amnion; in monochorionic twins, there is no chorionic layer. In dichorionic twins, there is a thick septum between the two gestational sacs, which, at the base of the membrane, appears as a triangular tissue projection called the lambda sign, which is not present in monochorionic twins. The lambda sign is readily visible in the late first trimester but becomes progressively more difficult to identify with advancing gestation (Fig. 2.11).

Fig. 2.11. (a) Twin pregnancy at 9 weeks; transvaginal ultrasound. Thick septum between the two sacs. (b) Triplet pregnancy, of which one is monochorionic with a thin interamniotic septum (arrow). (c) Transabdominal ultrasound: dichorionic twins with thick septum (arrow). (d) Transabdominal ultrasound: quadruplets

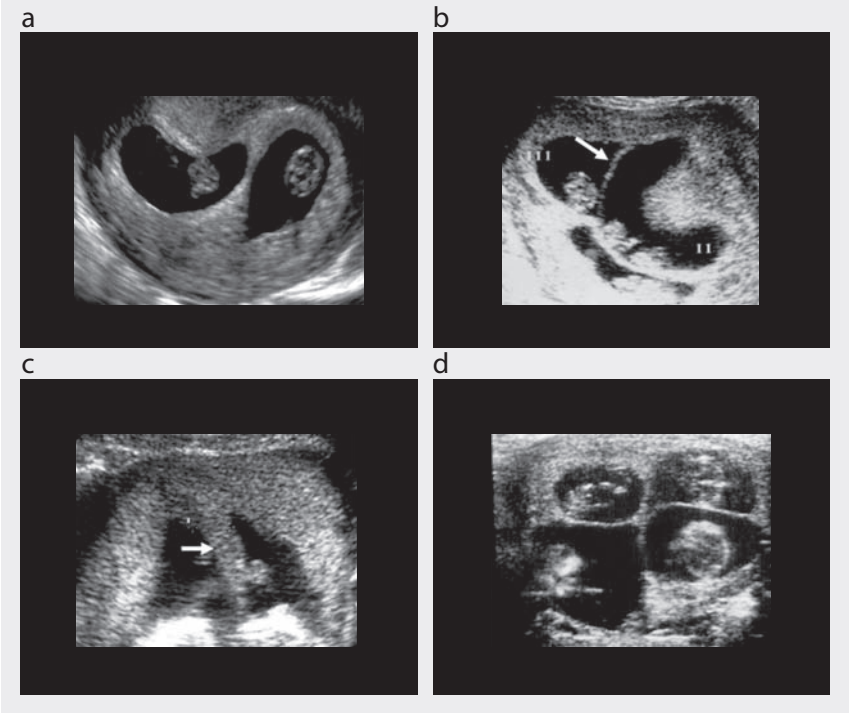

First-trimester screening for aneuploidy

In 1995, it was established that about 75% of fetuses with aneuploidy have greater nuchal translucency thickness, and 65–70% have no nasal bone between 11 and 13 weeks + 6 days of gestational age (crown–rump length, 45–84 mm). Fetal nuchal translucency normally increases with gestation and crown–rump length. The technical reasons for selecting 13 weeks + 6 days as the upper limit for measuring fetal nuchal translucency are that the incidence of abnormal fluid accumulation in fetuses with abnormal karyotypes is maximal before 14 weeks and the success rate of nuchal translucency measurements is 98–100% at 11–14 weeks, falling to 90% after 14 weeks because of the more frequent vertical position of the fetus. The normal upper limit for nuchal translucency changes with gestational age and crown–rump length and never exceeds 2.5 mm (Fig. 2.12).

Fig. 2.12. Nuchal translucency measurement (calipers) by transvaginal ultrasound. (a) Normal nuchal translucency. (b) Increased nuchal translucency with fetal hydrops. (c) Nasal bone (arrow) demonstrated by transvaginal sonography

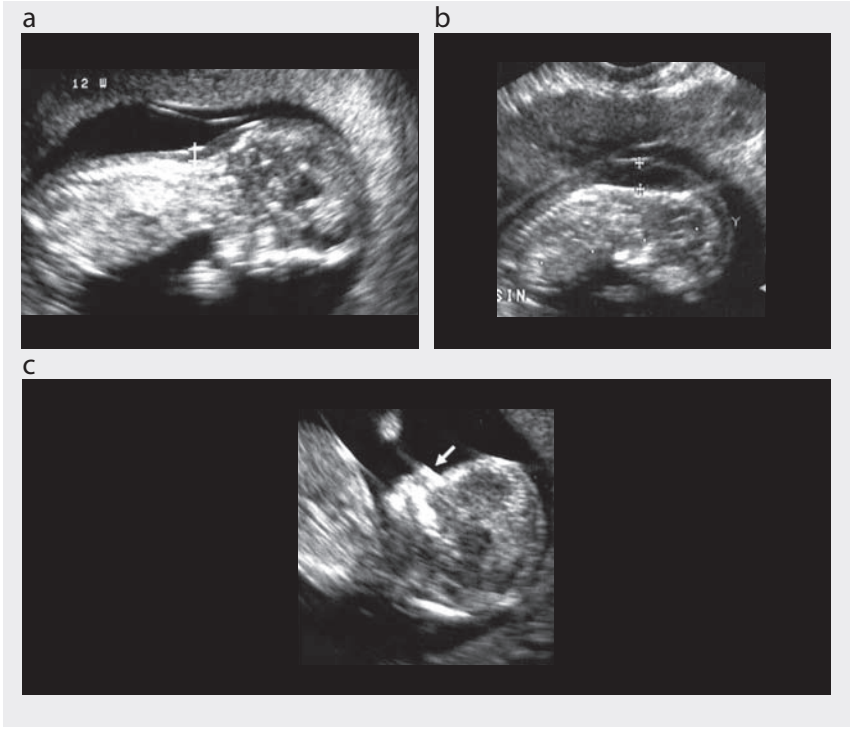

For computerized calculation of risk, abnormal nuchal translucency is expressed as the deviation from the expected normal median for a given crown–rump length.

The ultrasound machine should have high resolution, a video-loop function and calipers that provide measurements to one decimal point. Transabdominal

ultrasound is successful in about 95% of cases. Appropriate training of sonographers and adherence to a standard technique for measuring nuchal translucency are essential prerequisites for good clinical practice and for the success of a screening programme. To measure nuchal translucency:

- A mid-sagittal section of the fetus should be obtained, and nuchal translucency should be measured with the fetus in the neutral position and horizontal on the screen.
- Only the fetal head and upper thorax should be included in the image.
- The magnification should be as great as possible, such that a slight movement of the calipers causes only a 0.1-mm change in the measurement.
- The maximum thickness of the subcutaneous translucency between the skin and the soft tissue overlying the cervical spine should be measured.
- The calipers should be placed on the lines that define the thickness of the nuchal translucency.
- More than one measurement should be taken during the scan, and the maximum should be recorded.

The fetal nasal bone can be visualized at 11–14 weeks. Several studies have shown a strong association between an absent nasal bone in the late first trimester and trisomy 21, as well as other chromosomal abnormalities. The fetal profile can be examined in more than 95% of cases at 11–14 weeks (Fig. 2.12). In chromosomally normal fetuses, the nasal bone is absent in less than 1% of Caucasians and Asians and in about 10% of Afro-Caribbeans. It is absent in 65–70% of cases of trisomy 21, more than 50% cases of trisomy 18 and 30% of cases of trisomy 13. For examination of the nasal bone:

- The image should be magnified so that only the fetal head and upper thorax are included.
- A mid-sagittal view of the fetal profile should be obtained with the ultrasound transducer held in parallel to the direction of the nose.
- The image of the nose should contain three distinct lines: the top line represents the skin, the thicker, more echogenic line represents the nasal bone, and the third line, in continuity with the skin but higher, represents the tip of the nose (Fig. 2.12).

Pathological findings

Because of the complexity of first-trimester development, complications are frequent. Spontaneous miscarriage occurs in approximately 15% of clinically diagnosed pregnancies, but the loss rate is estimated to be two to three times higher in very early, often unrecognized pregnancies. Vaginal bleeding or spotting occurs in 25% of first-trimester pregnancies. Often, the bleeding is mild and self-limited, and

ultrasound usually shows normal findings. In cases of severe pain, uterine contractions, heavy bleeding or a dilated cervix, however, the pregnancy will probably fail, and ultrasound shows abnormal findings.

Intrauterine blood

In many cases of threatened abortion in the first trimester, but also in asymptomatic women, intrauterine blood collections are found on ultrasound examination. In early pregnancy, the genesis of such collections is usually normal implantation; later, it is often due to venous bleeding associated with separation of the placental margin or marginal sinus, with blood collection between the chorion and the endometrium. The finding of an intrauterine fluid collection near the gestational sac is due to subchorionic haemorrhage. The echogenicity of the blood depends on its age and the amount of clotting: recent haemorrhages are echo-poor or isoechoic, depending on the location (Fig. 2.13).

Fig. 2.13. Examples of large subchorionic haemorrhage (arrows) surrounding the gestational sac (dotted arrows). (a), (b) Recent echo-free haemorrhage. (c) Partially organized subchorionic haematoma

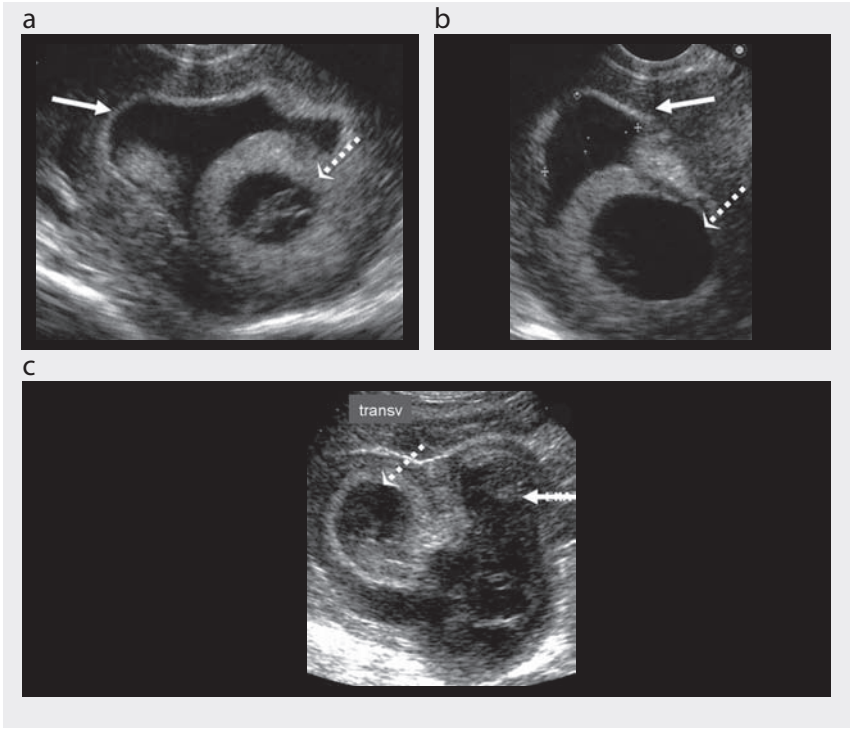

The pregnancy outcome in cases of visible intrauterine haematoma depends on the location and the size of the haematoma. The prognosis of a retroplacental

haematoma or a progressively larger haematoma is poor, but the evidence is equivocal. Despite vaginal bleeding, most women with intrauterine haematoma have successful pregnancy outcomes.

Abortion

Spontaneous abortion is defined as termination of a pregnancy before 20 completed weeks' gestational age. Sixty-five per cent of spontaneous abortions occur during the first 16 weeks of pregnancy. Recurrent abortion is defined as three or more consecutive spontaneous abortions; its occurrence is 0.4–0.8% of all pregnancies.

In cases of threatened abortion (vaginal bleeding with a long, closed cervix), ultrasound examination gives information about the evolution of the pregnancy. The term 'missed abortion' is not clear, and the term 'embryonic demise' should be used when a non-living embryo is found, whereas the term 'blighted ovum' should be used when a gestational sac with no visible embryo is found. Other entities that can present with symptoms suggesting threatened abortion are ectopic pregnancy and gestational trophoblastic disease. The ultrasonographic findings in women with threatened abortion are crucial both for diagnosis and therapy. Sometimes, for a more precise diagnosis, it is necessary to integrate the ultrasound images with the quantity of serum human chorionic gonadotropin (hCG).

The term 'incomplete abortion' is used when partial expulsion of products occurs. The ultrasound scan reveals retained products of conception, endometrial blood and trophoblastic tissue, with no normal gestational sac. In cases of 'complete abortion', with complete expulsion of the products of conception, the ultrasound scan shows an empty uterus with a normal or slightly thickened endometrium. For practical reasons, the ultrasound findings in diagnoses of abortion are divided into those that reveal an absent intrauterine sac, a sac with no embryo visible and a sac containing an embryo.

Absent intrauterine sac: On ultrasound examination, if the uterus appears normal or if the endometrial echoes appear thickened without a visible gestational sac, the differential diagnosis may be early spontaneous abortion, very early intrauterine pregnancy or ectopic pregnancy. The woman's history and the quantity of hCG can often clarify the sonographic findings. With transvaginal ultrasound, the gestational sac is usually visible at 4 weeks' gestational age, when the mean sac diameter is 2–3 mm and the hCG level 800–2600 IU/l; with both transvaginal and transabdominal ultrasound, a sac should be detected when its mean diameter is 5 mm, corresponding to 5 weeks' gestational age. If the hCG concentration is less than 1000 IU/l, it is difficult to identify the gestational sac. In these cases, it is advisable to repeat the hCG measurement and ultrasound after at least 48–72 h. If the hCG level is more than 2500 IU/l and no gestational sac is visible inside the uterus, the probability of an ectopic pregnancy is high.

Intrauterine sac without an embryo or yolk sac: In this situation, there are three possible diagnoses: a normal early intrauterine pregnancy, an abnormal intrauterine pregnancy or a pseudogestational sac in an ectopic pregnancy. In theory, an

Fig. 2.14. Transvaginal ultrasound in cases of spontaneous abortion. (a) Intrauterine sac containing a yolk sac and a small embryo (> 5 mm) without a heartbeat. (b) Non-living embryo (crown–rump length, 20 mm). (c) Bright yolk sac (arrow), often seen in abortion. (d) Twin abortion at 10 weeks' gestational age: transverse scan demonstrates an empty gestational sac (right) and a gestational sac containing a small embryo (< 5 mm; left) near the inter-twin membrane

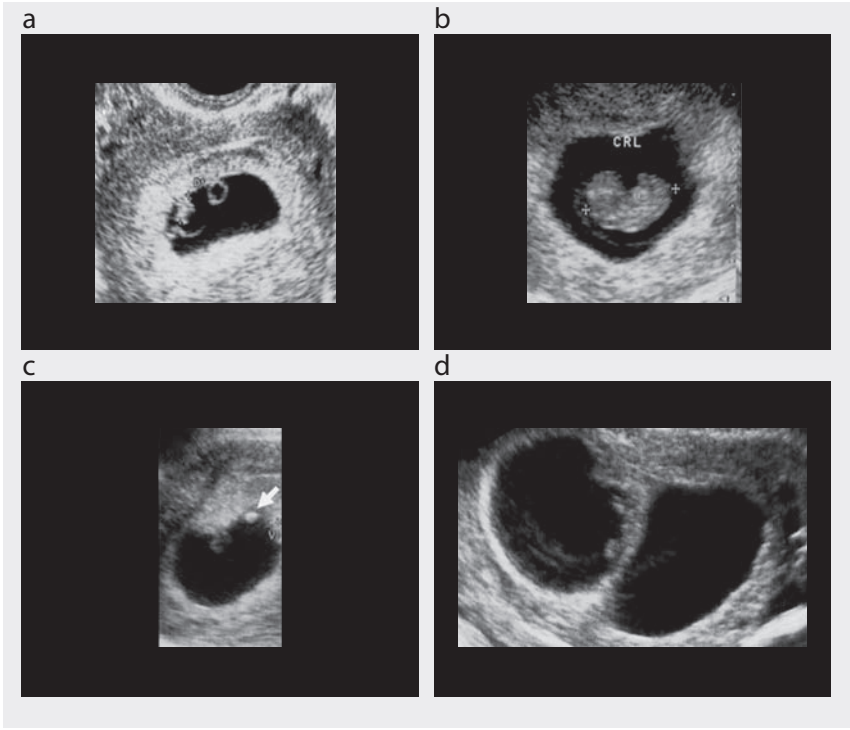

intrauterine sac can be distinguished from a pseudogestational sac, as the former is located within the decidua and the latter is within the uterine cavity. In practice, this distinction is often difficult, and a follow-up ultrasound should be made to verify the subsequent appearance of the yolk sac or the embryo. Size criteria can be used to differentiate a normal from an abnormal intrauterine sac. With transabdominal ultrasound, discriminatory size criteria suggestive of an abortion include: failure to detect a double decidual sac with a mean gestational sac diameter of ≥ 10 mm; failure to detect a yolk sac with a mean gestational sac diameter of ≥ 20 mm; and failure to detect an embryo and its cardiac activity with a mean gestational sac diameter of ≥ 25 mm. With transvaginal ultrasound, the discriminatory size criteria are: failure to detect a yolk sac with a mean gestational sac diameter of ≥ 8 mm; and failure to detect an embryo and its cardiac activity with a mean gestational sac diameter of ≥ 20 mm. The normal gestational sac grows at 1.13 mm/day, whereas an abnormal sac is estimated to grow at only 0.70 mm/day. If the ultrasound findings are controversial, the examination is difficult or the sonographer is inexperienced, caution is

warranted, and follow-up ultrasound should be done after an appropriate interval to obviate the risk of terminating a normal intrauterine pregnancy.

Intrauterine sac containing an embryo: When an embryo is visible with transabdominal ultrasound but cardiac activity is absent, the prognosis is poor. Nevertheless, cardiac activity is not detectable in very small embryos; the discriminatory embryonic size for detecting cardiac motion by transabdominal ultrasound is 10 mm. With transvaginal ultrasound, the discriminatory crown–rump length for visualizing cardiac motion is 5 mm. If the embryonic length is less than the discriminatory size, women should be managed expectantly, and follow-up ultrasound should be done when the expected crown–rump length exceeds the discriminatory value. When the crown–rump length exceeds the discriminatory length and cardiac activity is absent, a nonviable gestation is diagnosed (missed abortion or embryonic demise). Observation of the heartbeat inside the embryo is helpful for evaluating its relation to the yolk sac. At 6–7 weeks' gestational age, the embryo and the yolk sac

Fig. 2.15. Transabdominal ultrasound in cases of spontaneous abortion. (a) Empty gestational sac at 7 weeks + 3 days, with a leiomyoma of the posterior uterine wall (arrow). (b, c) Spontaneous expulsion of gestational sac and placenta (visible as a complex mass) in transverse (b) and longitudinal (c) scans of the uterine cervix. (d) Embryonic demise at 16 weeks' menstrual age, 8 weeks' gestational age: a large gestational sac, filling the uterine cavity completely, shown in transverse (top) and longitudinal (bottom) scans of the uterus

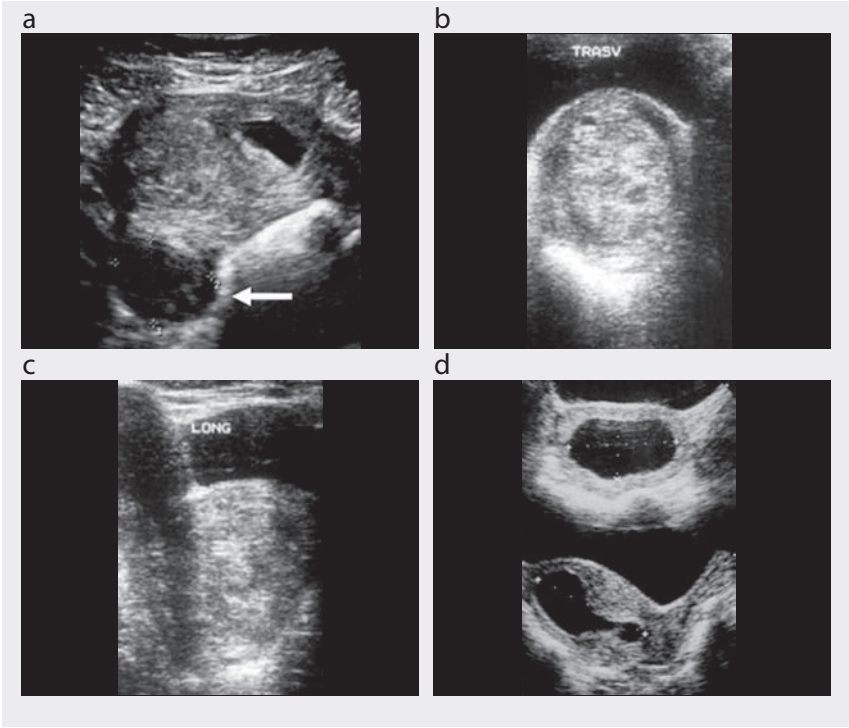

are contiguous; they diverge after 7 weeks. Cardiac activity should be recorded at the highest transducer frequency available in real-time or M-mode; for safety reasons, Doppler should be avoided before 10 weeks' gestational age. The normal cardiac rate should be > 100 beats per min up to 6 weeks + 2 days and > 120 beats per min later (Fig. 2.14, Fig. 2.15).

Ectopic pregnancy

An ectopic pregnancy is defined as a pregnancy that occurs outside the uterine cavity. The incidence of ectopic pregnancy is increasing (2% of all first-trimester pregnancies today) with the steady increase in risk factors (pelvic inflammatory disease and assisted reproductive techniques) and better diagnosis. Ectopic pregnancy can occur in 10% of all cases of medically assisted conception. It is still associated with high morbidity and mortality (6% of all pregnancy-related deaths). Most ectopic pregnancies are implanted in the Fallopian tube (95–97%), although implantation can occur in the ovary (1–3%), abdomen (< 1%), uterine cervix or cornua (interstitial) (< 1%) (Fig. 2.16).

Recently, ectopic pregnancies implanted on the scar of a previous Caesarean section have been described. Heterotopic pregnancies (simultaneous occurrence of two or more implantation sites) can also occur, commonly manifested as concomitant intrauterine and ectopic pregnancies, mainly in women who have undergone assisted reproduction. Diagnosis of this form of ectopic pregnancy is difficult and often delayed. Early detection of ectopic pregnancy can lead to successful medical management and prevention of maternal morbidity and mortality. Diagnosis has been based on clinical examination and physical symptoms of tubal rupture, while it is now possible to diagnose an early ectopic pregnancy before rupture, from serial measurements of hCG associated with serial ultrasonography. With transvaginal ultrasound, it is possible to visualize a gestational sac measuring 2 mm with an hCG level of 1000 IU/l.

Fig. 2.16. Intrauterine ectopic pregnancies. (a) Transvaginal ultrasound of a cervical pregnancy at 8 weeks' gestational age (arrow). (b) Same case seen by transabdominal ultrasound: living embryo present inside the sac (arrow). (c) Longitudinal section by transabdominal ultrasound of an interstitial ectopic pregnancy in the right uterine cornua (arrow) at 8 weeks: no visible embryo (embryonic demise). (d) Same case on transverse transabdominal ultrasound

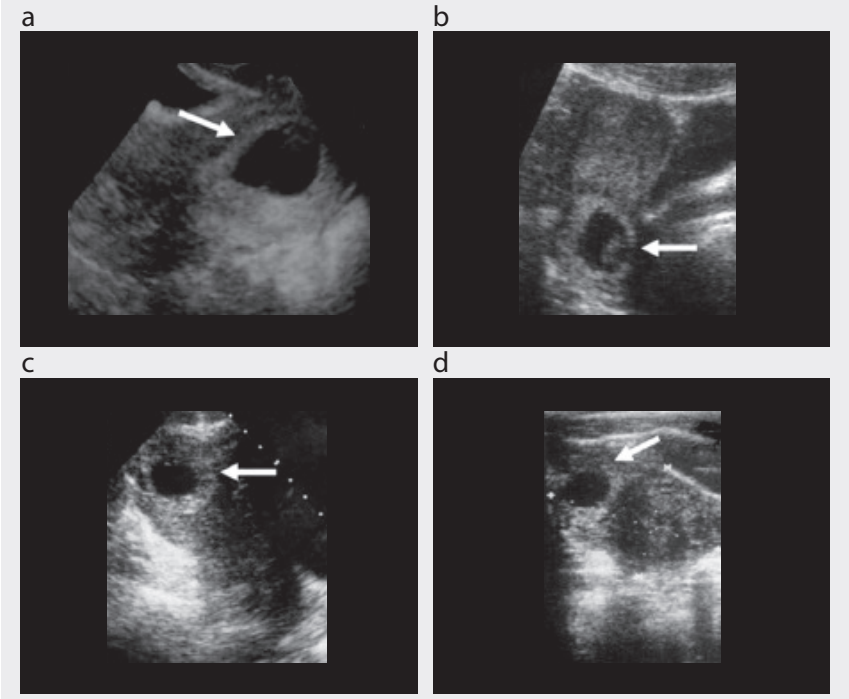

The diagnostic signs of an ectopic pregnancy can be direct or indirect:

Direct sign: visualization of the ectopic sac with or without a yolk sac and embryo (detected in 9–64% of cases) (Fig. 2.17);

Indirect signs: non-visualization of an intrauterine sac (empty uterus) with the hCG level greater than the discriminatory zone (1500–2000 IU/l); pseudogestational sac inside the uterus (detected in 10–20% of cases); complex, poorly defined, extra-ovarian adnexal mass (80%); tubal ring (echo-free structure inside the tube, 68–78%); abnormal tubal content (due to clots [haematosalpinx] and ovular material); intra-peritoneal free fluid collection (Douglas pouch, pelvis or abdomen, 60%) (Fig. 2.18).

A differential diagnosis must be made from other tubal pathological conditions (hydrosactosalpinx) sometimes associated with ectopic pregnancies, or from normal structures, such as a luteal body or bowel. The accuracy of ultrasound for detecting an ectopic gestation is about 80–85%, with a specificity of 96% and a false-positive rate of 0.5–1%.

Fig. 2.17. Tubal ectopic pregnancies. (a) Transvaginal ultrasound: tubal ring (arrow) at 6 weeks' gestational age. (b) Transabdominal ultrasound: ectopic pregnancy at 7 weeks with a visible embryo inside the sac (arrow). (c) Transvaginal ultrasound: tubal gestational sac at 5 weeks (arrow), with the whole tube visible (dotted arrow on the ampulla)

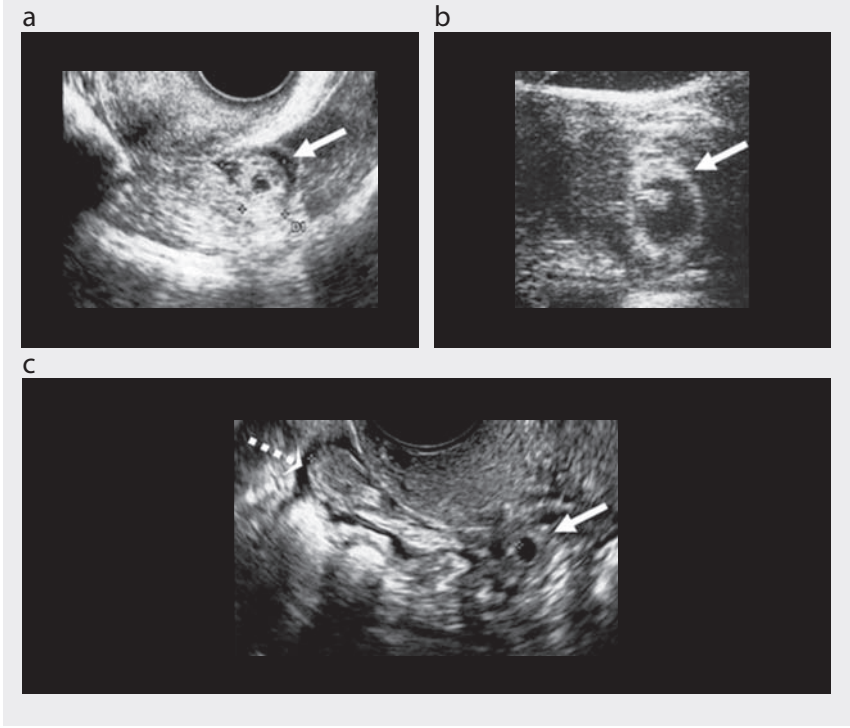

Fig. 2.18. Transvaginal ultrasound in cases of tubal ectopic pregnancy. (a) Large pseudogestational sac inside the uterine cavity (arrow), with the ectopic gestational sac containing an embryo (dotted arrow) visible inside a hydrosalpinx. (b) Complex mass (dotted arrow) and fluid collection in the cul-de-sac (arrow). (c) Small pseudogestational sac in the middle of the uterine cavity (arrow)

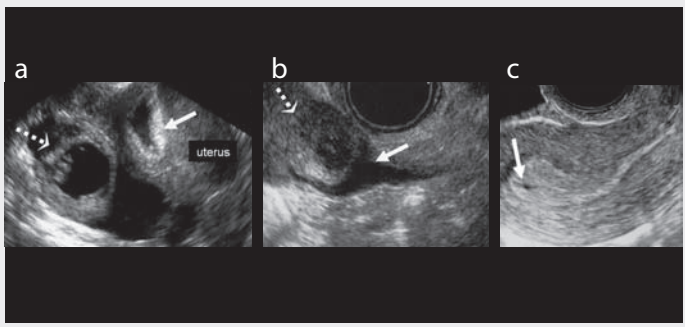

Gestational trophoblastic disease

Gestational trophoblastic disease is a spectrum of conditions, including hydatidiform mole, invasive mole and chorioncarcinoma. First-trimester bleeding is often the commonest clinical presentation of these disorders, with excessive, rapidly growing uterine size, exceeding the normal size for gestational age. Other clinical features are hyperemesis gravidarum or pre-eclampsia before 24 weeks. Maternal blood contains excessive hCG due to abnormal proliferation of trophoblastic tissue.

Hydatidiform mole (molar pregnancy)

Hydatidiform mole is a gestational complication that occurs in 1 out of 1000–2000 pregnancies. Complete and partial molar pregnancies have been described. **Complete hydatidiform mole** is the commonest trophoblastic disease, resulting from fecundation of an egg with no active nucleus: all the chromosomes present in the product of conception are of paternal origin (complete hydatidiform mole is also known as uniparental disomy, with a 46,XX karyotype in 90% of cases). The uniparental disomy causes early embryonic demise and proliferation of trophoblastic tissue, with the gross pathological appearance of a complex multicystic mass, shown as a snowstorm pattern with the oldest ultrasound equipment. The current ultrasound appearance of a complete hydatidiform mole is a heterogeneous echogenic endometrial mass with multiple cysts of variable size and necrotic–haemorrhagic areas. Doppler examination reveals increased uterine vascularity with high velocities and a low resistance index in the uterine arteries. In 50% of cases of complete hydatidiform mole, theca lutein cysts are present in the adnexa, resulting from hCG stimulation of the ovaries. On ultrasound, theca lutein cysts appear as multiple, large, bilateral, multiseptated ovarian cysts, sometimes haemorrhagic or complex, described as clusters of grapes (Fig. 2.19).

Partial hydatidiform moles result from fecundation of a normal egg with two spermatozoa or a diploid sperm, known as diandry (extra haploid set from the father). The abnormal karyotype is triploid (69,XXY) or tetraploid (92,XXXY). In partial moles, the triploidy is always paternal. In cases of maternal triploidy (digyny, an extra haploid set from the mother), other disorders, such as intrauterine growth retardation or spontaneous abortion, occur, with a non-molar placenta. In partial molar pregnancy, the ultrasound scan shows a gestational sac containing a fetus and an enlarged placenta with focal areas of multiple cysts. Often, the fetus coexisting with a molar pregnancy shows growth retardation and congenital anomalies (Fig. 2.20).

The differential diagnosis of a partial mole includes:

- twin pregnancy with one normal fetus and placenta and an accompanying complete hydatidiform mole; in this case, the fetal growth and anatomy are normal;
- fetal demise with hydropic degeneration of the placenta; the ultrasound presentation can be identical to that of a partial molar pregnancy, and pathological diagnosis is needed;
- placental pseudomole, due to mesenchymal dysplasia with villous hydrops, seen in pre-eclampsia. This placental pathology is rare in the first trimester.

Fig. 2.19. Complete hydatidiform mole. (a) Transvaginal ultrasound showing ovarian theca lutein cysts. (b), (c) Transabdominal ultrasound showing cystic villus degeneration (dotted arrows) and necrotic–haemorrhagic areas (arrows)

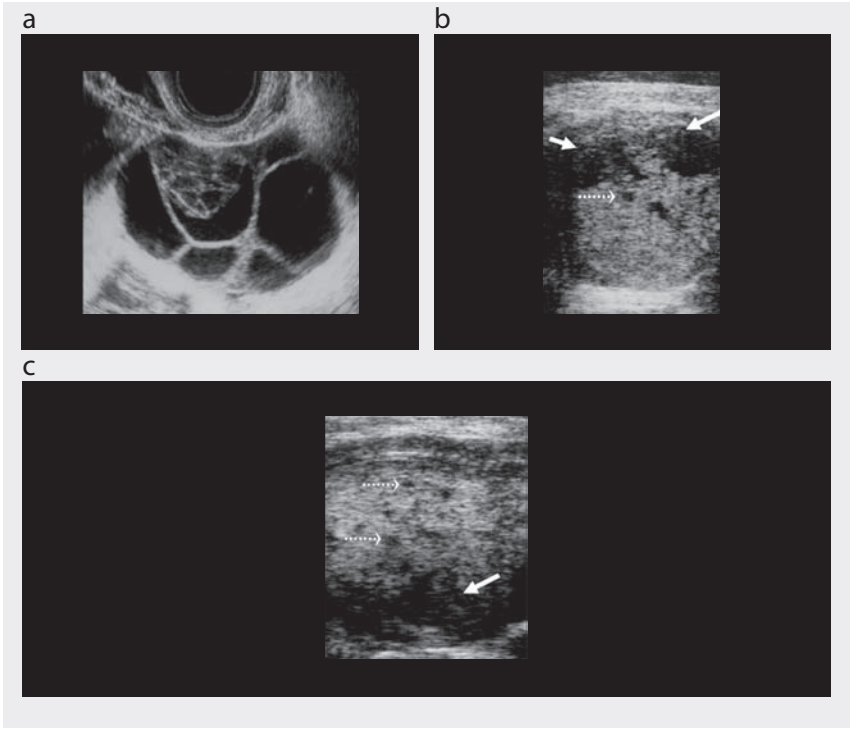

Fig. 2.20. Partial hydatidiform mole. (a), (b) Transabdominal ultrasound showing cystic degeneration of the placenta associated with a gestational sac and a non-living embryo (arrows)

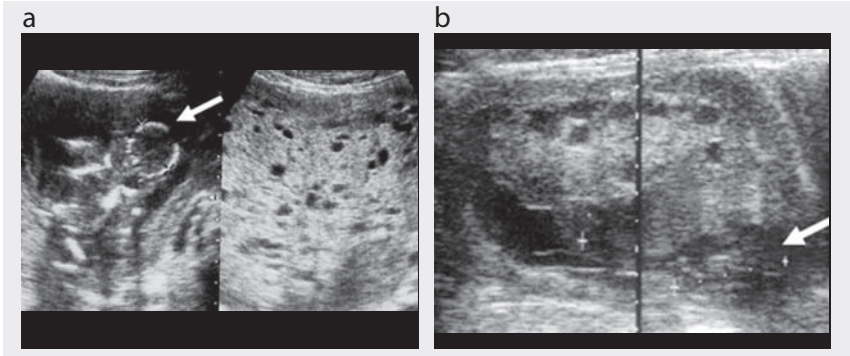

Invasive mole and chorioncarcinoma

Invasive mole presents as a deep growth into the myometrium and beyond, sometimes with penetration into the peritoneum and parametria. This tumour is locally invasive and rarely metastasizes, in contrast to chorioncarcinoma, which typically metastasizes extensively to the lung and pelvic organs. Of these tumours, 50% derive from a molar pregnancy, 25% from an abortion and 25% from an apparently normal pregnancy. A diagnosis is made when hCG levels remain elevated after evacuation of a pregnancy or after a delivery. Ultrasound may show the presence of a uterine mass similar to a complete hydatidiform mole and sometimes myometrial trophoblastic invasion. Haemorrhagic areas are often present inside the molar tissue, giving a complex aspect, mainly in chorioncarcinoma. Doppler shows increased myometrial flow, with abnormal vessels and shunts.

Computed tomography (CT) is useful for detecting metastases, and magnetic resonance imaging (MRI) demonstrates myometrial and vaginal invasion.

Embryo–fetal anomalies

Although many congenital anomalies cannot be diagnosed with confidence until the middle of the second trimester, imaging of the embryo has improved with continued technological advances, and many major fetal defects (such as acrania or anencephaly, large encephalocoele, holoprosencephaly, ventral wall defects, megacystis and conjoined twins) can be detected in the latter part of the first trimester. By 10 weeks' gestational age, the fetal cranium, brain, trunk and extremities can be visualized.

Anencephaly is characterized by the absence of the cranial vault (acrania), with dystrophic brain tissue exposed to the amniotic fluid: the fetal head has an irregular shape, and no cranial bones are visible (Fig. 2.21a).

Hydranencephaly is a lethal condition caused by complete occlusion of the internal carotid artery and its branches, resulting in the absence of cerebral hemispheres. This condition in early pregnancy appears as a large head with a fluid-filled (echo-free) intracranial cavity and no midline echo. Severe cases of ventriculomegaly (**hydrocephaly**) can be diagnosed during the first trimester (Fig. 2.21b).

Large **meningo-encephalocoele** is due to a defect in the skull, usually in the occipital region, through which the intracranial contents herniate. Either meninges (meningocoele) or both meninges and brain tissue (encephalocoele) protrude through this opening. This defect can be diagnosed in early pregnancy, but the diagnosis is difficult before ossification of the cranial vault (Fig. 2.21c).

In **alobar holoprosencephaly**, the prosencephalon fails to cleave into the two cerebral hemispheres. A large central cystic space is present inside the head and the falx and choroid plexus are absent. In 30% of cases, this condition is associated with trisomy 13 or 18 (Fig. 2.21d).

Cystic hygromas are large fluid collections behind or lateral to the fetal head, neck and trunk, sometimes associated with generalized hydrops. Hygromas can be septated or not and of variable size; they are associated in 70–90% of cases with Turner syndrome and trisomy 13, 18 or 21 (Fig. 2.22).

Fig. 2.21. Transvaginal ultrasound of central nervous system anomalies. (a) Acrania at 11 weeks' gestational age: meninges (arrow) without skull covering the abnormal brain tissue. (b) Hydrocephaly of the posterior horns of the lateral ventricles. (c) Occipital cephalocoele (arrow). (d) Holoprosencephaly

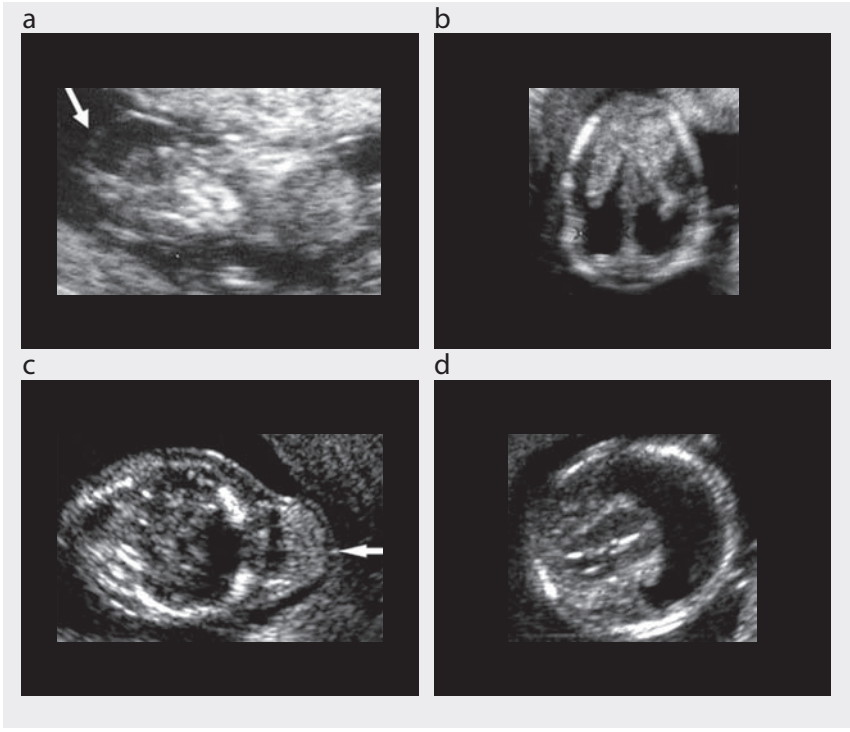

Large ventral wall defects, such as **omphalocoele (exomphalos)** and **gastroschisis**, should be differentiated from physiological bowel herniation, a normal finding up to 12 weeks' gestational age. Before 12 weeks, if the mass protruding outside the ventral wall is greater than 7 mm, a ventral wall defect should be suspected. In exomphalos, the extruded abdominal content is covered by a peritoneal membrane and has a smooth, rounded contour. In 60% of cases, exomphalos is associated with chromosomal anomalies (mainly trisomy 18). Gastroschisis results from a defect involving the entire thickness of the abdominal wall and is usually located to the right of the umbilical cord insertion. In gastroschisis, the protruding small bowel loops are not covered by a membrane, and the contour of the lesion is irregular; the cord insertion is normal. This condition is not associated with an increased risk for aneuploidy (Fig. 2.23a, b).

Megacystis is diagnosed when the fetal bladder length exceeds the normal value of 6 mm at 11–14 weeks' gestational age. Megacystis with a longitudinal bladder diameter of 7–15 mm is associated in 20% of cases with trisomy 13 or 18. If the bladder is more than 15 mm long, the incidence of chromosomal defects is only 10%, but there is a strong association with progressive obstructive uropathy (Fig. 2.23a–c).

Fig. 2.22. Transvaginal ultrasound in cases of cystic hygroma. (a) Trisomy 21 fetus: left, longitudinal scan showing nuchal translucency enlargement (calipers) and neck hygroma; right, echo-rich bowel (dotted arrow) and hypoplastic middle phalanx of the fifth digit (arrow) in the same fetus. (b) Transverse section of the neck with septated bilateral cystic hygromas. (c) Longitudinal scan of a fetus with large cystic hygromas and generalized hydrops

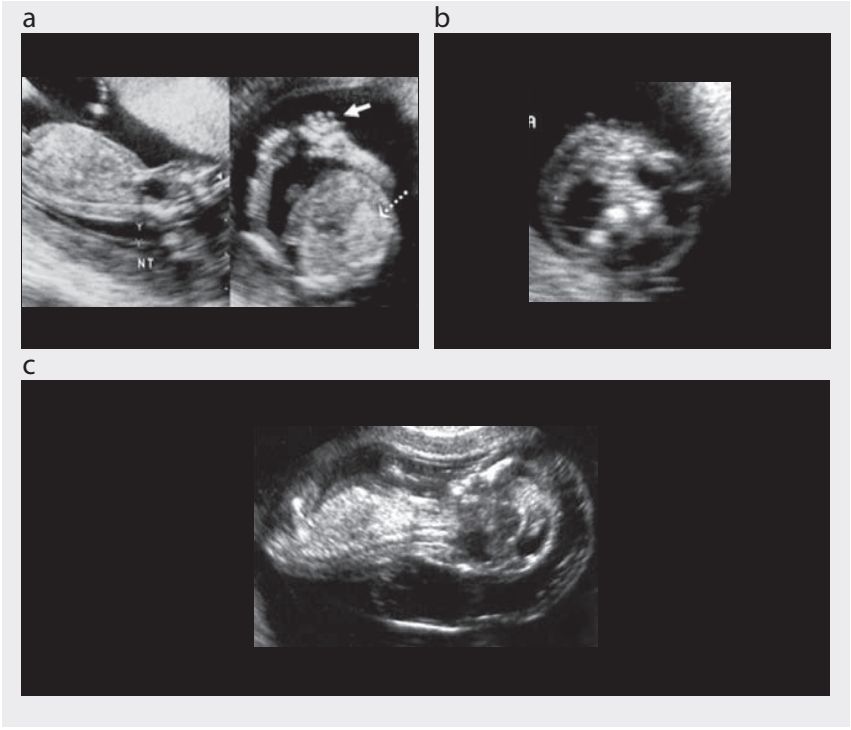

Conjoined twins are a complication of a monoamniotic monochorionic twin pregnancy and are due to an abnormality of monozygotic twinning, with incomplete division of an embryonic cell mass. Conjoined twins are sporadic and rare (one of 30 000–100 000 live births). They are, however, frequent in fetal life, because this condition is associated with a high rate of spontaneous abortion and stillbirth. Early in pregnancy, it can be difficult to differentiate conjoined twins from two separated but close monoamniotic twins; by the end of the first trimester, as the amniotic cavity enlarges, such differentiation becomes possible (Fig. 2.24).

Cardiac defects can be detected even in the first trimester of pregnancy due to improvements in the resolution of ultrasound machines. Increased nuchal translucency is known to be associated with all types of heart lesions, the prevalence of major cardiac defects being 1% with a nuchal translucency of 2.5–3.4 mm and 30% with a nuchal translucency of 6.5 mm or more. For fetuses with a nuchal translucency above the 99th centile, echocardiography is recommended. An echocardiogram, whether in the first trimester or later, must be done by an expert sonographer who has received specific training.

Fig. 2.23. (a) Transvaginal ultrasound in a 13-week + 4-day fetus with omphalocoele (arrow) and megacystis (dotted arrow). (b) Transvaginal ultrasound in a case of large gastroschisis with protrusion of bowel loops (arrow) at 14 weeks' gestational age. (c) Megacystis (arrow) at 14 weeks

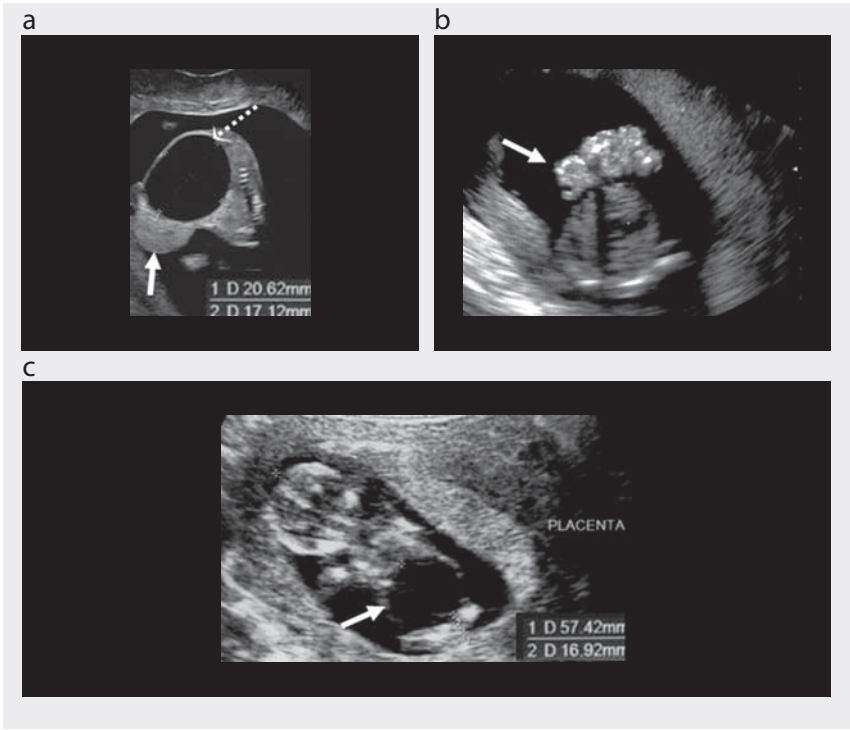

Fig. 2.24. Transabdominal ultrasound of monoamniotic conjoined twins. (a) Two fetuses close within the same sac. (b) Conjunction between the two fetal abdomens (arrow)

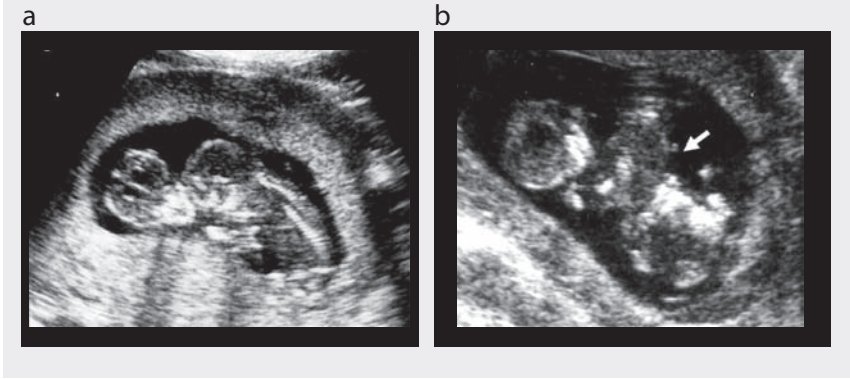

Second trimester

Indications

Sonographic examination in the second trimester of pregnancy should include: evaluation of the situation, presentation and cardiac activity of the fetus; placental localization (Fig. 2.25); assessment of the amniotic fluid; fetal biometrics; and assessment of fetal anatomical structures and movements. Sonography in the second trimester is also recommended in cases of vaginal bleeding, risks for fetal malformations and requests for invasive antenatal diagnosis.

Fig. 2.25. Placental localization. Sagittal scan of the uterus shows the anterior placenta, with its distal margin reaching the internal uterine orifice, and the fetus in a breech position

Estimation of gestational age

Gestational age (dating of pregnancy), unless already estimated in the first trimester, is based on the biparietal diameter and other biometric parameters (femur length, cranial circumference, transverse diameter of cerebellum). All these parameters should be compared to reference curves. If the discrepancy between anamnestic (i.e. menstrual) gestational age and ultrasound-derived gestational age is ≥ 2 weeks, the pregnancy should be re-dated.

Assessment of fetal morphology

Fetal morphology should be studied between 19 and 21 weeks to exclude the most serious malformations. It requires systematic scanning of the head, chest, abdomen and extremities, with assessment of placental and amniotic fluid volume.

Head

This study includes measurement of the biparietal diameter and cranial circumference, the thickness of the atrium (atrial width) of the lateral ventricles and the transverse

diameter of the cerebellum; the morphology of the orbits must also be demonstrated (Fig. 2.26, Fig. 2.27). The fetal brain should be scanned in at least four planes (transthalamic, transventricular, transcerebellar, transorbital), in which the examiner should measure the above-mentioned structures and identify all relevant cerebral structures, such as the falx, the ventricular walls, the cisterna magna, the septum pellucidum, the thalami, the brain peduncles, the cerebellar hemispheres and the vermis.

Transthalamic scanning (Fig. 2.27) is recommended for measuring the biparietal diameter, the frontal-occipital diameter and the cranial circumference (derived from the previous two measurements by means of the ellipsoid formula or traced directly on the ultrasound monitor). The cerebral structures to be assessed in this plane are the cavum septi pellucidi, the third ventricle, the thalami and the Sylvian fissures; when these structures are normal, many conditions can be excluded.

Fig. 2.26. Left, width (caliper 1) of the atrium of the lateral cerebral ventricles (atrial width). Right, transverse diameter of cerebellum (caliper 2) and anteroposterior diameter of the cisterna magna (caliper 3)

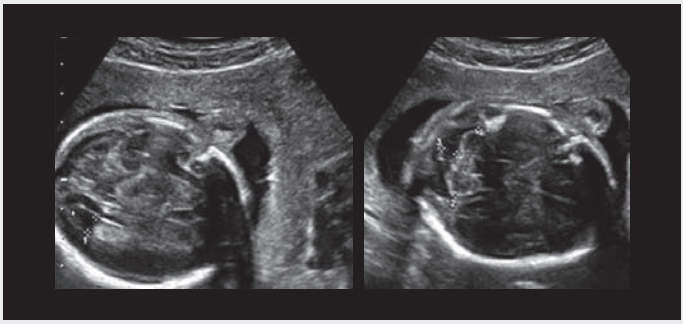

Fig. 2.27. Transthalamic scanning plane: biparietal diameter (caliper 1) and frontal–occipital diameter (caliper 2), from which the cranial circumference can be calculated

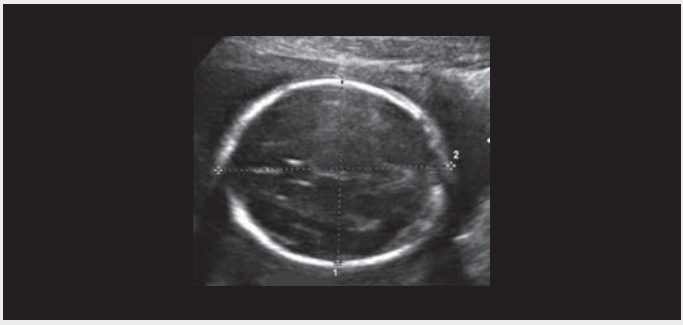

Transventricular scanning is done at a plane slightly higher than the previous one, allowing visualization at the median line of the same structures and the front and rear of the ventricular cavities. The atrial width of the frontal horns must be measured and reported at each examination: its average value is 7.5 ± 0.5 mm and its maximum value is 10 mm. After the 30th week, the cavity of the frontal horns can no longer be seen in the normal fetus.

Transcerebellar scanning (Fig. 2.28) allows a clear view of the cerebellum, the vermis, the cisterna magna (depth range: 4 to 10 mm) and the fourth ventricle.

Transorbital scanning (Fig. 2.29) can show the orbits, which should be symmetrical and of equal size.

Fig. 2.28. Transcerebellar scanning plane: cavum septi pellucidi and cerebellar hemispheres (calipers)

Fig. 2.29. Transorbital scanning plane

Vertebral column

Study of the vertebral column requires a longitudinal scan along the entire column (Fig. 2.30).

Fig. 2.30. Vertebral column. Longitudinal scans of the cervical and upper thoracic spine (a) and lower thoracic and lumbar spine (b)

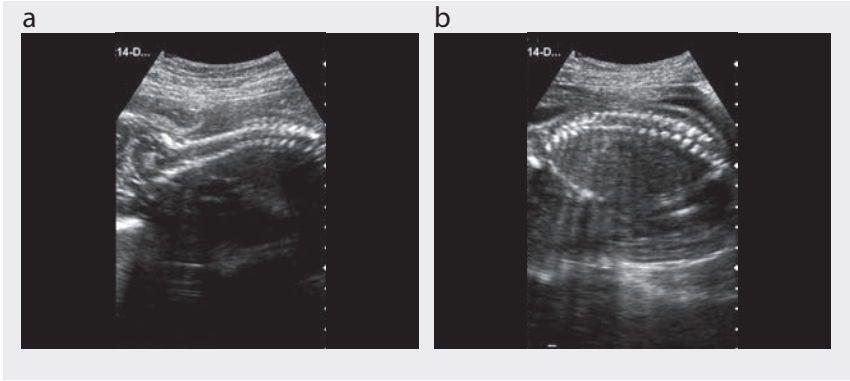

Chest

The examiner must obtain a display of the lungs, cardiac situs, four cardiac chambers (Fig. 2.31, Fig. 2.32) and left and right outflows (Fig. 2.33, Fig. 2.34). A scanning plane that shows the four cardiac chambers is best for assessing the chest anatomy.

Fig. 2.31. Chest. Sagittal (a) and transverse (b) scans of the chest, showing heart, lungs, diaphragm and fluid-filled stomach (a), and heart (view of four chambers), ribs, and spine (b)

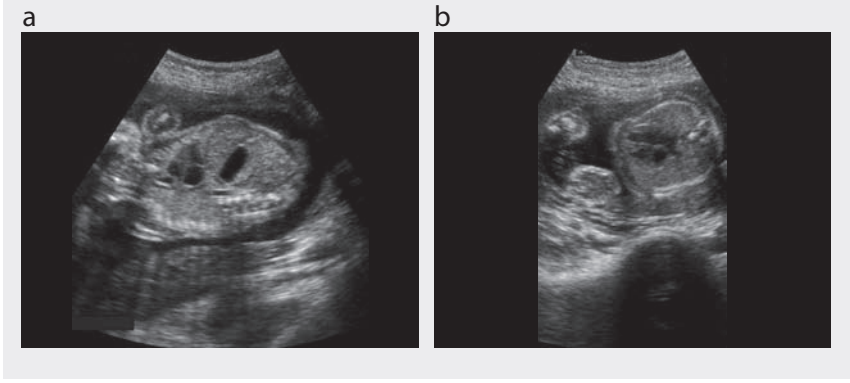

Fig. 2.32. Four cardiac chambers

Fig. 2.33. Right outflow

Fig. 2.34. Left outflow

Abdomen

This study requires measurement of the abdominal circumference and visualization of the stomach, anterior abdominal wall, bladder and kidneys. The best plane for measuring the abdominal circumference is that in which the portal vein is visualized on a tangential section; the plane in which the stomach is visualized is also acceptable (Fig. 2.35). With accurate measurement of the abdominal circumference, the examiner will be able to obtain an accurate estimate of fetal weight, which is essential for assessing intrauterine fetal growth.

The stomach appears as a round, echo-free structure located in the upper part of the left abdomen. The shape and volume of the stomach are highly variable according to the degree of filling and peristalsis. If this organ is not visualized, the examination should be repeated later.

Assessment of urinary morphology requires a systematic sequential study to establish the location, volume and echogenicity of both kidneys; identification of renal vessels may be helpful in the assessment of congenital anomalies of the kidneys (Fig. 2.36 and Fig. 2.37). Ultrasound has an indirect role in the evaluation of renal function, from the measurement of amniotic fluid, the presence of urine in the bladder, the relation between abdominal and renal circumference and the cortical thickness of the kidneys.

Fig. 2.35. Abdominal circumference. Axial scan of the fetal abdomen showing the correct plane for measuring the transverse abdominal diameter and abdominal circumference: the portal vein (on a tangential section) and the fluid-filled stomach are both visualized

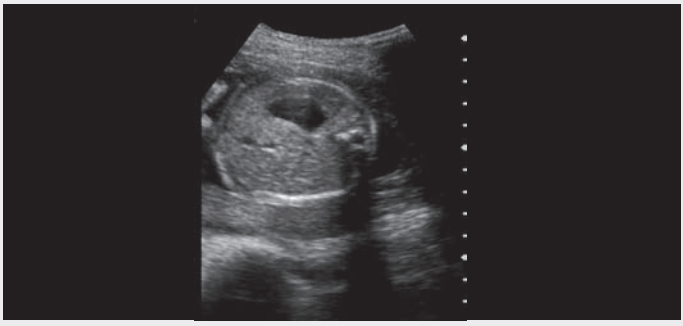

Fig. 2.36. Sagittal scan of the kidney (calipers)

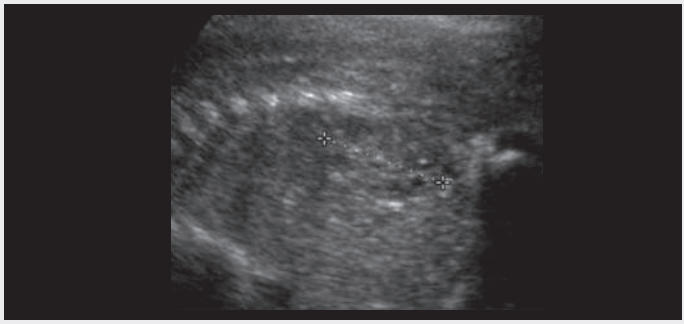

Fig. 2.37. Coronal plane (colour Doppler), with the kidneys, aorta and renal vessels (arrowheads)

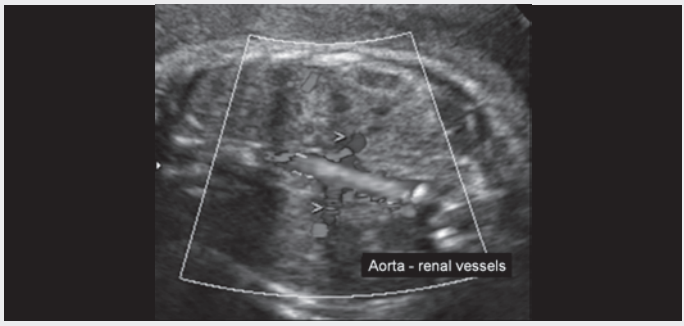

Extremities

The examiner must obtain a display of the long bones of the four limbs and of the distal extremities (hands and feet) to determine their presence. The femur length must be measured (Fig. 2.38), and the length, morphology and echogenicity of the limbs must be assessed (Fig. 2.39).

By convention, measurement of femur length (Fig. 2.38) is considered accurate only when the femoral bone on the image shows two blunted ends. The extension to the greater trochanter and the head of the femur should not be included. The measurement is also considered inaccurate when the femur image is at an angle of over 30° to the horizontal.

Fig. 2.38. Lower limbs: femur length (FL; calipers)

Fig. 2.39. Upper limb: hand, wrist, forearm and elbow

Amniotic fluid volume

Both a subjective evaluation and more objective estimates of the quantity of amniotic fluid can be made. The amniotic fluid index is calculated by measuring the deepest pocket of fluid in each of the four quadrants that ideally divide the uterus and by adding the four values; polydramnios is indicated if the resulting value is > 20 cm, and oligohydramnios is indicated if it is < 5 cm. The size of the greatest vertical pocket of fluid can also be measured. The normal values are 2–8 cm; a pocket measuring < 2 cm indicates oligohydramnios, while one > 8 cm indicates polydramnios (see section below on Amniotic fluid).

Placenta

The examiner should identify the location of the placenta and assess the normality of the umbilical cord and of the placental implant and its relation to the internal uterine orifice (see section below on Placenta). (Fig. 2.25, Fig. 2.40).

Fig. 2.40. Normal umbilical cord and placenta. Sagittal scans in different pregnancies show normal anterior (a)and posterior (b) localization of placenta; normal umbilical cord (arrows), with two arteries and one vein

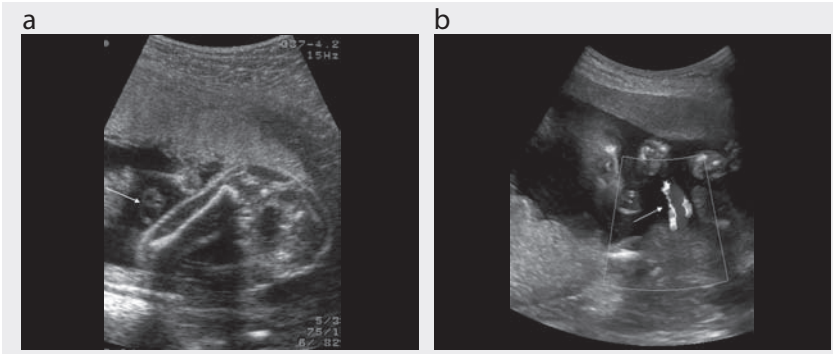

Third trimester

Introduction

Fetal biometry is an important part of routine examinations in the third trimester of pregnancy. Fetal measurements can be combined to estimate fetal weight or can be compared with previous measurements in the same fetus to evaluate growth longitudinally. The growth kinetics of normal fetuses has been studied extensively with ultrasound, to track parameters such as head and abdominal diameter and limb dimensions. The progression in growth of the fetal head and body is variable and the changes in fetal morphological characteristics are dynamic, responding to a complex array of environmental and genetic factors. The growth of these parameters appears to be different in the different periods of normal pregnancy and to vary even more in relation to pathological conditions that can affect fetal growth. Most measurements are plotted on reference charts for gestation to compare the measurements with the normal distribution. Growing interest in adjusting fetal size charts for genetic influence has resulted in publications on race-adjusted or customized fetal size charts.

Biometric parameters

The most important biometric parameters evaluated in the third trimester of pregnancy are head measurements (biparietal diameter and head circumference), abdominal circumference and limb dimensions (femur and humerus length).

Head measurements

The biparietal diameter is measured by positioning the calipers at the outer limits of the proximal and distal borders of the fetal skull (Fig. 2.41). All reports on biparietal diameter have shown it to be an accurate predictor of menstrual age before 20 weeks,

with a variation of ± 1 week (2 standard deviations [SD]). Virtually all studies showed a progressive increase in variation between 20 weeks and term, but the variation increases by ± 2 to ± 3.5 weeks (2 SD) in the late third trimester of pregnancy.

The head circumference (Fig. 2.41) and the abdominal circumference are measured directly with the ellipse facility around the perimeters of the head and abdomen. Head measurements are taken on the classic axial plane of the fetal head, identified from the cerebral peduncles, the thalami and the cavum septum pellucidum, which interrupts the continuous midline echo in its anterior third. Head circumference can be derived from measurements of the occipito-frontal diameter and the biparietal diameter from the formula $\pi (d_1 + d_2)/2$. Several authors have reported that head circumference is one of the most reliable parameters for estimating menstrual age because of its shape independence, its ease of measurement (and therefore accuracy) and its predictive value for gestational age. It can predict menstrual age to within 1 week (2 SD) before 20 weeks' gestation to 3.8 weeks (2 SD) in the late third trimester.

Fig. 2.41. Measurement of biparietal diameter (BPD; calipers) and head circumference (dotted ellipse). GA, gestational age; OFD occipito-frontal diameter; CC head circumference

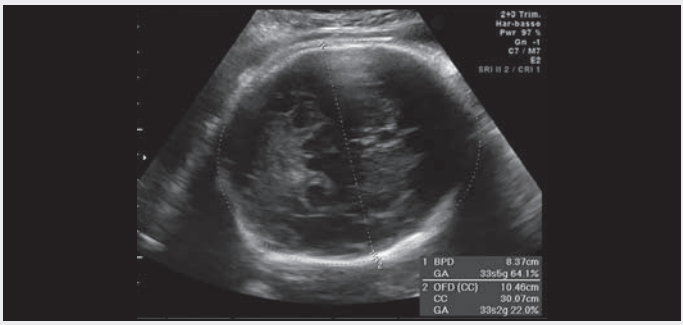

Abdominal measurements

The abdominal circumference is measured in a location that allows an estimate of liver size. The liver is the largest organ in the fetal torso, and its size reflects aberrations of growth, both restriction and macrosomia. The fetal abdominal circumference is measured at the position where the transverse diameter of the liver is greatest, which corresponds sonographically to the plane at which the right and left portal veins are continuous. The abdominal circumference is obtained on a transverse circular section of the fetal abdomen, identified by the stomach and the intrahepatic tract of the umbilical vein, just above the level of the umbilical cord insertion (Fig. 2.42).

Of the basic ultrasound measurements, abdominal circumference is reported to be the most variable, partly because it is more acutely affected by growth disturbances, but this variation is probably due more to measurement error than to biological differences. Furthermore, measurements of abdominal circumference are

the most difficult to obtain. Variability in predicting menstrual age from abdominal circumference increases as pregnancy advances, reaching a peak of approximately 4.5 weeks (2 SD) in the late third trimester of pregnancy.

Fig. 2.42. Measurement of the transverse diameters (calipers) and circumference (dotted circle) of the fetal abdomen. APAD, anteroposterior abdominal diameter; TAD, transverse abdominal diameter; CA, abdominal circumference; GA, gestational age; EFW, estimated fetal weight

Limb measurements

Femur length is measured on a longitudinal scan showing the whole femur diaphysis, imaged on a plane as close as possible at right angles to the sonographic beam. The measurement is taken from one end of the diaphysis to the other (Fig. 2.43). The same technique is used to measure the length of other bones, such as the humerus, tibia, fibula, ulna and radium (Fig. 2.44).

Fig. 2.43. Femur length (FL; calipers). GA, gestational age

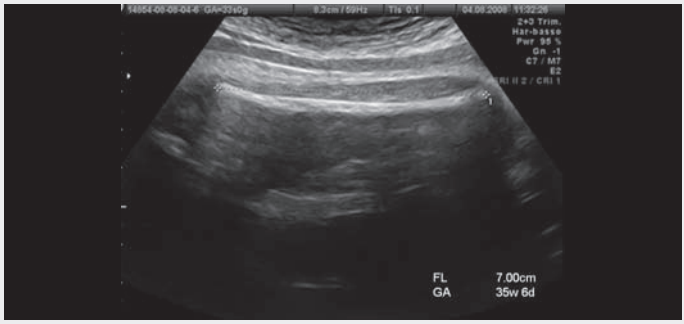

Fig. 2.44. Longitudinal measurement (calipers) of the humerus (left) and femur (right)

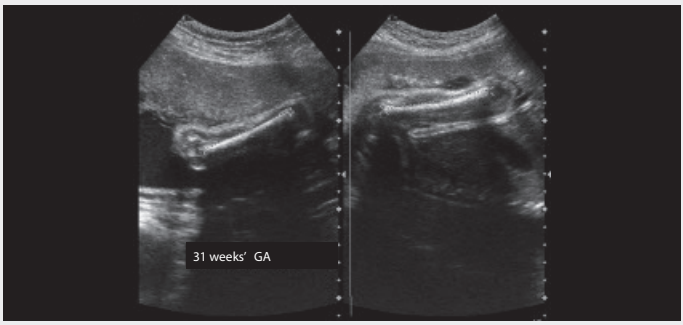

Most studies suggest that the femur length is an accurate predictor of menstrual age in the early second trimester, with a variation of ± 1 week (2 SD). Again, however, variation increases as pregnancy advances, reaching a peak of approximately 3.5 weeks in the late third trimester. It is important to emphasize that the variability of head and femur measurements is small early in gestation.

Biometric charts of size or volume have been obtained for some fetal organs, such as the orbits, cerebellum, liver, kidney and heart, which can be useful for suspected or diagnosed malformations. Kidney volume is reported to be linked with all fetal growth parameters in late pregnancy (Fig. 2.45).

Fig. 2.45. Kidneys. Sagittal (left) and axial (right) scan of the fetal abdomen showing normal kidneys

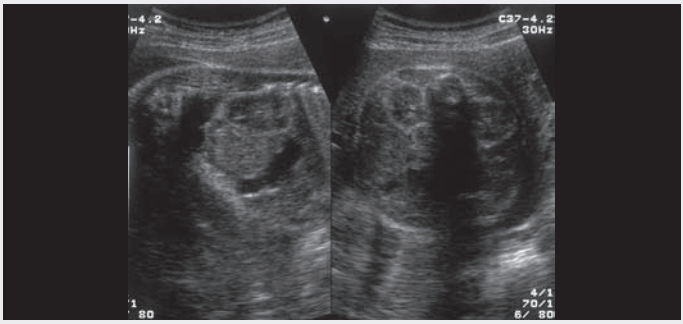

Amniotic fluid

Evaluation of amniotic fluid is now considered an integral, important part of the ultrasound evaluation of gravid women, particularly in situations such as intrauterine growth restriction or post-term pregnancy. Several subjective and objective methods are available. Subjective assessment of amniotic fluid volume involves comparing the echo-free fluid areas surrounding the fetus with the space occupied by the fetus and placenta (Fig. 2.46). The most commonly used objective methods are measurement of the single deepest amniotic fluid pocket free of umbilical cord and fetal parts (maximum vertical pocket), and the amniotic fluid index, which is the sum of the deepest amniotic fluid pockets measured in the four quadrants of the gravid uterus (see section below on Amniotic fluid).

Many studies have shown that the amniotic fluid index is more closely related to the amniotic fluid volume found in dye-dilution studies and, in many cases, is more accurate than measuring a single pocket. Other investigators do not agree. Neither fetal movements nor maternal position seem to adversely affect the assessment of amniotic fluid volume; however, fetal position may influence measurements. Similarly, excessive transducer pressure on the maternal abdomen can affect measurements of the amniotic fluid index. Other potential pitfalls exist. An umbilical cord-filled amniotic fluid pocket should not be used in assessing amniotic fluid volume. Colour Doppler flow imaging is often useful in identifying the umbilical cord. Obese women may appear to have significantly less fluid because of artefactual echoes into the amniotic fluid. This problem can be overcome by using a lower-frequency transducer. Similarly, in the third trimester, free-floating particles, perhaps resulting from vernix, can make the true amniotic space less conspicuous.

Amniotic fluid volume begins to decline near term and may do so precipitously in post-term women. This could be related to placental insufficiency, such as in cases of intrauterine fetal growth restriction, due to redistribution in cardiac blood flow such that renal perfusion is decreased, whereas cerebral blood flow is increased.

Fig. 2.46. Amniotic fluid. Normal amount of amniotic fluid subjectively assessed in comparison with fetus and placenta

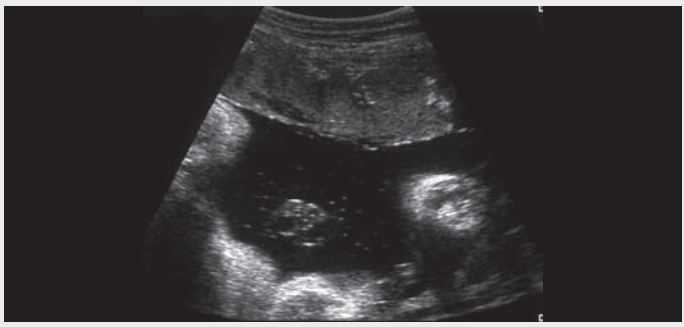

Estimation of fetal weight with ultrasound

Fetal biometrics can be used alone or in combination with mathematical formulas to predict fetal weight. Many formulas, broadly classified as linear or exponential, are used to estimate fetal weight in clinical practice (Table 2.3). In exponential formulas, the logarithm of the weight is expressed as a polynomial function of the ultrasound parameters. Early formulas used to predict birth weight with ultrasound were based on measurements of abdominal circumference alone or abdominal circumference and biparietal diameter. The model that included the two parameters predicted fetal weight to within 10% of the actual weight in 85% of cases; by incorporating another fetal parameter, the random error in estimating fetal weight was reduced by 15–25%. Use of three variables repetitively in the same formula is, however, cumbersome and sometimes requires multiple mathematical manipulations, which could limit its clinical usefulness.

The population-based reference ranges used to assess fetal growth have some limitations. Moreover, most of the formulas are based on a general fetal population, which includes a wide range of birth weights at term or close to term. For these reasons, some authors have suggested that these formulas are not relevant to very preterm fetuses. As preterm labour is often triggered by pathological conditions that affect growth, preterm birth weights are significantly lower than those of fetuses delivered at term. Individualized growth models have therefore been proposed: by defining a growth curve specific to a particular fetus, the obvious limitations of population-based growth charts should be eliminated. In a normal fetus, growth before 28 weeks' gestation predicts its subsequent growth pattern. In this approach, each fetus acts as its own control. The method is limited, however, by its dependence on normal second trimester growth and is useful when a growth abnormality occurs in the third trimester.

Another complex weight prediction formula has been proposed, which includes not ultrasound parameters but length of gestation, the sex of the fetus, the height of the mother, third-trimester maternal weight-gain rate and parity. This equation could be used when a fast, approximate estimation is required. Not all physicians are skilled in ultrasound biometry, and the cost of an ultrasound examination is much greater than the cost of this complex weight prediction method, which can be performed even by women themselves.

Accurate assessment of fetal weight is an integral part of obstetrics practice. It is well known that both low birth weight and excessive fetal weight are associated with increased risks for complications in the newborn during labour and puerperium. The optimal range of birth weights is considered to be 3000–4000 g. Exact estimation of birth weight is important, particularly for fetuses with an inappropriate weight, such as small-for-gestational age or macrosomic fetuses. Most universally applicable formulas were derived in studies in which few small or macrosomic infants were included. In contrast, targeted formulas derived specifically for these infants are generally based on small numbers of cases. Moreover, small-for-gestational age fetuses are frequently delivered extremely prematurely.

Table 2.3. Biparietal diameter (BPD), head circumference (HC), femur length (FL), abdominal circumference (AC), estimated fetal weight (EFW), birth weight (BW), mean abdominal diameter (mAD), calculated as the mean of anteroposterior and transverse abdominal diameters

Reference	Parameter	Regression equation
Warsof, 1977	AC	$\text{Log}_{10}\text{EFW} = -1.8367 + 0.092(\text{AC}) - \frac{0.019(\text{AC} \times \text{AC} \times \text{AC})}{1000}$
Hadlock, 1984	AC	$\log_e\text{EFW} = 2.695 + 0.253(\text{AC}) - 0.00275\ (\text{AC} \times \text{AC})$
Campbell & Wilkin, 1975	AC	$\log\ \text{EFW} = -4.564 + 0.282(\text{AC}) - 0.00331(\text{AC})^2$
Eik-Nes, 1982	BPD/AC	$\log\ \text{BW} = 1.85628(\log\ \text{BPD}) + 1.34008(\log\ \text{mAD}) - 2.8442$
Warsof, 1977	BPD/AC	$\log_{10}\text{EFW} = -1.599 + 0.144(\text{BPD}) + 0.032(\text{AC}) - \frac{0.111(\text{BPD} \times \text{BPD} \times \text{AC})}{1000}$
Shepard, 1982	BPD/AC	$\log_{10}\text{EFW} = -1.7492 + 0.166(\text{BPD}) + 0.046(\text{AC}) - \frac{2.646(\text{AC} \times \text{BPD})}{1000}$
Birnholz, 1986	BPD/AC	$\text{BW} = \frac{3.42928(\text{BPD} \times \text{mAD} \times \text{mAD})}{1000} + 41.218$
Vintzileos, 1987	BPD/AC	$\log_{10}\text{BW} = 1.879 + 0.026(\text{AC}) + 0.084(\text{BPD})$
Hadlock, 1984	AC/FL	$\log_{10}\text{BW} = 1.304 + 0.05281(\text{AC}) + 0.1938(\text{FL}) - 0.004(\text{AC} \times \text{FL})$
Warsof, 1977	AC/FL	$\log_n\text{BW} = 2.792 + 0.108(\text{FL}) + 0.000036(\text{AC}^2) - 0.00027(\text{FL} \times \text{AC})$
Nzeh, 1992	BPD/AC/FL	$\log_{10}\text{BW} = 0.470 + 0.488(\log_{10}\text{BPD}) + 0.554(\log_{10}\text{FL}) + 1.377(\log_{10}\text{AC})$
Hill, 1985	BPD/AC/FL	$\text{BW} = -3153.1 + 13.645(\text{AC} \times \text{BPD}) + 2753.97(\text{FL/BPD})$
Ott, 1986	BPD/AC/FL	$\log\ \text{BW} = 0.04355(\text{HC}) + 0.05394(\text{AC}) - 0.0008582(\text{HC} \times \text{AC}) + 1.2594(\text{FL/AC}) - 2.0661$
Hadlock, 1985	BPD/AC/FL	$\log_{10}\text{EFW} = 1.5662 - 0.0108(\text{HC}) + 0.0468(\text{AC}) + 0.171(\text{FL}) + 0.00034(\text{HC} \times \text{HC}) - 0.003685(\text{AC} \times \text{FL})\ln(\text{BW}) = 0.143(\text{BPD} + \text{mAD} + \text{FL}) + 4.198$
Sabbagha, 1989	BPD/AC/FL	$\text{EFW} = -55.3 - 16.35(\text{GA} + \text{HC} + 2\text{AC} + \text{FL}) + 0.25858((\text{GA} + \text{HC} + 2\text{AC} + \text{FL}) \times (\text{GA} + \text{HC} + 2\text{AC} + \text{FL}))$
Hadlock, 1985	BPD/AC/FL	$\log_{10}\text{BW} = 1.3596 + 0.00386(\text{AC} \times \text{FL}) + 0.0064(\text{HC}) + 0.00061(\text{BPD} \times \text{AC}) + 0.0424(\text{AC}) + 0.174(\text{FL})$
Rose & McCallum, 1987	BPD/AC/FL	$\log_n\text{BW} = 0.143(\text{BPD} + \text{mAD} + \text{FL}) + 4.198$

Fetal macrosomia

Macrosomic fetuses, defined as fetuses with a birth weight over 4000 g, represent about 10% of all newborns, but the percentage has been increasing over the past few decades in western countries because of nutrient supplements and better nutrition. During the past 2–3 decades, an overall 15–25% increase in the proportion of women giving birth to large infants has been found in various populations around the world, with a few exceptions, such as the United States. Fetal macrosomia is frequently associated with neonatal morbidity and traumatic birth, and the complications associated with this condition include increased maternal and fetal trauma, shoulder dystocia with resulting Erb palsy, perinatal asphyxia, meconium aspiration, increased frequency of labour disorders, postpartum atonia and haemorrhage, lacerations of the birth canal and haematomas.

Weight prediction by ultrasound gives adequate results for the general fetal population, but the results are less satisfactory for the macrosomic population. Nevertheless, sonographically estimated fetal weight, obtained with models that include abdominal circumference and femur length, remains a useful method for evaluating women at risk for macrosomia.

Many methods for ultrasound determination of fetal weight have been reported; in most, the predictive accuracy declines as the fetal weight approaches 4000 g. A major problem in the estimation of macrosomic fetal weight with ultrasound is the high degree of inherent error. Moreover, most formulas for estimating fetal weight are derived from cross-sectional data on unselected patient populations, a minority of whom probably have diabetes. The proposed ultrasound methods do not appear to differ substantially in terms of accuracy in predicting macrosomia. The mean absolute percentage error in predicting fetal birth weight was about 7%, but the sensitivity of ultrasound in detecting macrosomia was only 65%.

As clinical and ultrasound methods have similar limited power to predict fetal weight greater than 4000 g, the American College of Obstetricians and Gynecologists cited a third method, namely the mothers' own estimate of fetal size. The probability that this method could predict macrosomia is similar to that of clinical and ultrasound methods.

Because fat is less dense that lean mass and because of the disproportionate increase in the fetal fat component of infants of women with diabetes, the weight of their fetuses, especially those with excessive birth weight, may be systematically overestimated by ultrasound with these formulas. The results of studies addressing this issue are, however, inconsistent. Because of the increased contribution of fat mass to the fetal weight of infants of women with diabetes, formulas based exclusively on soft tissue measurements might be more accurate than those with measures of both fat and lean tissue. Although a good correlation has been found between ultrasound measures of fetal body composition and those taken at birth, the usefulness of the approach of measuring fetal fat for detecting macrosomic newborns was not confirmed, and its clinical use in comparison with other predictors remains to be defined.

Fetal body configuration may be more important than an arbitrarily defined birth weight threshold. Macrosomic fetuses are in fact characterized by larger trunk and chest circumference and an increased bisacromial diameter as fetal weight increases. Macrosomic infants of diabetic mothers are also characterized by larger shoulder and extremity circumferences, a decreased head-to-shoulder ratio, significantly higher percentages of body fat and thicker upper extremity skin folds than controls of similar birth weight and length. Use of other, nonstandard ultrasound measurements, such as humeral soft tissue thickness, ratio of subcutaneous tissue to femur length and cheek-to-cheek diameter, to estimate fetal weight does not, however, significantly improve the predictive value of obstetric ultrasound for birth weight.

In normal pregnancies, fetal abdominal subcutaneous tissue thickness at term is positively associated with birth weight. With increasing thickness, the likelihood of operative vaginal and Caesarean delivery increases; however, this measure is not associated with perinatal outcome.

Advancements in ultrasound technology have not changed this situation. The introduction of three-dimensional ultrasound led some authors to propose new formulas that incorporate volumetric data on fetal limbs. Application of these techniques was generally limited by the excessive time required for measuring volume and by the need for a three-dimensional machine with specific software. Similarly, the clinical usefulness of MRI to estimate fetal weight requires further documentation.

Clinical indications for ultrasound examination: placenta praevia and accreta

In late pregnancy, diagnostic ultrasound is used selectively for specific clinical indications, and the value of routine ultrasound screening during late pregnancy in unselected populations is controversial. The Cochrane Database used existing evidence to conclude that routine ultrasound in late pregnancy in low-risk or unselected populations provided no benefit for the mother or the infant. Information is lacking about the potential psychological effects of routine ultrasound in late pregnancy and the effects on both short- and long-term neonatal and childhood outcomes. Ultrasound examination could be useful in certain situations, such as a suspected anomalous placental location (placenta praevia) or adherence (placenta accreta–percreta).

Placenta praevia

While clinical judgement remains crucial in suspecting and managing placenta praevia, a definitive diagnosis of most low-lying placentas is now achieved with ultrasound imaging. Clinical suspicion should, however, be raised in any case of vaginal bleeding. Transvaginal ultrasound, if available, can be used to investigate placental location at any time in pregnancy and in particular in the third trimester, if the placenta is thought to be low-lying. The transvaginal approach is significantly more accurate than transabdominal ultrasound

and is highly recommended, especially in the case of a posteriorly situated placenta, with the additional benefit of reduced scanning time. Its safety is well established, as confirmed in numerous prospective observational studies in which transvaginal ultrasound scanning was used to diagnose placenta praevia with no haemorrhagic complications.

In 60% of women who undergo transabdominal ultrasound, the placental position may be reclassified when they undergo transvaginal scan. On the basis of the increased prognostic value of a transvaginal ultrasound diagnosis, sonographers are encouraged to report the actual distance between the placental edge and the internal cervical os at transvaginal scan, using the standard terminology of millimetres from the os or millimetres of overlap (a placental edge that reaches exactly the internal os is described as 0 mm).

Placenta accreta

Placenta accreta are abnormal adherences of the placenta to the uterus, with subsequent failure to separate after delivery of the fetus. The most frequent predisposing conditions are previous Caesarean section and placenta praevia. The type of accreta varies according to the depth of invasion: villi penetrate the decidua but not the myometrium (accreta); villi penetrate and invade the myometrium but not the serosa (increta); and villi penetrate the myometrium and may perforate the serosa, sometimes into adjacent organs (percreta).

The diagnosis can be made by ultrasound. The features of placenta accreta include irregularly shaped placental lacunae (vascular spaces) with turbulent internal flow shown by Doppler, thinning of the myometrium overlying the placenta, loss of the retroplacental echo-poor clear zone, absence of a decidual interface with normal placental echogenicity, interruption or increased vascularity of the uterine serosa–posterior bladder wall interface, and apparent bulging or protrusion of the placenta into the bladder (Fig. 2.47).

Fig. 2.47. Placenta accreta: the placenta appears heterogeneous with prominent vascular spaces (Swiss-cheese appearance) and loss of the retroplacental echo-poor zone

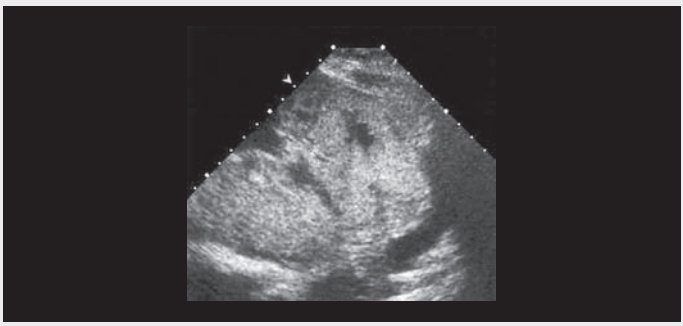

In addition to grey-scale ultrasound findings, targeted Doppler assessment should be performed. Sometimes, MRI may be considered in this evaluation, as it can provide additional diagnostic information in equivocal cases or when the placenta is in a posterior location.

Fetal growth restriction

Fetal growth depends on genetic, placental and maternal factors. Each fetus has an inherent growth potential which, under normal circumstances, yields a healthy newborn of appropriate size. The maternal–placental–fetal unit acts in harmony to provide the needs of the fetus while supporting the physiological changes of the mother. In normal pregnancy, the fetus and the placenta grow at different rates. The placenta expands early and develops into a large tertiary villus structure, with maximum surface area and thus functional activity for exchange peaking at about 37 weeks' gestation; at this time, it weighs about 500 g. From then until delivery, its surface area decreases slightly as microinfarctions occur. The placenta partially regulates fetal growth. The fetus grows throughout pregnancy, but the rate of weight increase per week begins to slow from the 36th week of gestation.

The fetus requires three kinds of substrate for its growth. Glucose freely crosses the placental barrier by facilitated diffusion, while maternal amino acids are actively transported to the fetus, so that their concentration is higher in fetal blood that in the maternal circulation. Oxygen passes to the fetal circulation by simple diffusion. Glucose is burnt with oxygen to produce energy and to convert amino acids into structural proteins: the result is a normally growing fetus. Regulation of the fetal growth rate depends not only on the availability of substrates from placental transfer but also on the activity of fetal hormones, such as insulin and insulin-like growth factors.

Causes of intrauterine growth restriction

The causes of intrauterine growth restriction (Table 2.4) can be grouped into three categories on the basis of substrate availability and consumption:

- **Maternal substrate availability**: Maternal nutrition before and during pregnancy is crucial for normal fetal development. Abnormalities may occur if the mother has chronic disorders that reduce substrate availability, e.g. chronic lung disease for oxygen supply or malabsorption syndromes.
- **Placenta group**: Women may have poor uterine blood flow or a small placental surface-active area. Even cigarette smoking can affect this area, because it both causes endothelial damage and releases vasospastic modulators that reduce uterine and placental blood flow. The commonest clinical symptom of constricted uterine vessels is maternal hypertension, and this is also the commonest maternal factor associated with intrauterine growth restriction.

- **Fetal group**: In some fetuses, substrate consumption is impaired due to a genetic disorder, major congenital anomalies, metabolic disorders or accelerated metabolism and impaired growth caused by congenital intrauterine infection.

Table 2.4. Causes of intrauterine growth restriction

Maternal causes	Fetal causes
Disease	
Poor nutritional status	Genetic disorders
Cardiovascular disease	Malformations
Diabetes	Infections
Placental insufficiency	
Idiopathic	
Pre-eclampsia and other hypertensive disorders of pregnancy	
Abnormal placentation	
Substance abuse (smoking, alcohol, drugs)	Metabolic disorders
Multiple pregnancy	
Cord anomalies	
Autoimmune diseases	

Diagnosis and definition

Intrauterine growth restriction refers to conditions in which a fetus is unable to achieve its inherent growth potential. This functional definition applies to fetuses at risk for various poor outcomes. It intentionally excludes fetuses who are small for gestational age, i.e. at or below the 10th percentile for weight of normal fetuses of the same gestational age, but not pathologically small. A certain number of fetuses at or below the 10th percentile may be constitutionally small. In these cases, maternal or paternal features, the neonate's ability to maintain its own growth rate even if at a low centile, and the absence of other signs of uteroplacental insufficiency (e.g. oligohydramnios, abnormal Doppler findings) can be reassuring. Some fetuses who are pathologically growth-restricted may nevertheless be over the 10th percentile of estimated fetal weight. An estimated fetal weight at or below the 10th percentile is therefore used only to identify fetuses at risk.

The incidence of intrauterine growth restriction in the general obstetric population is estimated to be approximately 5%. Identification of this condition is crucial because proper evaluation and management can result in a favourable outcome. Certain pregnancies are at high risk for growth restriction, although a substantial percentage of cases occur in the general obstetric population. Accurate dating early in pregnancy is essential for a diagnosis; ultrasound biometry on serial longitudinal evaluation is the gold standard for determining fetal size and the amount of amniotic fluid, while Doppler assessment of fetal circulation may be of value in determining fetal status and assessing well-being.

In 1977, Campbell and Thoms introduced the concept of symmetric versus asymmetric growth-restriction. Symmetric growth restriction results in a fetus whose entire body is proportionally small, often due to a condition occurring in the first trimester, such

as a congenital anomaly, a genetic disorder or congenital infection. Asymmetric growth restriction results in a fetus who is undernourished and is directing most of its energy to maintaining the growth of vital organs, such as the brain and heart, at the expense of other structures, such as muscle, fat and the abdomen, especially its storage organ, the liver. This type of growth restriction is usually the result of placental insufficiency.

This differentiation has been questioned, because intrauterine growth restriction due to placental causes that have been present for a long time may present as symmetric growth impairment, as even brain development may be adversely affected. In growth-restricted hypoxic fetuses, redistribution of well-oxygenated blood to vital organs, such as the brain, heart and adrenal glands, is a compensatory mechanism to prevent fetal damage. When the reserve capacity of circulatory redistribution reaches its limit, fetal deterioration may occur rapidly. The most widely used definition of intrauterine growth restriction is now a fetus whose estimated weight is below the 10th percentile for gestational age and whose abdominal circumference is below the second percentile.

Accurate dating in early pregnancy is essential in diagnosing intrauterine growth restriction. The most reliable dating method is an ultrasound examination performed during the first trimester and no later than 20 weeks' gestation. Pregnancy can be re-dated by ultrasound scanning if the difference between menstrual age and ultrasound parameters is 7 days or more in the first trimester or 2 weeks or more in the second trimester. Re-dating during the second trimester should be avoided if an ultrasound scan from the first trimester is available. A woman's due date should never be changed on the basis of a third-trimester sonogram.

Ultrasound biometry

Ultrasound biometry of the fetus from measurements of the biparietal diameter, head circumference, abdominal circumference and femur length is now the gold standard for assessing fetal growth (Fig. 2.48). The percentiles have been established for each of these parameters, and fetal weight can be calculated.

In the presence of normal head and femur measurements, an abdominal circumference measurement less than 2 SD below the mean is considered a reasonable cut-off for considering a fetus to be asymmetric. The most sensitive indicator of symmetric and asymmetric intrauterine growth restriction is the abdominal circumference, which has a sensitivity of over 98% if the measurement is below the 2.5th percentile and has the lowest positive predictive value (36.3%). It may also be useful to calculate the ratio of the head circumference to the abdominal circumference. Between 20 and 36 weeks of gestation, this ratio normally drops almost linearly from 1.2 to 1.0. It is normal in a fetus with symmetric growth restriction and increased in asymmetric growth restriction.

Evidence of a hostile intrauterine environment can be obtained by looking specifically at the amniotic fluid volume. A decreased volume is strongly associated with intrauterine growth restriction. Significant morbidity has been found in pregnancies

with an amniotic fluid index of less than 5 cm, and a decreased index may be an early marker of declining placental function. The combination of oligohydramnios and intrauterine growth restriction portends a less favourable outcome, and early delivery should be considered. Generally, if the pregnancy is at 36 weeks or more, the high risk for intrauterine loss may mandate delivery.

Fig. 2.48. Asymmetric growth restriction. Ultrasound biometry in a 33-week fetus shows severe growth restriction, as demonstrated by the measurements of the biparietal diameter (top left), femur length (top right), and abdominal circumference (bottom left), all below –2 SD, and by the abnormally increased ratio of the head circumference to the abdominal circumference (bottom right; upper, middle, lower lines: 95th, 50th, 5th percentiles)

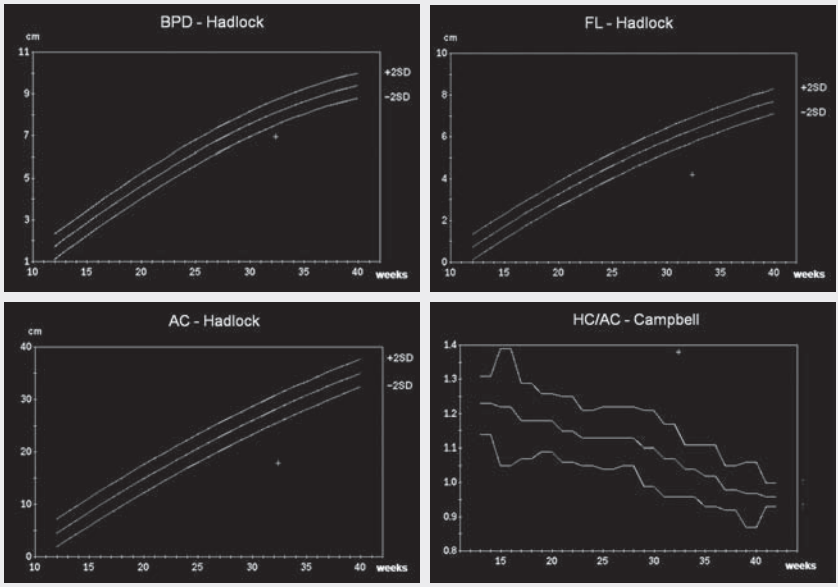

Haemodynamic modifications

During the past few years, technological advances in ultrasound have made it possible to study haemodynamic modifications in both physiological and pathological pregnancies. Both arterial and venous Doppler have been used to identify fetuses with intrauterine growth restriction and also to obtain additional information for planning delivery of fetuses at risk.

Placental insufficiency can be quantified on the basis of a reduction in end-diastolic Doppler flow velocity. Umbilical artery resistance decreases continuously in normal pregnancies but not in fetuses with uteroplacental insufficiency. The commonest measure of gestational age-specific umbilical artery resistance is systolic:diastolic

flow, which increases from baseline with worsening disease. As the insufficiency progresses, end-diastolic velocity is lost and, finally, reversed (Fig. 2.49).

Fig. 2.49. Umbilical artery: normal impedance to flow (a) and absent end-diastolic flow (b)

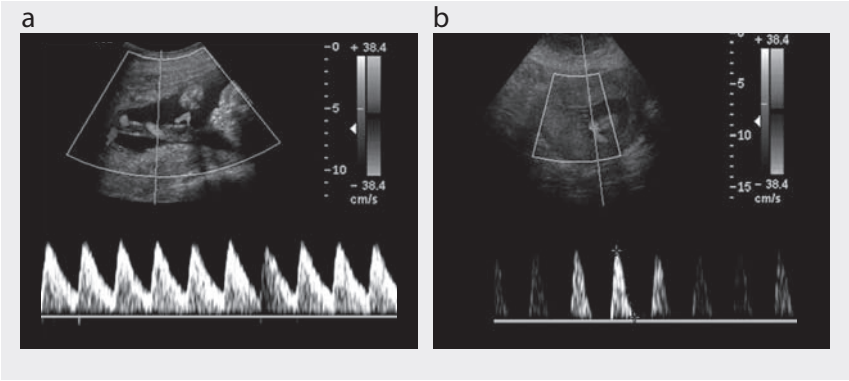

Fetuses with intrauterine growth restriction due to uteroplacental insufficiency are characterized by selective changes in peripheral vascular resistance, the so-called brain-sparing effect (Fig. 2.50), with increased blood supply to the brain, heart and adrenal glands and reduced perfusion of the kidneys, gastrointestinal tract and lower extremities. This mechanism allows preferential delivery of nutrients and oxygen to the vital organs, thereby compensating for diminished placental resources. Compensation through cerebral vasodilatation is, however, limited, and the maximum vascular adaptation to hypoxaemia precedes critical impairment of fetal oxygenation. In a series of intrauterine growth-restricted fetuses, examined longitudinally, a curvilinear relation was described between impedance in cerebral vessels and the state of fetal oxygenation; the progressive fall in impedance reached a nadir 2 weeks before the onset of late fetal heart rate deceleration.

Secondary to the brain-sparing condition, selective modifications occur in cardiac afterload, with a decreased left ventricle afterload due to cerebral vasodilation and an increased right ventricle afterload due to systemic and pulmonary vasoconstriction. In the first stages of the disease, the intrinsic myocardial function takes part in compensation for intrauterine growth restriction after establishment of the brain-sparing effect, as the supply of substrates and oxygen can be maintained at near-normal levels despite an absolute reduction in placental transfer.

The next phase of the disease is abnormal reversal of blood velocity, first in the inferior vena cava and then in the ductus venous, increasing the ratio of peak systolic velocity to end-diastolic velocity, mainly due to a reduction in the atrial component of the velocity waveforms (Fig. 2.51).

Fig. 2.50. Middle cerebral artery. Colour flow imaging (top) and spectral Doppler (bottom) in a normal fetus (bottom left) and in a growth-restricted fetus (bottom right). Normal (bottom left) and low (bottom right, with brain-sparing effect) impedance to flow

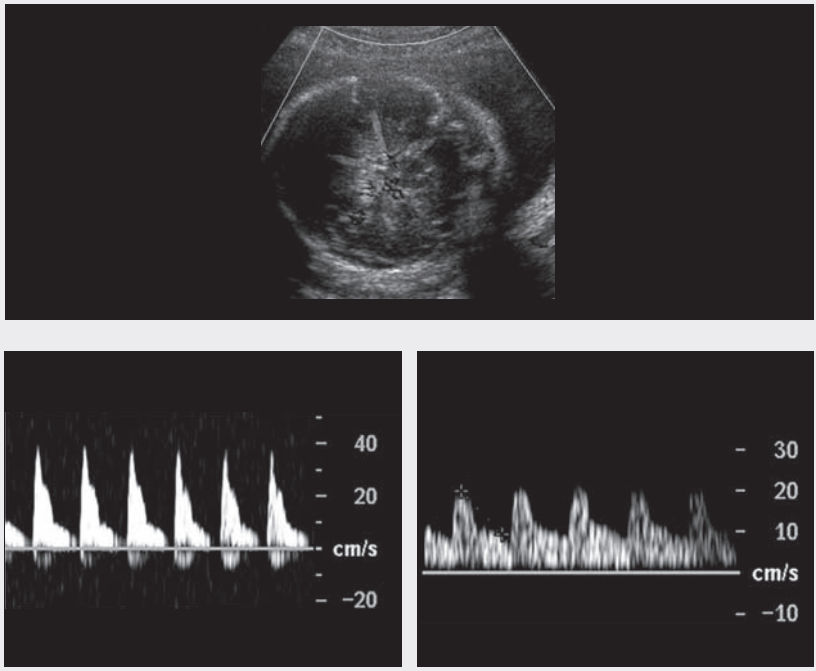

The high venous pressure induces a reduction in velocity at end diastole in the umbilical vein, causing typical end-diastolic pulsations. Development of these pulsations occurs close to the onset of fetal heart rate anomalies and is frequently associated with acidaemia and fetal endocrine changes. At this stage, reduced or reverse end-diastolic velocity may also be present in pulmonary veins, and coronary blood flow can be seen to be faster than in normal third-trimester fetuses. If the fetuses are not delivered, intrauterine death may occur after a median of 3.5 days.

Fig. 2.51. Ductus venous (top). Normal flow waveform (bottom left) and reversal of blood flow during atrial contraction (bottom right)

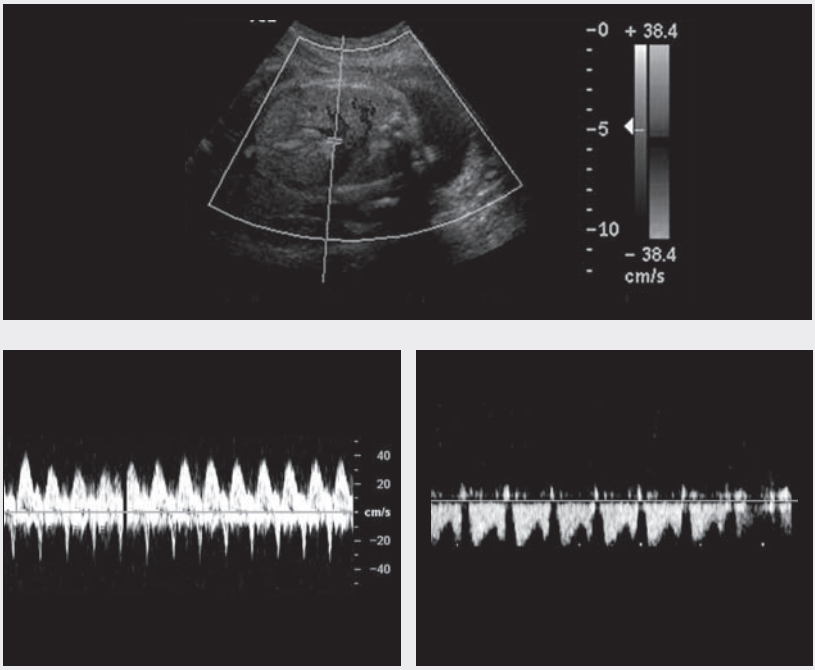

Management and delivery planning

Once a small-for-gestational age fetus is identified, intensive efforts should be made to determine whether there is growth restriction and, if so, its cause and severity, first by excluding structural or chromosomal abnormalities and possibly congenital infections.

Proper clinical management of intrauterine growth restriction requires maternal hospitalization and strict fetal surveillance, including a non-stress test (depending on gestational age) and serial Doppler velocity waveform measurements. For severely growth-retarded fetuses remote from term, the timing of delivery depends on an evaluation of the risk presented by intrauterine stay as compared with that of a very preterm birth. As no effective treatment of intrauterine growth restriction is available, the goal of management is to deliver the most mature fetus in the best physiological condition possible, while minimizing the risk to the mother. This requires antenatal testing to identify intrauterine growth restriction before acidosis.

Numerous protocols have been suggested for antenatal monitoring of such fetuses, including the non-stress test, amniotic fluid volume determination, biophysical profiles, venous and arterial Doppler measurements and fetal heart rate.

Harman and Baschat suggested a strategy for monitoring intrauterine growth restriction, which integrates fetal testing for increasing orders of severity, from 1 to 5.

Step 1

- *Test results*: abdominal circumference less than the fifth percentile, low abdominal circumference growth rate, high ratio of head circumference to abdominal circumference; biophysical profile score ≥ 8 and normal amniotic fluid volume; abnormal umbilical artery or cerebroplacental ratio; normal middle cerebral artery;
- *Interpretation*: intrauterine growth restriction diagnosed, asphyxia extremely rare, increased risk for intrapartum distress;
- *Recommended management*: intervention for obstetric or maternal factors only, weekly biophysical profile score, multivessel Doppler every 2 weeks.

Step 2

- *Test results*: intrauterine growth restriction criteria met, biophysical profile score ≥ 8, normal amniotic fluid volume, umbilical artery with absent or reversed end-diastolic velocities, decreased middle cerebral artery;
- *Interpretation*: intrauterine growth restriction with brain sparing, hypoxaemia possible and asphyxia rare, at risk for intrapartum distress;
- *Recommended management*: intervention for obstetric or maternal factors only; biophysical profile score three times a week; weekly umbilical artery, middle cerebral artery and venous Doppler.

Step 3

- *Test results*: intrauterine growth restriction with low middle cerebral artery pulsatility index; oligohydramnios; biophysical profile score ≥ 6; normal inferior vena cava, ductus venous and umbilical vein flow;
- *Interpretation*: intrauterine growth restriction with significant brain sparing, onset of fetal compromise, hypoxaemia common, acidaemia or asphyxia possible;
- *Recommended management*: if at more than 34 weeks' gestation, deliver (route determined by obstetric factors); if at less than 34 weeks' gestation, administer steroids to achieve lung maturity and repeat all testing after 24 h.

Step 4

- *Test results*: intrauterine growth restriction with brain sparing, oligohydramnios, biophysical profile score ≥ 6, increased inferior vena cava and ductus venous indices, umbilical vein flow normal;
- *Interpretation*: intrauterine growth restriction with brain sparing, proven fetal compromise, hypoxaemia common, acidaemia or asphyxia likely;
- *Recommended management*: if at more than 34 weeks' gestation, deliver (route determined by obstetric factors and oxytocin challenge test results); if at less

than 34 weeks' gestation, individualize treatment with admission, continuous cardiotocography, steroids, maternal oxygen or amnioinfusion, then repeat all testing up to three times a day, depending on status.

Step 5

- *Test results*: intrauterine growth restriction with accelerating compromise, biophysical profile score ≤ 6, abnormal inferior vena cava and ductus venous indices, pulsatile umbilical vein flow;
- *Interpretation*: intrauterine growth restriction with decompensation, cardiovascular instability, hypoxaemia certain, acidaemia or asphyxia common, high perinatal mortality, death imminent;
- *Recommended management*: if fetus is considered viable by size, deliver as soon as possible at tertiary centre (route determined by obstetric factors and oxytocin challenge test results); fetus requires highest level of natal intensive care.

In all cases, a diagnosis of intrauterine growth restriction before 32 weeks' gestation is associated with a poor prognosis. Therapy must be highly individualized. Several studies have shown that the ductus venous pulsatility index and short-term variation in fetal heart rate are important indicators for the optimal timing of delivery before 32 weeks' gestation. Delivery should be considered if one of these parameters is persistently abnormal, and it should be delayed for 48 h to allow maximum fetal benefit of maternal administration of glucocorticoids. Worsening of the mother's condition because of the pregnancy must be considered in deciding on the delivery of a severely growth-retarded fetus.

Perinatal and long-term sequelae

As the likelihood of severe distress in growth-retarded fetuses during labour is considerably increased, they should be monitored closely and Caesarean section should be considered. Moreover, the lack of amniotic fluid predisposes to cord accidents and their consequences. Growth-retarded newborns are also susceptible to hypothermia and other metabolic effects, such as serious hypoglycaemia. Polycythaemia and blood hyperviscosity (due to chronic hypoxia in utero) may occasionally cause cardiac heart failure at birth.

Most infants who have growth restriction in utero have normal rates of growth in infancy and childhood, although at least one third of them may show impaired growth and neurological development of various degrees. Many of these infants are also born prematurely, with additional morbidity. Children with a history of intrauterine growth restriction have been found to have attention and performance deficits. Minimizing hypoxic episodes during labour and delivery and intensive neonatal care at birth are mandatory for the best outcome.

Future directions and prevention

Prevention of intrauterine growth restriction is highly desirable. Investigators have suggested altering the thromboxane:prostacyclin ratio by administering aspirin with or without dipyridamole to mothers of fetuses with intrauterine growth restriction. Despite the theoretical benefit of aspirin, its role in preventing intrauterine growth restriction is still unclear. A large randomized controlled trial with a standardized high-risk population and a standardized treatment regimen could better answer this question.

Placenta, umbilical cord, amniotic fluid

Placenta

Normal findings

The echo pattern of the placenta changes during pregnancy. The intervillous spaces appear as lacunae 10–13 days after ovulation. Until 10–12 weeks, because of the proliferation of villi, the placenta appears as a hyperechoic rim of tissue around the gestational sac. At 12–16 weeks, the chorion normally apposes with the amnion. By 14–15 weeks, the placenta appears as a prominent echo-poor area. At 16–18 weeks, small intraplacental arteries may be visible. In the third trimester, the placenta is a highly vascularized organ.

Sonographic evaluation of the placenta begins with localization, but ultrasound can also be used to assess placental size, thickness and echo texture. The normal at-term placenta measures 15–20 cm in diameter, with a volume of 400–600 ml. The normal placental thickness is approximately 1 mm per week of gestation (at term 45 mm). Common causes of homogeneous thickening are diabetes mellitus, anaemia, hydrops, infection and aneuploidy.

Abnormalities

Placenta bipartita or bilobata: The placenta is separated into lobes, but the division is incomplete and the fetal vessels traverse the membranes, extending from one lobe to the other, before uniting to form the umbilical cord (Fig. 2.52).

Placenta succenturiata: In this condition, one or more small accessory lobes develop in the membranes at a distance from the main placenta and can be recognized on ultrasound as a distinct, apparently separate mass of placental tissue. There is a strong association with placental infarction and velamentous insertion of the umbilical cord.

Placenta circumvallata: The chorionic plate, on the fetal side of the placenta, is smaller than the basal plate, on the maternal side; the fetal surface of the placenta presents a central depression, surrounded by a thickened ring composed of a double fold of amnion and chorion. The fetal surface presents the large vessels that terminate at the margin of the ring.

Placenta circummarginata: The chorionic plate, on the fetal side of the placenta, is smaller than the basal plate, on the maternal side, but the ring does not have

Fig. 2.52. At 27 weeks, a bilobate placenta (large arrowhead shows separation of the two lobes), with the two lobes (small arrowheads) originating from the anterior and posterior wall of the uterus

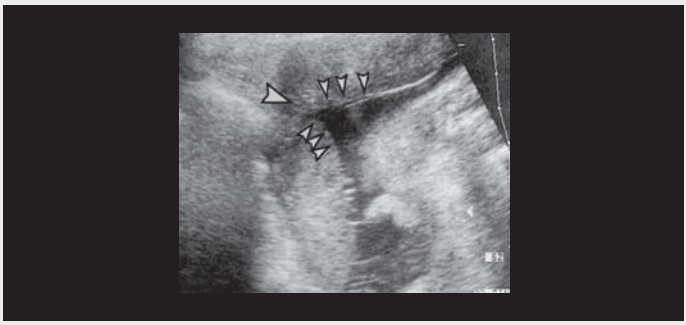

a central depression with the fold of membranes seen in placenta circumvallata, and the fetal membrane insertion is flat.

Placental calcifications

The placenta can mature and calcify. Although there is a system for grading placentas in utero, only premature or accelerated placental calcification has been associated with maternal or fetal disorders, such as hypertension and intrauterine growth restriction.

Focal lesions

Focal lesions, which are often of no clinical significance, can be cystic or echo-poor. They may result from intervillous thrombus, decidual septal cysts or perivillous fibrin deposition and are usually < 3 cm in diameter (Fig. 2.53).

Fig. 2.53. Placental cyst (arrowheads) centrally located and situated below the chorionic plate, at 24 weeks. Colour Doppler velocimetry failed to demonstrate flow within the echo-poor area

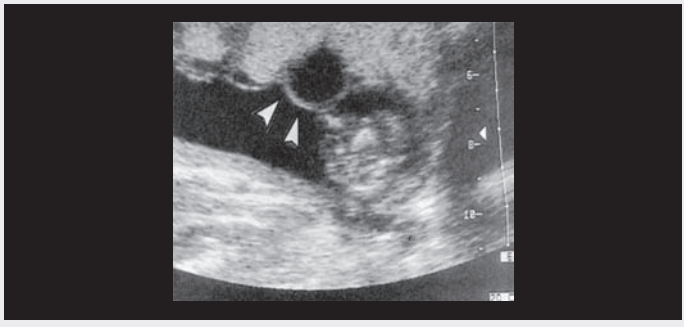

Vascular abnormalities

Placental infarct: A placental infarct is a localized area of ischaemic villous necrosis, more commonly at the periphery of the placenta. In almost 90% of cases, it is located at the placental margin and is < 1 cm. This type of limited infarction results from occlusion of the maternal uteroplacental circulation and usually represents normal ageing. Placental infarcts can be an incidental, normal finding, but placental insufficiency may develop if they are numerous.

Most placental infarcts are not readily detectable by ultrasound because they are isoechoic with adjacent placental tissue; in rare instances, an acute placental infarct may be visible as a slightly echo-rich region. Most infarcts are small and are not clinically significant. When they are thick, centrally located and randomly distributed, they may be associated with pre-eclampsia or lupus anticoagulant.

Maternal floor infarct: This uteroplacental vasculopathy differs from the previously described infarcts in that there are no large areas of villous infarction. Instead, fibrinoid deposition occurs within the decidua basalis, usually confined to the placental floor. These lesions are not detectable by antenatal ultrasound.

Haematomas

The location, cause, sonographic findings and clinical impact of haematomas should be determined. Subchorionic or marginal haematomas are located at the lateral margin of the placenta. Retroplacental haematomas, which can manifest as placental abruption, are of the greatest clinical consequence. When the placenta is imaged, the retroplacental echo-poor complex, composed of uteroplacental vessels (veins) and myometrium, should be observed. When this region appears thicker, the possibility of retroplacental haemorrhage should be considered.

Placental abruption

The clinical condition (abruption) and the pathological condition (haematoma) both involve abnormal accumulation of maternal blood within or above the placenta or membranes. The sonographic appearance of retroplacental haemorrhage depends on age and location of bleeding. Characteristically, haemorrhage may be hyperechoic acutely (0–48 h), isoechoic at 3–7 days and hypoechoic at 1–2 weeks. After 2 weeks, portions of the clot may become echo-free.

Placenta praevia

In placenta praevia, the placenta is located over or very near the internal os (Fig. 2.54). Four degrees of this abnormality have been recognized:

- **Total placenta praevia**: the internal cervical os is completely covered by placenta.
- **Partial placenta praevia**: the internal os is partially covered by placenta.
- **Marginal placenta praevia**: the edge of the placenta is at the margin of the internal os.

Fig. 2.54. Placenta praevia

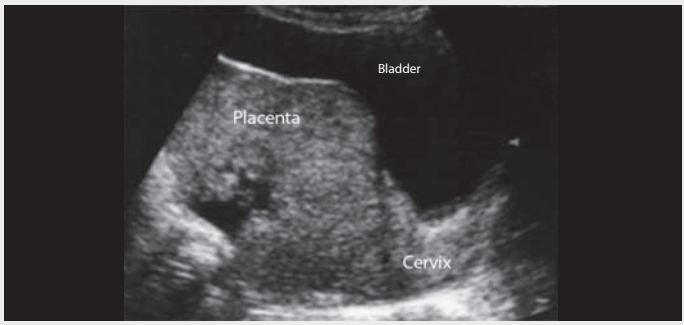

- **Low-lying placenta**: the placenta is implanted in the lower uterine segment such that the placental edge does not reach the internal os but is in close proximity to it.

Sonographic evaluation of the placental location with respect to the internal cervical os is reliable, and a diagnostic accuracy of 90–95% has been reported. Placenta praevia can also be diagnosed transvaginally, particularly for a posteriorly implanted placenta. The positive predictive value is 71% with the transvaginal approach and 31% with the transabdominal approach. The high false-positive rate with transabdominal ultrasound may be due to technical reasons. Excessive distension of the urinary bladder can result in approximation of the anterior and posterior lower segments, creating a false impression of placenta praevia. Therefore, the evaluation should be performed with the bladder partially full and not overdistended. A laterally implanted placenta, in conjunction with normal uterine rotation and a distended bladder can also lead to a false diagnosis. It is important to identify the cervix. Parasagittal evaluation of a laterally located placenta or isolated contractions of the lower segment in conjunction with a distended bladder can lead to a false diagnosis.

Accurate diagnosis of placenta praevia thus requires knowledge of the location of the cervix, the internal cervical os and the placenta. The diagnosis should be confirmed by sonographic examinations with the urinary bladder both filled and partially empty. A careful transvaginal technique can confirm the diagnosis.

Placenta accreta

The term 'placenta accreta' is used to describe any placental implantation in which there is abnormally firm adherence to the uterine wall. Placenta praevia can be associated with placenta accreta or one of its more advanced forms, placenta increta or

Fig. 2.55. Placenta accreta: longitudinal power Doppler sonogram in the 19th week of gestation shows arcuate and radial arteries within the bladder muscle layer. P, placenta; U, urinary bladder

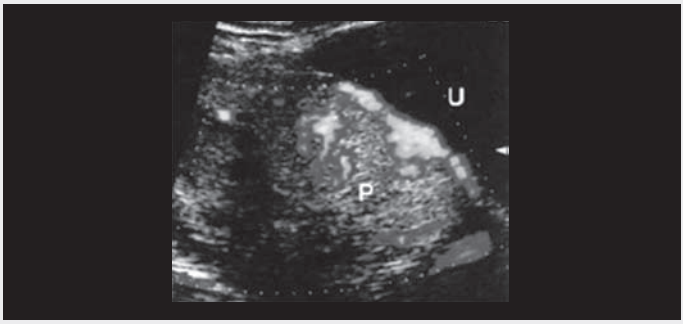

percreta (Fig. 2.55). As a consequence of the partial or total absence of the decidua basalis and imperfect development of the fibrinoid layer, placental villi are attached to the myometrium in placenta accreta and actually invade the myometrium in placenta increta or penetrate through the myometrium in placenta percreta.

Ultrasound is only 33% sensitive for detecting placenta accreta; however, with ultrasound Doppler colour flow mapping, two factors are highly predictive of myometrial invasion: a distance < 1 mm between the uterine serosal bladder interface and the retroplacental vessels and the presence of large intraplacental lakes.

Tumours

Chorioangioma (haemangioma): Chorioangiomas are unique, non-trophoblastic placental tumours, which are present in approximately 1% of all placentas examined. Antenatal diagnosis is possible. Morphologically, they appear most commonly on the fetal surface of the placenta but can occur within the substance. The sonographic features are complex. Colour flow Doppler can reveal highly turbulent flow or low flow. Small chorioangiomas are often benign, whereas large tumours have been associated with polyhydramnios in 15–30% of cases.

Gestational trophoblastic neoplasia: Benign gestational trophoblastic neoplasia is commonly referred to as hydatidiform mole (Fig. 2.56). The clinical course is benign in 80–85% of cases. The sonographic features of hydatidiform mole are distinctive and characteristic at advanced gestational ages. Sonographically, the uterus is usually filled with multiple isoechoic-to-hyperechoic areas which are highly correlated with the presence of vesicles, the size of which depends on gestational age. During the first trimester, the vesicles are not easily delineated and the uterine cavity appears echo-rich, generating the classical snowstorm appearance seen in the old B-mode static scanning. This appearance may not be as evident using current ultrasound technology. The diameter of the vesicles can reach 10 mm during the second

Fig. 2.56. Hydatidiform mole (Doppler signals in white)

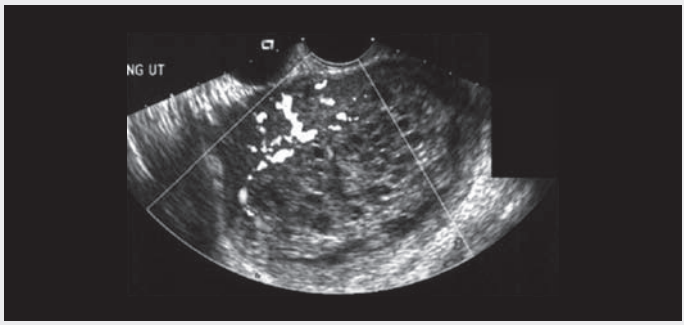

trimester. Areas of haemorrhage can also be seen. Theca lutein cysts of the ovaries can be demonstrated sonographically. Other gynaecological conditions that can be mistaken for a molar pregnancy on ultrasound examination are embryonic demise, anembryonic pregnancy, leiomyoma and retained products of conception associated with an incomplete abortion.

A coexisting fetus, which is often dead, is seen in approximately 2% of cases. It is thought that this association is probably the result of molar transformation of one placenta in a dizygotic twin pregnancy. The hydatidiform mole frequently has a parental 46,XX (dispermy) karyotype, while the coexisting fetus generally has a normal karyotype. Fetal karyotypic analysis of this twin is recommended if the woman wishes to continue the pregnancy. It is important to distinguish between a partial hydatidiform and a molar pregnancy with a coexisting fetus, as a partial mole is considered to have less malignant potential than a complete hydatidiform mole.

The sonographic characteristics of a partial mole include a large, thickened placenta containing cystic spaces and a gestational sac with a fetus. If the fetus is alive, it is often severely growth-restricted. Fetal triploidy is characterized by severe growth restriction, oligohydramnios, hydrocephaly and hydropic placental changes.

Umbilical cord

The umbilical cord is first visualized by ultrasound at 8 weeks, when the length of the cord is approximately equal to the crown–rump length; it usually remains at the same length as the fetus throughout pregnancy. The diameter of the umbilical cord is normally < 2 cm. It usually contains two arteries and one vein; early in development, there are two umbilical veins, but the right vein atrophies and the left vein persists. The presence of two umbilical arteries can be confirmed on a short axis view or by visualizing vessels on each side, lateral to the fetal bladder (Fig. 2.57, Fig. 2.58).

The average length of the umbilical cord is 59 cm (range, 22–130 cm). The two factors that determine its length are sufficient space in the amniotic cavity for

movement and the tensile force applied to the cord during fetal movement. The vessels of the cord are surrounded by Wharton jelly, a gelatinous connective tissue that protects the umbilical vessels from compression.

The commonest abnormality of the umbilical cord is a single umbilical artery, which may occur as aplasia or as the consequence of atrophy of one artery secondary to thrombosis. Normally, the umbilical cord has a central insertion within the placenta. In 7% of pregnancies, there is an insertion of the cord at the margin of the placenta. Insertion of the cord beyond the placental edge into the free membranes is referred to as a velamentous insertion. Focal abnormalities within the umbilical cord may be seen incidentally during routine ultrasound. Single or multiple cysts are occasionally seen, whereas focal masses are rare and include tumours, haematomas, varices and aneurysms.

Fig. 2.57. Two vessels in an umbilical cord (short axis view of the cord)

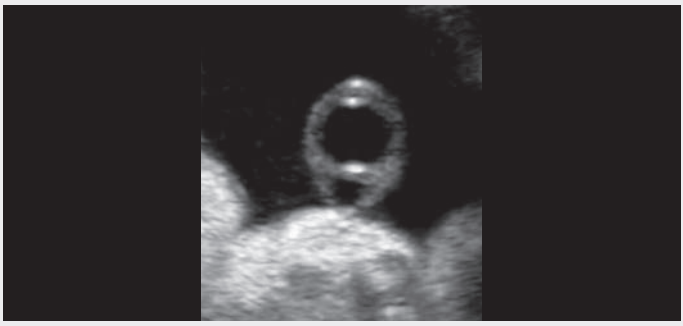

Fig. 2.58. Two vessels in an umbilical cord. Sagittal scan lateral to the fetal bladder (left); long axis view of the cord (right). RT UMB ART, right umbilical artery; BL, urinary bladder; 2VC, two-vessel cord

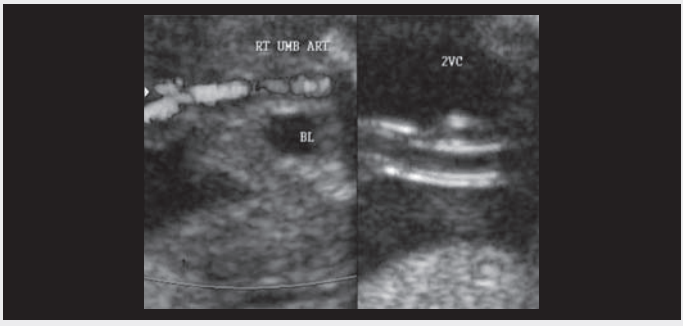

Amniotic fluid

Over the past two decades, estimation of amniotic fluid volume has become part of the standard evaluation in antenatal surveillance and intrapartum management in both normal and high-risk pregnancies. Although progressive improvement of ultrasound techniques and of clinical expertise has led to sophisticated methods for quantifying amniotic fluid volume with highly reproducible accuracy, there is still no unanimous agreement on which method of measuring the fluid is the best prognostic indicator of pregnancy outcome.

Methods for evaluating amniotic fluid

Today, ultrasound visualization of amniotic fluid pockets allows both subjective and objective estimates of amniotic fluid volume, the former being closely dependent on the sonographer's experience and the latter providing more accurate trends in volume over time and comparison with standard values. Semiquantitative methods are described below.

Single deepest pocket technique: The concept of estimating amniotic fluid volume from the depth of the maximum vertical pocket observed with ultrasound was first introduced in 1984 by Chamberlain. This technique consists of measuring the deepest clear amniotic fluid pocket (free from umbilical cord and small fetal parts) in its anteroposterior diameter within the uterus. **Oligohydramnios** is a pocket < 1 cm in depth, while a reduced fluid volume is a pocket measuring 1–2 cm. Measured pockets deeper than 8 cm are classified as **hydramnios**. Although the criteria for normal amniotic fluid volume in the study of Chamberlain were based on a population of high-risk, post-date pregnancies, this technique has the virtues of simplicity, reproducibility and a large body of experience; moreover, it is probably the best method for estimating amniotic fluid volume in the sacs of multifetal pregnancies.

Amniotic fluid index: The amniotic fluid index was used for the first time in 1987 by Phelan. It is obtained by summing the maximum vertical pocket in each of four quadrants of the uterus; the uterine quadrants are defined sagittally by the linea nigra for left and right and by the umbilicus for the upper and lower. When taking the measurements, the ultrasound transducer should be positioned parallel to the woman's sagittal plane and perpendicular to the coronal plane (not angled following the uterine curvature), and the pockets should be clear of umbilical cord and small fetal parts. To allow use of the amniotic fluid index in preterm pregnancies, the upper and lower quadrants are divided at half the fundal height, regardless of umbilical position.

The range and distribution of amniotic fluid indexes were more rigorously defined by Moore and Cayle (1990) in a group of normal pregnancies. These authors found that the mean amniotic fluid index in term pregnancies (40 weeks) was 12 cm, in hydramnios it was 21 cm (95th percentile) and in oligohydramnios it was 7 cm (5th percentile). Huge variations in amniotic fluid index were noted at different gestational ages, the median index varying from approximately 15 cm at mid-trimester to < 11 cm after 42 weeks.

Moore evaluated the interobserver and intraobserver variation in multiple measurements of the amniotic fluid index in the same woman and found an intertest variation of approximately 1 cm, which represents a variation of > 15% at low amniotic fluid indexes (< 7 cm). To obtain optimal accuracy with this technique, taking the average of three measurements at the same ultrasonographic session has been recommended.

Two-diameter pocket: In this method, the depth of the maximum vertical pocket in the uterus is multiplied by its largest horizontal diameter (again, the pocket must be free of cord or fetal extremities). With this technique, the normal amniotic fluid volume is defined as 15–50 cm^2, hydramnios as > 50 cm^2 and oligohydramnios as 0–15 cm^2.

Amniotic fluid volume in multiple pregnancies

Estimating amniotic fluid volume in multiple pregnancies is challenging, as the cavity occupied by each fetus is irregular and the position and limits of the intervening membranes may be difficult to discern. The three methods described above were evaluated and found to be approximately equivalent (80–98% accurate) when the amniotic fluid volume was in the normal range. When the volume measured with the dye infusion technique was < 500 ml (oligohydramnios), however, the accuracy of all three techniques fell to 3–57%. This finding, as for singleton gestations, confirms the difficulty of identifying oligohydramnios with ultrasound in multiple pregnancies.

Because of the convoluted position of the dividing membranes, the rapidly changing fetal position and pressure and volume differences within each sac, the four-quadrant approach (based on several angle-dependent measurements) might be even less accurate for multifetal gestations than for singletons.

Given the simplicity of the maximum vertical pocket and the two-diameter techniques, either will provide the most accurate and reproducible assessment of amniotic fluid volume in multiple pregnancies. Oligohydramnios should be suspected if no pocket at least 3 cm in depth can be measured in an individual sac, and hydramnios should be suspected if a single pocket exceeds 8 cm.

Cervix

The main aim of ultrasonographic evaluation of the cervix is to identify women at risk for preterm labour. It can also be used before medical induction of labour, with a clinical examination, to evaluate the probability of successful induction. A study with transvaginal ultrasound of the relation between placental insertion and uterine internal os is recommended in all cases of placenta praevia or low-lying placenta suspected on transabdominal ultrasound. For a differential diagnosis of complete placenta praevia, incomplete placenta praevia and low-lying placenta, transvaginal ultrasound of the uterine neck and its relation to the lower placental edge is advised between 32 and 37 weeks' gestational age in all cases suspected earlier (Fig. 2.59). If

Fig. 2.59. Transvaginal ultrasound in cases of placenta praevia. (a) 32 weeks: the inferior placental edge (dotted arrow) does not cover the internal uterine os (arrow). (b) 28 weeks: the placenta praevia covers the internal os (arrow); IUO, internal uterine os

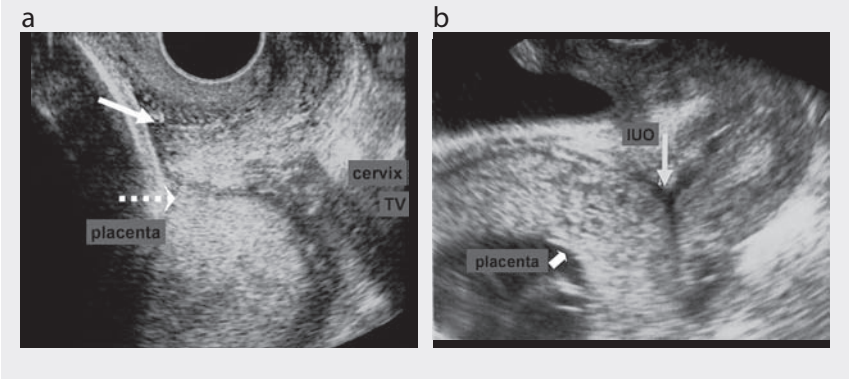

bleeding occurs, transvaginal ultrasound can be used at any time during gestation, but the diagnosis must be confirmed after 32 weeks.

Indication

Evaluation of the uterine cervix is indicated for women at risk for a preterm birth based on a previous history, women with symptoms of preterm labour and follow-up of women after cervical cerclage positioning. Evaluation is not indicated for low-risk populations, i.e. in screening to predict preterm labour. The value of ultrasound cervical examination in predicting the success of labour induction and mode of delivery is still being investigated.

Preparation

For transabdominal ultrasound, the woman should have a full bladder. To fill her bladder, the woman should drink 1 l (four glasses) of water 0.5–1 h before the procedure. If she cannot drink, the bladder can be filled with a saline solution through a Foley catheter. For transvaginal or transperineal ultrasound, the woman should void her bladder immediately before the procedure.

Examination techniques

For transabdominal, transperineal (translabial), or transvaginal ultrasound, the woman should lie on the examination bed on her back, with extended or flexed legs.

For **transabdominal ultrasound**, ultrasonographic gel is applied to the woman's skin, and the ultrasonographic probe is used to examine the pelvis and the lower part of the abdomen through horizontal (transverse), vertical (sagittal) and oblique

scanning planes. Unfortunately, this technique is not sufficiently reliable or valid, because bladder filling often elongates the cervix and masks the funnelling of the internal os; fetal parts can obscure the cervix, especially after 20 weeks; and the distance between the probe and the cervix degrades the image quality.

For **transperineal** (translabial) **ultrasound**, a gloved transducer in a sagittal orientation is positioned on the perineum, at the vaginal introitus between the labia majora, oriented in the direction of the vagina to visualize the uterine neck. This technique is well accepted by most women, as the transducer does not enter the vagina, avoiding pressure on the cervix; however, the technique is more difficult than transvaginal ultrasound, and gas in the rectum can impede satisfactory visualization of the uterine neck.

For **transvaginal ultrasound** (Fig. 2.60), a clean transvaginal probe, placed in an aseptic probe cover (condom) filled with ultrasonographic gel, is inserted into the anterior fornix of the vagina. The probe is close to the cervix, without the problem of obscuring bowel gas. This technique has become the preferred method of evaluating the cervix in all clinical settings. Recommendations for transvaginal ultrasound examination of the cervix are to:

- obtain a sagittal long-axis view of the endocervical canal, along its entire length;
- withdraw the probe until the image is blurred and apply just enough pressure to restore the image, avoiding excess pressure, which can elongate the cervix;
- enlarge the image so that the cervix occupies two thirds of the picture, with both the external and the internal os clearly visible;

Fig. 2.60. Transvaginal ultrasound of normal cervical length. (a) Uterine neck at 24 weeks: normal cervical length after cervical cerclage (arrowheads), internal os (arrow), external os (dotted arrow). (b) Normal cervix at 25 weeks: closed and curved endocervical canal from internal (arrow) to external os (dotted arrow); IUO, internal uterine os

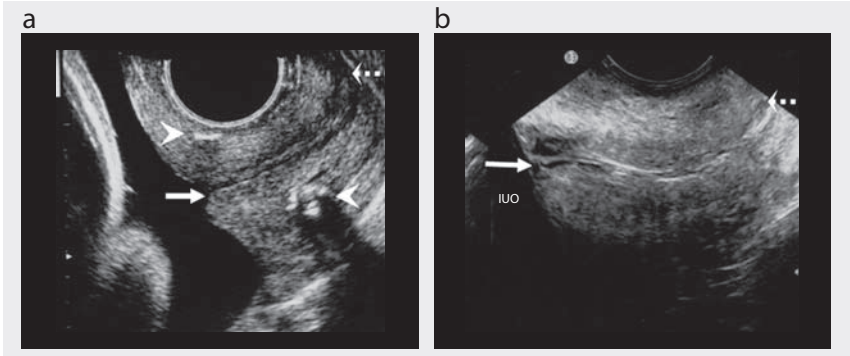

- measure the cervical length from the internal to the external os along the endocervical canal (take at least three measurements and record the shortest, best measurement in millimetres);
- apply transfundal pressure for 15 s and record the cervical length again;
- describe the presence of funnelling (opening) of the internal os and cervix and measure its length and width.

Normal findings

Transvaginal sonography has been shown to be superior to manual examination for evaluating the cervix. Various cervical parameters have been evaluated, but cervical length, measured from the internal os to the external os along the endocervical canal, is the most reproducible and reliable measurement. If the cervical canal is curved, the cervical length can be measured on a straight line between the internal and external os or as the sum of two straight lines that follow the curve.

The normal cervical length is 25–50 mm at 14–30 weeks' gestational age in singleton pregnancies. A cervical length > 25–30 mm is a reassuring finding. After 30 weeks, the cervix progressively shortens in preparation for term labour, so that a length of 15–24 mm can be physiological in asymptomatic women. In normal pregnancies, the internal os is flat, the cervical canal and the internal os are closed, and the length of the cervix is the only measurement to be made (Fig. 2.60). The length may change dynamically during a 5- to 10-min examination, and in some cases funnelling of the upper cervical canal may appear and resolve. This occurs in women having contractions, and, similarly, the cervix may shorten in response to transfundal pressure in an otherwise normal cervix.

In multiple pregnancies, cervical length measured at 14–19 weeks is similar to that in singleton pregnancies, but in multiple pregnancies the cervix is progressively much shorter, starting from 20 weeks' gestational age.

Pathological findings

Risk of preterm birth and patient with preterm birth

The changes in the cervix that lead to preterm or term labour, seen by transvaginal ultrasound, include: initial opening of the internal os of the cervix; progressive cervical shortening and widening along the endocervical canal (from the internal to the external os); and opening of the external os. A short cervical length (< 25 mm) is the best predictor of preterm birth at 16–24 weeks: the shorter the cervical length, the higher the risk for preterm birth. In high-risk women, preterm birth after the detection of a short cervix (< 10 mm) is often preceded by premature rupture of the membranes. When funnelling occurs, the internal os and the open part of the cervical canal have a triangular shape, and the total cervical length is the sum of the funnel (open portion of the cervix) length and the functional cervical length (closed portion of the endocervical canal). It is also possible to measure the internal os diameter (funnel width) (Fig. 2.61).

Fig. 2.61. Different degrees of cervical shortening and funnelling. (a) 31 weeks: cervical length, 36 mm, funnelling of the internal os, 4.5 mm (calipers). (b) 19 weeks: cervical length, 33 mm (calipers), evident funnelling. (c) 22 weeks: cervical length, 36 mm, funnel width, 11.3 mm (calipers). (d) 27 weeks: cervical length, 15 mm (calipers), broad funnelling

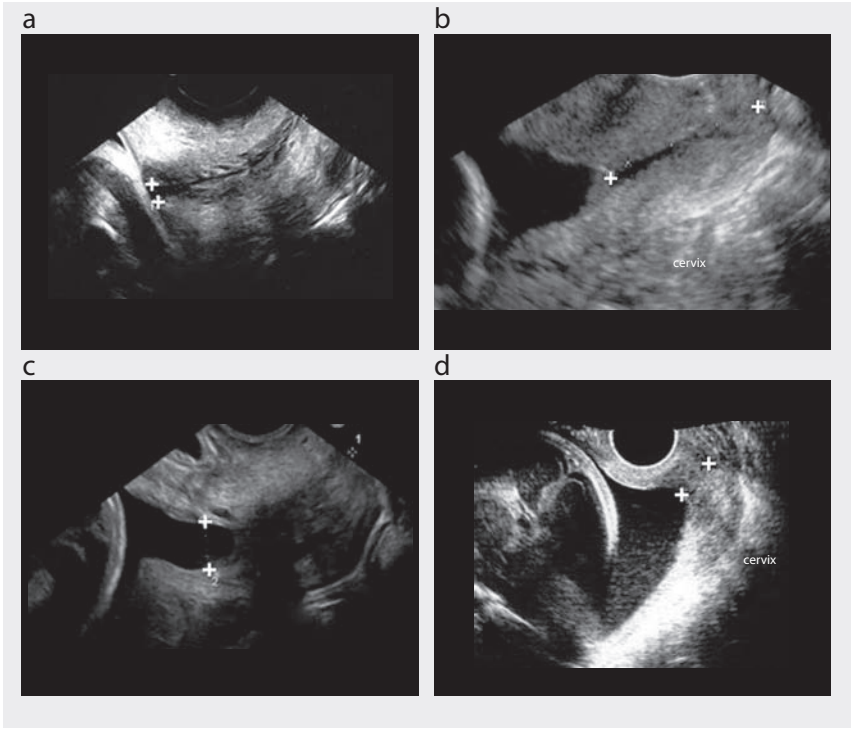

After measurement of a cervix < 25 mm before 24 weeks by transvaginal ultrasound, cervical cerclage is suggested in women with a singleton pregnancy and a previous preterm birth. The sensitivity of such measurements for predicting preterm birth in high-risk singleton pregnancies is often > 60%. Unfortunately, the sensitivity for predicting preterm births in low-risk women is low for singleton pregnancies (< 40%), twin pregnancies (30%) and triplet pregnancies (10%). Given these findings, routine screening for cervical length with transvaginal ultrasound is not recommended for all pregnant women.

Follow-up after cervical cerclage

Transvaginal sonography of the cervix has been evaluated in women with cerclage in place (indicated by history, physical examination or ultrasound). Evaluations of pre- and post-cerclage cervical length have shown that it usually increases after cerclage and that the increase is associated with a higher rate of term delivery. In women with cerclage, the best indicators for preterm birth are a cervical length < 25 mm and an upper cervix length (the closed cervical portion above the cerclage) < 10 mm.

Fig. 2.62. Ultrasound follow-up after cervical cerclage. (a) Transabdominal ultrasound, cerclage in place, 17 weeks; the two arrows show anterior and posterior views of the neck suture. (b) Transabdominal ultrasound, cerclage displacement, 24 weeks; left, longitudinal scan; right, transverse scan; the arrows show the suture displaced anteriorly with the protruding inferior pole of the membranes. (c) Transvaginal ultrasound, cerclage in place, 31 weeks; the arrows show the normal suture position

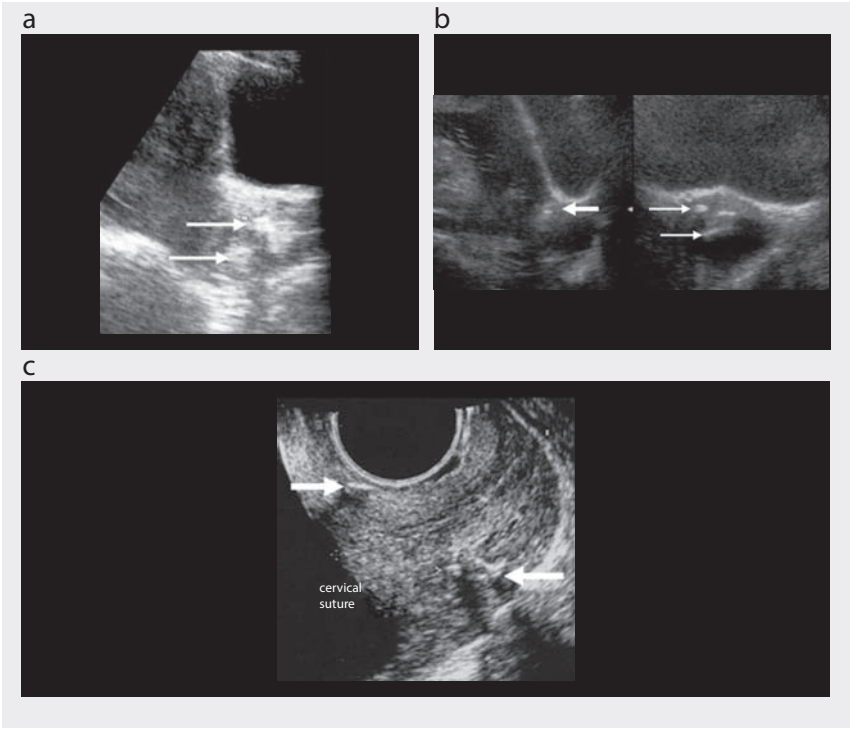

Transabdominal or transvaginal ultrasound or physical (manual, digital) examination can be used to detect cerclage displacement (Fig. 2.62).

Predicting the success of labour induction and mode of delivery

Some studies show that cervical length measured by transvaginal ultrasound at 37 weeks correlates with the mean gestational age at delivery: 38 weeks for women with a cervical length of 10 mm at 37 weeks, 41 weeks for women with a cervical length of 35 mm and > 41 weeks if the cervical length is > 40 mm. A short cervical length is associated with a short duration of labour and a higher incidence of vaginal delivery compared with a cervix measuring > 26–30 mm at the onset of labour. Caesarean delivery was recorded for only 4% of women in spontaneous labour with a cervical length < 20 mm but for 12% of women with a cervical length > 40 mm. The Bishop score parameter was less sensitive than transvaginal ultrasound for evaluating the need for intracervical prostaglandin treatment before oxytocin labour induction.

Multiple pregnancies

The incidence of multiple pregnancies is 3%. Over the past 20 years, the number of twin births has increased by 50% and the number of multiple deliveries by 400%, primarily because of the availability and increased use of ovulation-inducing drugs and assisted reproductive techniques. The increase is also related to advanced maternal age, with the rate of dizygotic twinning peaking between 35 and 40 years of age, mainly in multiparous women. Heredity and a maternal history of twinning (either dizygotic or monozygotic) are particularly important for twinning, while the father's history plays little or no part. Race is also a factor: the percentage of dizygotic twins is 1% in whites, lower in blacks and higher in Asians.

There are two kinds of twins. Dizygotic twins are the result of simultaneous fertilization of two different oocytes by two different spermatozoa. Monozygotic or identical twins result from duplication of a single conceptional product. As dizygotic twins originate from multiple ovulations, they reflect the incidence of genetic and ethnic factors, whereas monozygotic twins result from duplication of a single zygote, with a constant frequency in all ethnic groups. Dizygotic twins have two different placentas and amniotic membranes in two amniochorionic membranes (dichorionic twins). They are the same sex in 50% of cases. In monozygotic twins, who are always the same sex, placentation depends on the time of embryo duplication:

- within 3–4 days after conception: dichorionic diamniotic;
- between 3 and 9 days after conception: monochorionic diamniotic;
- between 9 and 12 days after conception: monochorionic monoamniotic;
- at ≥ 12 days after conception: Siamese or joined.

The placenta can be mono- or dichorionic. Fetal risks increase in relation to monochorionicity and monoamnionicity. Fetal mortality is three times greater among twins than among singletons. The fetal risk for cerebral palsy is eight times greater than in singletons and 47 times greater in triplets. Maternal risks, such as hypertension, postpartum haemorrhage and mortality, are twice as high as in a single pregnancy.

The purposes of management are to:

- prevent preterm birth;
- identify growth alterations in one or both twins;
- recognize correlated pathological conditions and, if necessary, treat them;
- determine the timing and type of delivery.

Indications

Early diagnosis of multiple pregnancy is possible from the 5th to 6th week by ultrasound scan. The final diagnosis, however, relies on embryo individuation, which is possible from week 6–7.

An ultrasound scan should be performed in the first trimester to:

- visualize ovular implants (or gestational sacs) in the uterus and their number;
- verify the presence of embryos or fetuses, their number and their cardiac activity;
- date the pregnancy.

In the case of multiple pregnancies, chorionicity and amniocity should be evaluated.

Preparation

Pregnancy can be evaluated with transabdominal or transvaginal probes. The main advantage of transvaginal scan is the significant improvement in image resolution. For transabdominal scanning, a probe of at least 3.5 MHz should be used to scan through the abdominal wall, with a full bladder, at an early gestational age. For the transvaginal scan, with an empty bladder, a high-frequency probe (at least 5 MHz) can be used because of the shorter distance between the transducer and the organ target, with a large increase in resolution. The two methods are, however, complementary. Transvaginal scan is preferred at early gestational ages (first trimester).

Normal findings

A twin pregnancy can be diagnosed from week 5 with a transabdominal or transvaginal probe to evaluate the number of intrauterine gestational sacs.

The main aims of ultrasound scanning in the first trimester are:

- pregnancy dating
- evaluation of the number of embryos or fetuses
- evaluation of fetal heartbeat
- diagnosis of amnionicity and chorionicity
- exclusion of early morphological anomalies
- cervix evaluation.

In the second trimester, ultrasound is used for morphostructural examinations, fetal growth evaluation and cervix evaluation; and in the third trimester, ultrasound is used for fetal growth evaluation and assessment of fetal well-being (Doppler).

In multiple pregnancies, the determination of chorionicity, as a distinction between monochorionicity and dichorionicity, will differentiate between monozygotic and dizygotic twins.

The accuracy of ultrasound scanning for diagnosing chorionicity is nearly 100% in the first trimester (14 weeks), but ultrasonographic determination is not always possible at an advanced gestational age, especially for a differential diagnosis of a

single or seemingly single placenta. This may require identification of typical signs, such as the lambda sign, or the interamniotic septum thickness.

Lambda sign: The chorial septum that separates the dichorionic gestational sacs in the first trimester becomes thinner during pregnancy but remains thicker in the portion next to the placenta. It can be seen as a triangular projection of chorial tissue at the base of the septum that separates the amniotic membranes of the twins. This feature, known as the lambda or twin peak sign, indicates a dichorionic pregnancy, with 94% sensitivity, 88% specificity, 97% positive predictive value and 78% negative predictive value. This part of the chorial tissue can, however, grow thin and become invisible in the second half of pregnancy.

Thickness of the interamniotic septum: This septum is thicker in cases of dichorionicity. Although there is no consensus on a cut-off, a 2-mm interamniotic septum indicates a dichorionic pregnancy. As septum thickness decreases in all pregnancies during the second trimester, the evaluation is subjective and the measurement is not reproducible.

In advanced pregnancies, a membrane between the two amniotic sacs is not always visible. When the insertion of the membranes on the uterine wall cannot be seen, the lambda sign is the index of a dichorionic twin pregnancy. While a diagnosis of chorionicity can be made reliably at the beginning of the second trimester with the lambda sign, its absence after the 20th week cannot exclude dichorionicity.

The type of twin pregnancy is determined in the first trimester as follows:

- **dichorionic, diamniotic**: Two chorions visible as two separate hyperechoic rings; the septum is thicker, with more intense echogenicity; four membranes (two chorions and two amnions) can be seen (Fig. 2.63);
- **monochorionic, diamniotic**: Only one hyperechoic chorionic ring, with two separate yolk sacs and two embryos separated by amniotic membranes; the septum is < 2 mm (Fig. 2.64, Fig. 2.65). In the early phases of gestation, only the two vitelline sacs are observed, before the embryos become visible;
- **monochorionic, monoamniotic**: Only one hyperechoic chorial sac, with two separate embryos; no membrane of separation between the twins is seen; the fetuses are free to move inside the uterine hollow; the amniotic fluid appears evenly distributed (Fig. 2.66, Fig. 2.67).

In the first trimester, a dichorionic pregnancy appears on an ultrasound scan as two separate hyperechoic rings in the endometrium. To confirm this diagnosis, a yolk sac and a fetus must be demonstrated in each chorionic sac.

Monozygotic pregnancies are identical to dizygotic ones. A monochorial diamniotic pregnancy appears on ultrasound as a single chorionic hollow containing two yolk sacs and subsequently two embryos, each with its own cardiac activity. Because of the unfavourable prognosis and greater incidence of malformations and complications in monoamniotic twins, the amnion must be identified. Identification of the amnion between the two fetuses has 100% predictive value for a diamniotic twin pregnancy.

Fig. 2.63. Dichorionic biamniotic twins: interamniotic septum (arrow)

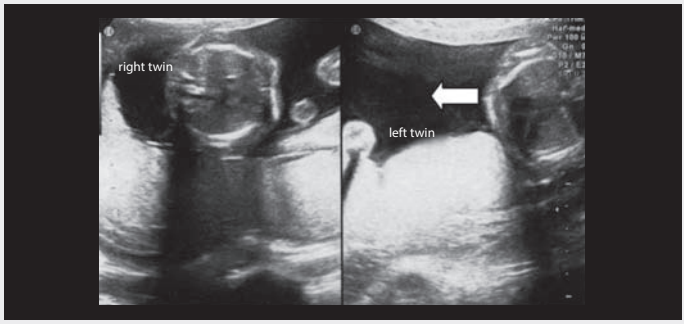

Fig. 2.64. Monochorionic biamniotic twins: ultrasound evaluation of cord insertions (arrows)

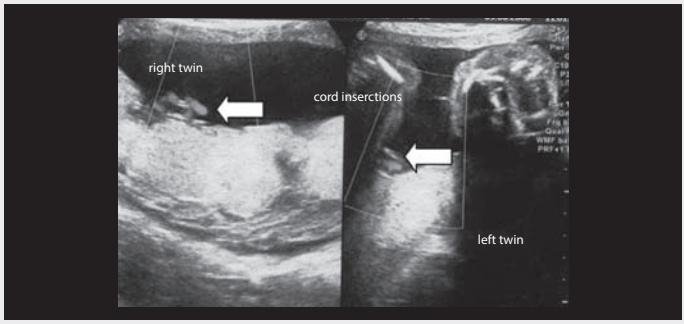

Fig. 2.65. Monochorionic biamniotic twins: ultrasound evaluation of twin sex (males)

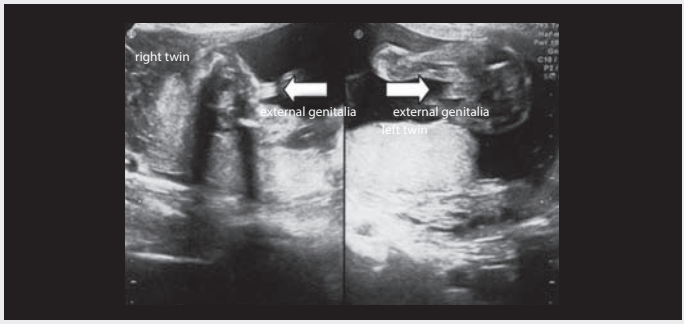

Fig. 2.66. Monoamniotic twins

Fig. 2.67. Monoamniotic twins: measurement of BPD of each twin (calipers 1; calipers 2)"

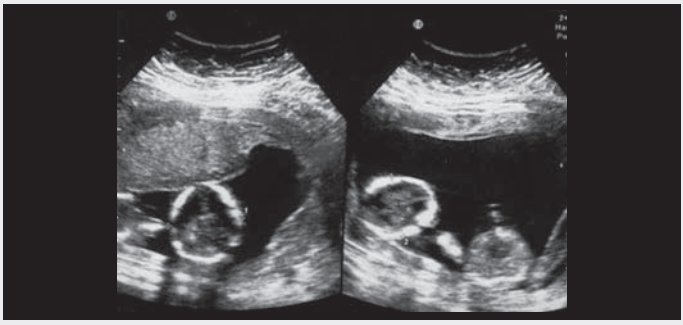

Mono- and dichorionic twins cannot be differentiated on the basis of identification of a membrane separating two fetuses after fusion of the amnion and the chorion from the 16th week. In monochorionic twins with a double amniotic sac, this membrane is composed of two layers, while in dichorionic twins it is formed from four layers: two chorions and two amnions. In both cases, the membranes can appear as a single echo-rich layer.

Biovular (dizygotic) twins have two different placentas, which, in cases of near ovular implant, can subsequently fuse. The chorion and amnion are always double. Monovular twins (monozygotic) generally have only one placenta, with a chorion containing one or two amniotic sacs. They can, however, have a fused placenta or two separate placentas, each with a chorion containing an amniotic sac. Therefore, it is not possible to establish whether one placenta indicates a mono- or a dichorionic pregnancy, unless the twins are of different sexes. When two placentas are observed,

the chorion–amniotic membrane extends sideways from the border of a placenta to the contralateral border. In the case of a single placenta, the chorion–amniotic membrane originates from the central portion of the placental implant. This typical aspect is useful for distinguishing it from the other membranes of the pregnancy, such as synechiae, the uterine septum and amniotic bands.

In early pregnancy, an intrauterine transonic area does not always indicate a gestational sac, unless an embryonic pole is seen, preferably with detectable cardiac activity. Similarly, not all hypoechoic areas near a gestational sac necessarily correspond to a second sac; they might, in fact, be due to a haematoma. If during the first trimester two amniotic sacs of different sizes are observed, it is reasonable to predict that the smaller sac is not viable and will be expelled or reabsorbed. Different growth rates of embryos in the early stage can be a sign of a malformation that will result in the death of the smaller twin.

Sonographic findings that can be misinterpreted as a second ovular sac are:

- an extracoelomatic space, visible up to 7–8 weeks in single pregnancies;
- subchorionic blood collection;
- pregnancy in a horn of a bicornate uterus and fluid collection in the other horn, or a pregnancy in a septated uterus with the septum mistakenly interpreted as a membrane separating two ovular sacs;
- a chorioangioma or a placental cyst.

Most authors agree that the pattern of growth in the first and second trimesters is the same in twins and in single fetuses. Various studies of fetal weight at birth have led to the hypothesis of a more rapid decrease in the growth curves of twins than of singletons between the 27th and the 37th week of pregnancy.

A decrease in the weight of fetal organs can be seen in cases of twins from the 30th week onwards. Some studies have shown a decrease in the rate of growth of the biparietal diameter of one of the two fetuses after week 31–32 and of the abdominal circumference after week 33–34, but no alteration in the rate of femoral growth in comparison with single fetuses.

The occurrence of a polydramnios is relatively frequent in twin pregnancies, especially if they are monovular. Any difference in growth between twins poses a risk for the smaller fetus. An apparent difference in the growth of the two biparietal diameters can be observed when one twin is in vertex and the other in breech presentation, a situation that provokes marked dolichocephaly. In such cases, the biparietal diameter is smaller, but the cranial circumference is in fact normal.

Serial measurements must be made of the growth parameters of twins in the second and third trimesters to detect and monitor intrauterine growth restriction or to identify serious pathological conditions such as the twin–twin transfusion syndrome.

Pathological findings

In modern obstetrical care, clinical management of a multiple pregnancy depends on sonography, which is irreplaceable for monitoring fetal growth and amniotic fluid volume. The frequency of monitoring is defined on the basis of chorionicity: monochorionic pregnancies should be monitored every 2 weeks, while monthly scans until birth are adequate for dichorionic pregnancies.

From the 16th week onwards, all monochorionic pregnancies should be examined to identify signs of twin–twin transfusion syndrome. All twin pregnancies should have a morphological ultrasound scan at the 20th week. Doppler velocimetry should be conducted in cases of a twin pregnancy with discordant growth. Transvaginal sonographic evaluation of the uterine cervix (length and funnelling) is also advisable. A cervix that is < 25 mm at the 24th week is strongly predictive of preterm birth before week 32.

Antenatal diagnosis of congenital anomalies

Increased maternal age enhances the risks for both aneuploidy and twin pregnancy. The general risk for aneuploidy in each twin depends on the zygosity. For dizygotic twins, who are genetically independent, the risk (related to maternal age and familial factors) is the same as that of a single fetus. Therefore, the risk that at least one fetus has a chromosomal anomaly is increased as many times as the number of fetuses, while the risk that both twins are affected is the same as that of a single fetus squared (or cubed if there are three or more fetuses).

The incidence of malformations is greater in twin pregnancies than in single pregnancies, particularly in monozygotic pregnancies. The risk is approximately doubled for major malformations (cardiac, central nervous system, intestinal; 2.12%) and a little less than doubled (4.13%) for minor malformations. Each fetus in a dizygotic pregnancy has the same risk as a single fetus, and the higher incidence of structural anomalies is attributable to defects in monozygotic twins. The most frequent anomalies are defects of the median line (holoprosencephaly), defects of the neural tube and cloacal exstrophy. Cardiac defects account for about 3.8% of defects in monozygotic pregnancies and 0.56% in dizygotic pregnancies.

Monozygotic twins have the same karyotype, and the risk for aneuploidy in relation to maternal age is identical to that of singletons. In dizygotic pregnancies, the risk for aneuploidy is twice that of single pregnancies at the same maternal age.

Defects that occur specifically in monozygotic twins are due to asymmetrical separation during division (joined twins) and the presence of placental anastomosis, which creates unbalanced perfusion of the two fetuses (twin–twin transfusion syndrome or twin reversed arterial perfusion). As zygosity cannot always be established, the probability that one or both fetuses are affected can be estimated from the chorionicity, keeping in mind that the risk is the same as that of a single pregnancy for 10% of monozygotic dichorionic pregnancies.

In twin pregnancies, invasive and noninvasive antenatal tests can be used. The best method for trisomy screening in twin pregnancies is evaluation of nuchal

translucency at 10–14 weeks. Serological screening has a low detection rate. The rate obtained by evaluation of nuchal translucency is similar to that in single pregnancies, but the percentage of false positives is higher (8% in monochorionic pregnancies). Evaluation of nuchal translucency in combination with serological screening increases the detection rate, but it is nevertheless 10% lower than in singleton pregnancies.

Invasive antenatal diagnosis, such as amniocentesis and villocentesis, is also possible. There is no agreement about the risk for fetal loss associated with diagnostic amniocentesis in the second trimester in twin pregnancies, and the issue must be discussed carefully with the couple. For expert operators, the risks associated with villocentesis are the same as those for amniocentesis.

Fetal growth

Twins weigh less at birth than infants born of single pregnancies, due to deceleration of the rate of intrauterine growth and to premature birth: a birth weight of < 2500 g is found in 50% of infants born of twin pregnancies and 5% of singletons. The intrauterine growth rate of twins is similar to that of single fetuses up to 30 weeks but then slows.

The growth of twins can differ in each trimester. When discordance occurs during the first trimester, it could indicate congenital anomalies in the smaller twin. A reduction in the growth of twins can also be detected at the end of the second trimester and at the beginning of the third. The percentage of discordance is assessed from a formula in which the difference in weight between twins is divided by the weight of the heavier twin. The greater the discordance in weight between two twins, the greater the risk for perinatal mortality. Although there is no agreement on a clinically relevant reference value, a discordance in weight of 20–25% is generally considered indicative of a worse perinatal outcome.

When there is both growth discordance and monochorionicity, the presence of unbalanced transfusion between the fetuses must be excluded. In dichorionic placentation, the fetuses may have different genetic codes, and the growth discordance might be due to subjective differences in each twin. The presence of two placentas could limit the uterine surface, with consequent suboptimal implantation of one, potentially detectable by spectral Doppler examination. In the case of dichorionic twins with discordant weights, the spectral Doppler reference point is the pulsatility index in the umbilical artery and its progressive increase, while in the case of monochorionicity, the spectral Doppler reference point is the increase in peak velocity of the cardiac outflow, a sign of anaemia in the smaller twin.

Intrauterine growth restriction

Intrauterine growth restriction is one of the most important causes of perinatal mortality in twins. The prevalence in twins is about 25%, 10 times greater than in single pregnancies. Generally, a difference of 20–25% in fetal weight between the two twins is considered clinically relevant. On the basis of the curves for fetal growth in single pregnancies, intrauterine growth restriction of one twin (rarely both) is found in

about one of three twin pregnancies. Such growth discordance is due mainly to the reduced space available in the uterine hollow or to fetal anomalies. In dichorionic pregnancies, intrauterine growth restriction can be due to differences in the growth potential of the twins or to different blood flow in the placentas. In monochorionic pregnancies, it can derive from unequal division of the initial cellular mass between the two embryos or from the presence of vascular communications in monochorionic placentas that causes imbalances in nutrition.

Criteria that can be used to diagnose differential growth in two fetuses include:

- a difference in the estimated weight of the two fetuses of at least 500 g;
- a difference in the estimated weight of the two fetuses of 15–20%;
- a difference in the abdominal circumference of the two fetuses of at least 2 mm.

The most useful measurements are abdominal circumferences and fetal weight. This method is sensitive (80%) and has a high negative predictive value (93%); furthermore, it can be combined with information on the amniotic fluid volume and a Doppler examination of fetal flows. This examination is necessary even though concordant intrauterine growth restriction is rare.

In monochorionic pregnancies, growth discordance can indicate either the presence of intrauterine growth restriction or twin–twin transfusion syndrome, which must be sought by suggestive signs.

Complications related to monochorionicity

Monochorionic twin pregnancies are associated with a fivefold greater risk for fetal and perinatal loss, a 10-fold greater risk for antenatally acquired cerebral paralysis and at least double the risk for intrauterine growth restriction in comparison with dichorionic pregnancies.

Twin–twin transfusion syndrome (imbalanced fetus–fetus transfusion) complicates 10–15% of monochorionic twin pregnancies. Generally, it is seen during the second trimester of pregnancy. The natural history of this syndrome results in approximately 80% mortality without treatment and severe newborn outcome. The demonstration of vascular anastomoses suggests that the physiopathology of this syndrome is based on impaired haematic exchange between the two fetuses. The donor twin generally appears hypovolaemic and, at times, anaemic, with delayed growth and a marked reduction in the amniotic fluid volume (oligoamnios; bladder poorly distended or not visualized; Fig. 2.68, Fig. 2.69, Fig. 2.70, Fig. 2.71). In contrast, the receiving fetus already appears hyperperfused and polyuric (polydramnios and hyperexpanded bladder), and signs of cardiac overload (cardiomegaly, fetal hydrops, myocardial hypertrophy) can be detected.

In the most serious cases, the donor twin is completely deprived of amniotic fluid, cannot move, leans against the uterine wall (stuck twin) and can have impaired

Fig. 2.68. Monochorionic biamniotic pregnancy complicated by twin–twin transfusion syndrome: different fetal growth and different amniotic fluid volume, with polyhydramnios of the recipient twin and oligoamnios of the donor twin

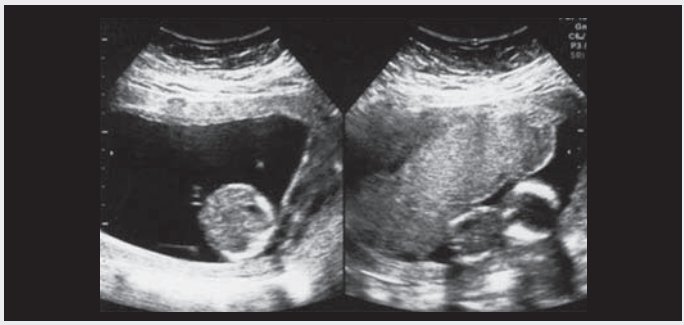

Fig. 2.69. Normal monochorionic biamniotic twins: no differences in bladder volumes (arrows)

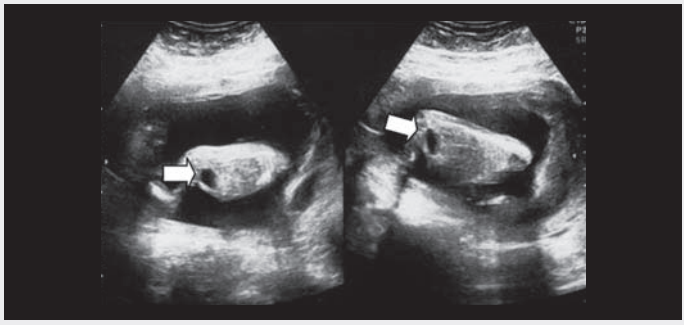

Fig. 2.70. Twin–twin transfusion syndrome: different bladder volumes (arrows)

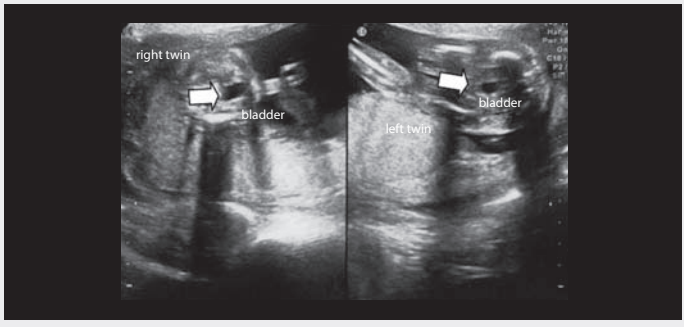

Fig. 2.71. Twin–twin transfusion syndrome: different amniotic fluid volume with hydramnios in the recipient twin and death of donor twin (stuck twin)

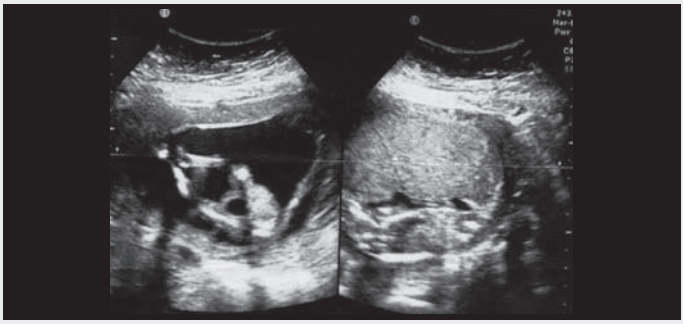

or pathological arterial flow. The resulting chronic hypoxia can induce cerebral lesions or bring about exitus in utero. The receiver twin shows signs of serious cardiac failure (tricuspid regurgitation, fetal hydrops, pathological venous flow), which can also bring about exitus in utero. The death in utero of one of the twins exposes the other to a 50% higher risk for death or at least results in neurological ischaemic injuries, as the surviving twin suffers acute hypovolaemia when part of its circulating mass is recalled into the dilated vessels and low pressure circle of the dying twin.

Antenatal ultrasound diagnosis of twin–twin transfusion syndrome is based on the following observations:

- a single placenta;
- a difference in the quantity of amniotic fluid: polydramnios in the receiving and oligoamnios in the donor twin;
- a difference in the degree of bladder filling: bladder hyperextended in the receiving twin and small or not visualized in the donor twin.

Additionally:

- hydrops in both fetuses or signs of congestive failure in the transfused fetus;
- weight discrepancy between the twins (on ultrasound);
- difference in haemoglobin levels between the two fetuses (on cordocentesis);
- differences in the dimensions or number of vases of the umbilical cords;
- pathological Doppler velocimetry (venous duct, umbilical vessels, fetal cerebral vessels).

Of the treatment options proposed, serial amnioreductions, septostomy, laser ablation and selective feticide are those most frequently practised. Fetus–fetus transfusion

can also occur acutely during labour. One of the two newborns will appear plethoric and the other strongly anaemic in a pregnancy without complications.

Fetal mortality in monoamniotic pregnancies is mainly due to twisting of the umbilical cord, which leads to fetal asphyxia. As fetal death is sudden and unpredictable, close sonographic checks are necessary to verify fetal comfort, especially if the cords are already entangled. Twisting of the umbilical cords occurs early in pregnancy, during the first or second trimester, when the fetuses can move freely within the uterus. In monochorionic monoamniotic pregnancies, in which the cords have a close placental insertion and there may be some large-calibre vascular anastomoses between the two fetal circulations, acute episodes of haemodynamic failure can also occur.

Intrauterine twin death

The incidence of death in twin pregnancies is greater in the first trimester than at birth. It has been estimated that about 12% of pregnancies are multiple at conception but only 2% evolve to twin births. About 20–70% of pregnancies diagnosed as twin in the first trimester result in a vanishing twin. In such cases, the prognosis of the surviving twin is good, although the risk for miscarriage is greater, particularly in monochorionic pregnancies.

The outcome of the surviving twin is poorer if one fetus is lost at a more advanced stage of pregnancy, particularly in the third trimester. The risk is estimated to be about 6% (about 8% in monochorionicity and about 4% in dichorionicity). The risk of death for the surviving twin reaches 30% and the risk for cerebral paralysis has been estimated variously to be 10–46% in monochorionic twins; in dichorionic twins, the outcome is favourable except for cases of congenital anomalies. The mechanism of the damage in the surviving twin is acute haemodynamic failure (hypotension and ischaemia) consequent to the passage of blood towards the vascular bed of the dead twin through the placental anastomosis.

Clinical management of such pregnancies is not simple. The most important elements are chorionicity and gestational age. In cases of dichorionicity, an immediate intervention is not necessary if the cause is established, and wait-and-see management associated with careful maternal and fetal monitoring shows no significant differences in terms of weeks and weight at birth of the surviving twin from interventional management. Moreover, in the presence of acute twin–twin transfusion syndrome, delivery immediately after the death of a twin does not prevent the ischaemic complications for the central nervous system of the surviving twin. Management greatly depends on gestational age, as delivery of the healthy twin at an early stage of pregnancy has little justification. If the cause of a twin's death in utero might also compromise the other (for instance, pre-eclampsia or chorioamniotitis), management must be adapted to avoid loss of the survivor. In monochorionic twin pregnancies, the risk for neurological damage can be monitored during the pregnancy with ultrasound or MRI. Evidence of a serious anaemic state is a poor prognosis, but the advantages of transfusion in utero through cordocentesis have not been clearly

demonstrated. Doppler measurement of peak velocity in the middle cerebral artery has been proposed as a noninvasive index for evaluating fetal anaemia.

Twin reversed arterial perfusion sequence

The twin reversed arterial perfusion sequence, also called the acardiac twin syndrome, is a rare disease that occurs in about 1% of monochorionic pregnancies. It is considered to be an extreme example of haemodynamic anomaly in a twin pregnancy with a single placenta: the acardiac twin receives blood into the umbilical artery through a large arterio-arterial anastomosis that allows the passage of blood from the umbilical artery of the twin cardiac donor (pump twin).

On colour Doppler, the cord of the perfused twin is composed of only two vessels, a single artery and a vein (there are only rarely two arteries), for arterial flow from the placenta to the fetus and venous flow from the fetus to the placenta. The perfused twin receives poorly oxygenated blood, which is distributed particularly to the iliac district; the affected twin's organs show anomalies that are probably due to hypoxic injuries, and the heart is completely absent or rudimentary. The cephalic extremity is usually absent (acardiac–acephalus twin), as are the upper extremities, while the lower part of the trunk is usually present. The acardiac twin often develops oedema and appears to be double the size of the other. Due to congestive cardiac failure and hydrops or as a result of prematurity induced by polydramnios, up to 50% of cardiac twins die during the perinatal period.

Joined twins

Joined twins occur in one of every 50 000 pregnancies. The cause is late, incomplete division of the embryonic disc around day 15–17 after conception. The twins are always monozygotic, monochorionic and monoamniotic. A diagnosis is based on the finding of a monochorionic monoamniotic pregnancy without separation of the vascular systems of the two fetuses.

If the two fetal heads are close to one another, there is a strong probability of Siamese twins, although the absence of this finding does not exclude the diagnosis. When the two twins are almost entirely formed, the point of union is often the anterior surface of the chest (thoracopagus) or more rarely the abdomen (omphalopagus), the back (pygopagus), the skull (craniopagus) or the pelvis (ischiopagus). When the duplication is less complete, the point of union is often lateral.

The survival of such twins is related to the gestational age at birth and the type of connection between the fetuses. In cases of extensive cardiovascular connections, the death of at least one twin is inevitable (Fig. 2.72).

Fig. 2.72. Monoamniotic twins (18 weeks' gestational age): conjoined twins with early death of one twin (arrow) (calipers: abdominal diameters of the dead twin)

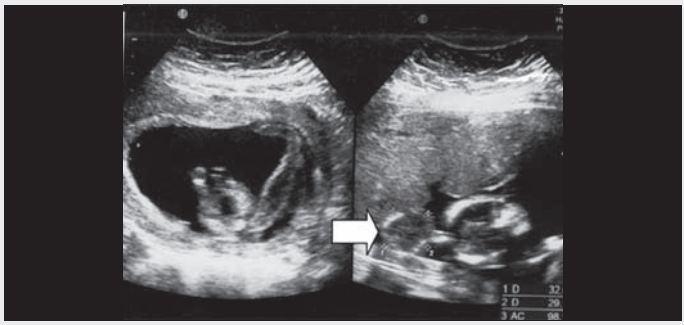

Fetus papyraceus is a dead twin pressed onto the uterine wall by the expanding amniotic hollow of the other twin. The dead fetus appears to be enclosed in its own membranes but with no amniotic fluid. The hydric content of the dead fetus is slowly reabsorbed, with further reduction of fetal size.

Fetus in fetu is a rare anomaly in which a parasitic twin is included in the retroperitoneum of the superior abdomen of the carrier fetus. The included fetus has a well-developed vertebral system, which is a distinctive sign for differential diagnosis with teratoma.

Fetal malformations

Antenatal ultrasound diagnosis of fetal malformations is the most difficult task of sonographers and sonologists in the field of obstetrics. The number of fetal malformations detectable by ultrasound is high and increasing with the development of technology and interest in the field of antenatal medicine. Fetal malformations are usually an unexpected finding during sonographic examination of an apparently healthy pregnant woman, as in most cases they are found in women with no risk factors. For this reason, in developed countries, ultrasonic examination of fetal anatomy has become a standard screening procedure, usually between 19 and 22 gestational weeks. This short interval has been chosen because: the development of fetal organs is almost complete; the amount of amniotic fluid is higher than the fetal body, allowing a good acoustic window for penetration of the ultrasound beam; and, if a fetal malformation is detected, it is still possible to plan other diagnostic procedures, such as amniocentesis, or offer the woman the option of terminating the pregnancy in the case of a severe anomaly.

If screening with ultrasound is accepted, a detailed survey of the fetal anatomy must be performed during the second trimester. The diagnostic results reported

in the literature for such a screening procedure vary widely in different countries, operators' skills and instrument characteristics. The most recent European multicentre trial showed a sensitivity of 60%. The aim of this section is not to describe how to diagnose all fetal congenital malformations (several textbooks are available on this topic) but how to suspect a malformation during a fetal anatomical survey. We therefore describe the findings suggesting malformations.

Fetal head

Evaluation of the fetal head requires visualization and measurement of the biparietal diameter and head circumference, measurement of the atrial width and transverse cerebellar diameter and visualization of the orbits (Fig. 2.73).

In cases of failed or abnormal measurement of biparietal diameter and head circumference, the malformations described below can be detected.

Fig. 2.73. Evaluation of a normal fetal head. (a) Transthalamic axial scan, in which the biparietal diameter and head circumference are measured. (b) Transventricular scan, in which the atrial width is measured (arrows). (c) Transcerebellar scan, in which the transverse cerebellar diameter (arrows) is measured. (d) Transorbital scan. CSP, cavum septum pellucidum; FH, frontal horns of lateral ventricles; T, thalamus; open arrow, insula

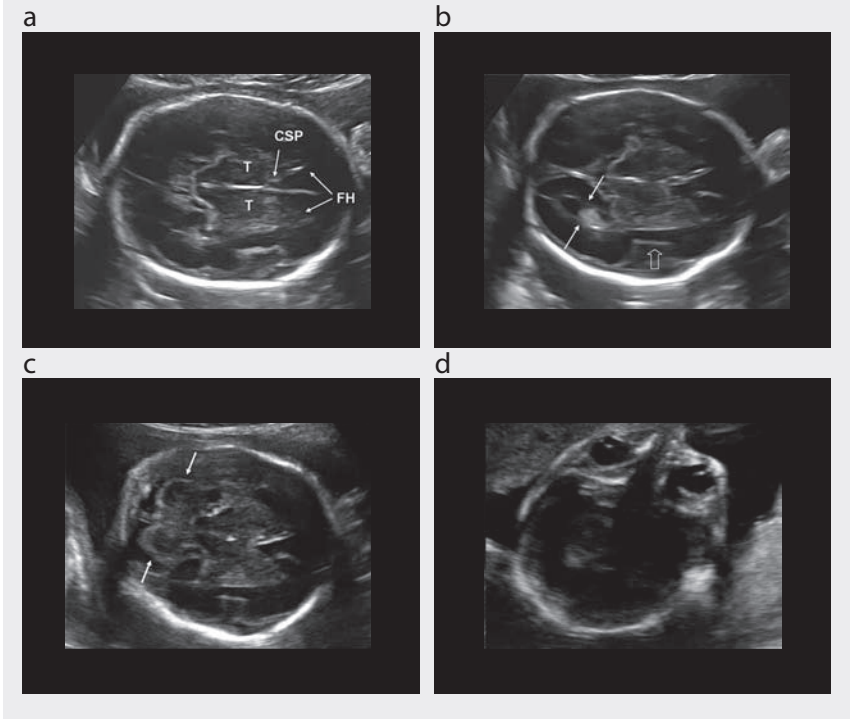

Anencephaly: severe anomaly incompatible with postnatal life, easily detectable from the first trimester by the absence of the fetal calvaria (Fig. 2.74).

Microcephaly: fetal head and brain smaller than normal. The diagnosis is difficult and frequently late. It is important to compare the head size with the abdominal circumference and femur length in order to confirm the diagnosis (Fig. 2.75).

Macrocephaly: an enlarged fetal head, usually due to severe hydrocephaly or the presence of intracranial masses such as tumours or cysts (Fig. 2.76). The brain anatomy is completely distorted by the severely enlarged ventricles in the first case, by a prevalently solid mass in the second case and by a prevalently cystic mass in the third one. In rare conditions, there is a large head with normal anatomy, which has a good prognosis but is sometimes a sign of severe neuronal migration disorder.

Fig. 2.74. Anencephaly. The fetal calvaria cannot be visualized

Fig. 2.75. Microcephaly. The fetal head is small in comparison with the face

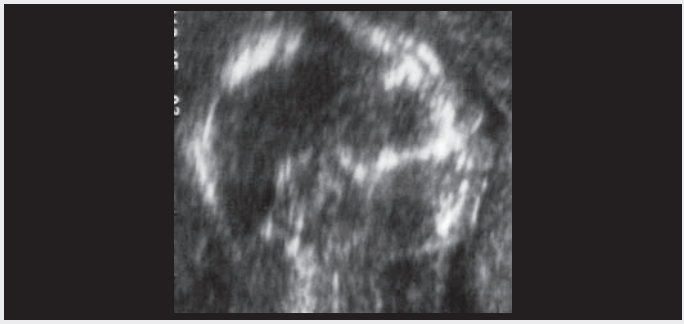

Fig. 2.76. Macrocephaly due to severe hydrocephaly (a), brain teratoma (b) and arachnoid cyst (c)

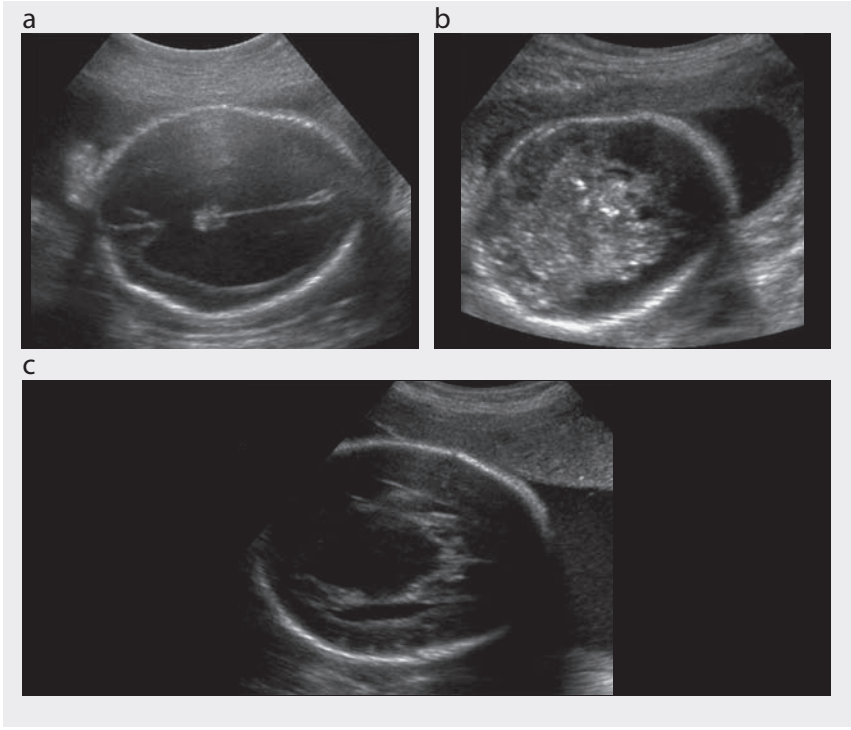

Cephalocoele: protrusion of meninges alone (meningocoele) or meninges and brain tissue (encephalomeningocoele) through a bony defect, usually located in the occipital pole (Fig. 2.77)

Fig. 2.77. Occipital cephalocele. A complex mass protrudes through a bony defect of the calvaria in the occipital pole

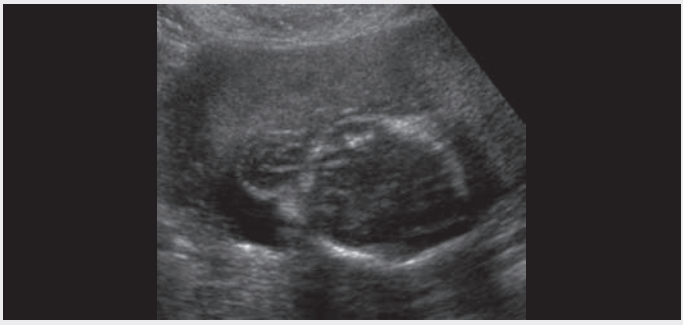

Abnormal findings and measurement of the atrium allow recognition of other malformations.

Ventriculomegaly: the ventricular size is considered normal when the atrial width is < 10 mm, independently of gestational age. Measurements of 10–15 mm are defined as borderline ventriculomegaly; dilatation > 15 mm is considered severe ventriculomegaly (Fig. 2.78). In cases of borderline ventriculomegaly, the prognosis depends mainly on the presence of associated anomalies; it is good in 90% of cases, particularly when the dilatation is 10–12 mm. In cases of severe ventriculomegaly (frank hydrocephalus), the prognosis is usually worse and depends mainly on the cause of the ventricular dilatation and the presence of associated anomalies.

Choroid plexus cysts are small fluid collections, usually bilateral, within the choroid plexus and are easily recognizable within the atrium (Fig. 2.79). In most cases, they are a transient finding and disappear by the end of the second trimester. If isolated, they have no clinical consequence; when associated with other anomalies, they may be a sign of chromosomopathy and especially trisomy 18.

Holoprosencephaly is the consequence of failed division of the prosencephalon into the two telencephalic vesicles in the early stages of brain development. They are classified according to the severity of the defect into alobar, semilobar and lobar. The first is easily detectable by the typical horse-shoe appearance of the single ventricular cavity with fused thalami (Fig. 2.80). In the semilobar variety, the frontal horns are fused, and abnormal occipital horns are present. The lobar variety is extremely difficult or impossible to diagnose, as the defect is limited to the area of septum pellucidum and olfactive tracts. Alobar and semilobar forms are frequently associated with other anomalies, mainly at the level of the face, such as cyclopia, hypotelorism, cleft palate (Fig. 2.80) and proboscis. In these cases, trisomy 13 or 18 should be suspected.

Abnormal findings and measurement of the cerebellum allow the detection of further anomalies.

Fig. 2.78. Borderline (a) and severe (b)ventriculomegaly

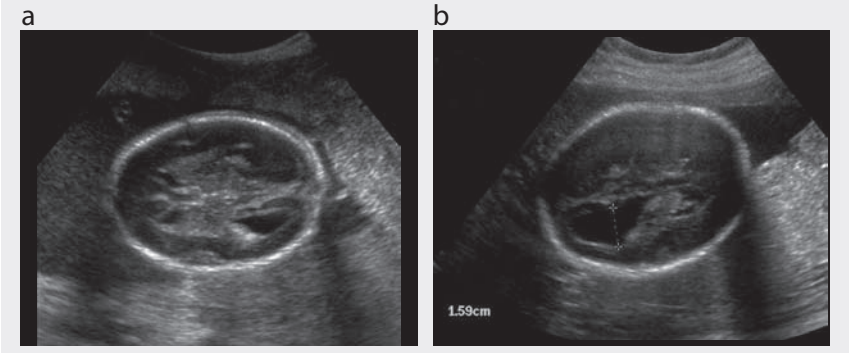

Fig. 2.79. Choroid plexus cyst

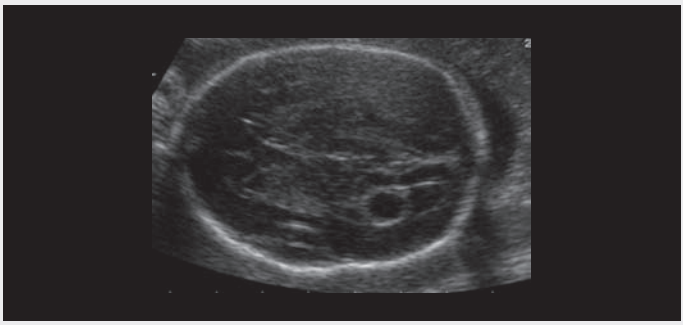

Fig. 2.80. Alobar holoprosencephaly: the single horse-shoe-shaped ventricular cavity (a) and the associated cleft palate (b, arrow) can be seen

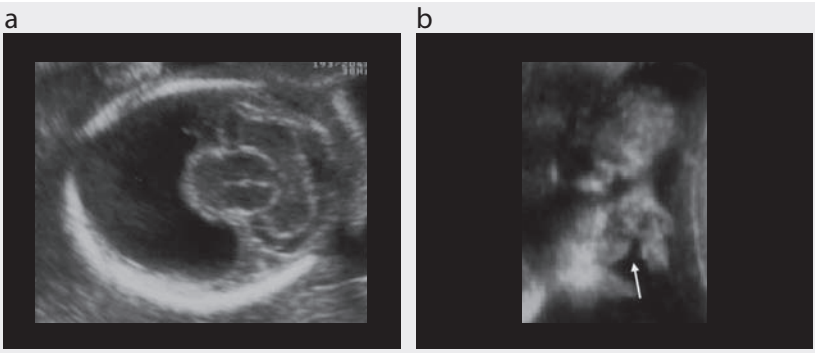

Dandy-Walker complex: This term covers anomalies characterized by various degrees of hypoplasia of the cerebellar vermis. In the classic Dandy-Walker malformation, the cerebellar vermis is severely hypoplastic and rotated upwards by an extremely enlarged fourth ventricle, which appears as a cyst in the posterior fossa; hydrocephaly is frequently associated (Fig. 2.81). In the so-called Dandy-Walker variant, the vermis is hypoplastic but still present and the enlarged fourth ventricle appears as a key-hole cystic structure between the two cerebellar hemispheres (Fig. 2.81). In this case, a difficult differential diagnosis is made from the Blake pouch cyst, which is a digit-like posterior protrusion of the fourth ventricle below a normal vermis. This condition usually has a better prognosis than Dandy-Walker complex.

Mega cisterna magna: The cisterna magna is considered enlarged when the anteroposterior diameter at the level of the cerebellar vermis is > 10 mm (Fig. 2.82). In these cases, a careful survey of fetal anatomy should be performed to rule out associated anomalies. The prognosis of the isolated forms is usually good.

Fig. 2.81. Dandy-Walker complex. Classical (a) and variant (b) malformations

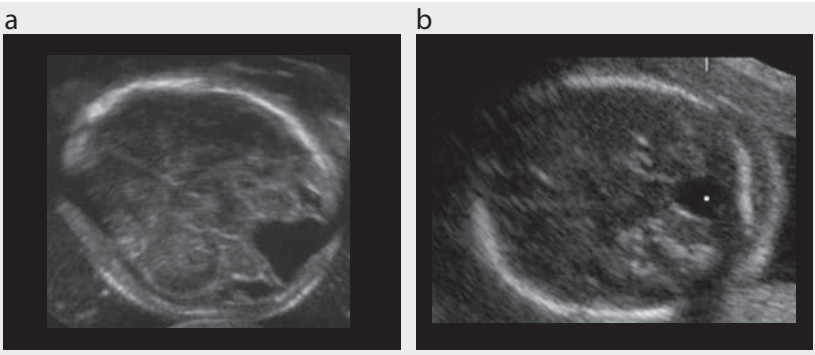

Fig. 2.82. Mega cisterna magna (calipers)

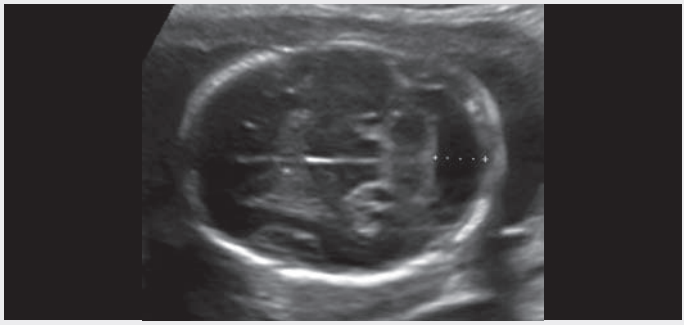

Fig. 2.83. Chiari II malformation. (a) Small cerebellum with effaced cisterna magna, 24 weeks' gestation. (b) Abnormal shape of the calvaria (lemon sign), 20 weeks' gestation

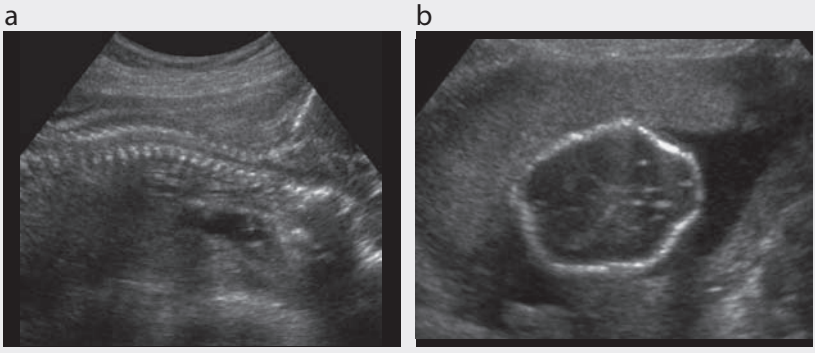

Fig. 2.84. Abnormal findings at the level of the orbits. Hypotelorism (a), cyclopia (b), unilateral microphthalmia (arrow) (c)

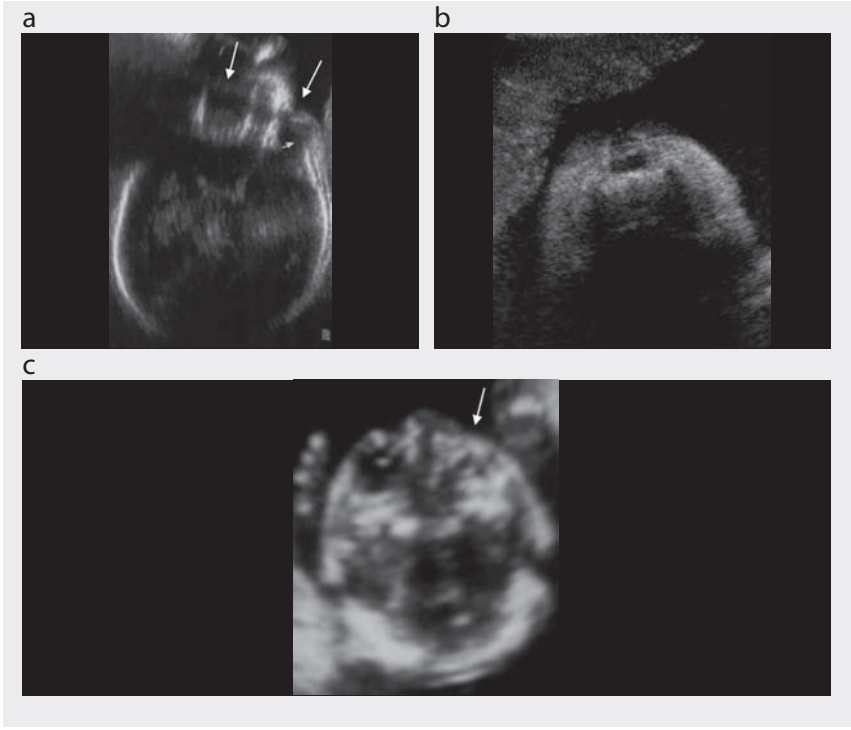

Chiari II malformation: The posterior fossa is small, the cerebellum shows a typical banana shape and the cisterna magna is effaced (Fig. 2.83a). Sometimes, the calvaria assumes a lemon shape (Fig. 2.83b). An open spina bifida is almost always associated.

Abnormal findings at the level of the orbits include hypotelorism, cyclopia, hypertelorism, microphthalmia and anophthalmia (Fig. 2.84).

Fetal spine

Routine examination of the fetal spine should include evaluation of its longitudinal view, to demonstrate the integrity of the spinal canal. In the transverse view, the spinal canal is delimited anteriorly by the ossification centre of the vertebral body and posteriorly by the ossification centres of the laminae (Fig. 2.85).

An abnormal appearance of the fetal spine may be due to several anomalies.

Spina bifida: In the longitudinal view, the spinal canal shows an enlargement at the level of the vertebral defect; the axial view at the same level shows lateral displacement of the laminae. The meningocoele protruding from the vertebral defect appears as a cystic structure of variable size (Fig. 2.86). Small spinal defects, however, can easily be missed; for this reason, it is easier to screen for open neural tube defects by

Fig. 2.85. Normal appearance of the fetal spine in the longitudinal (a) and axial (b) views

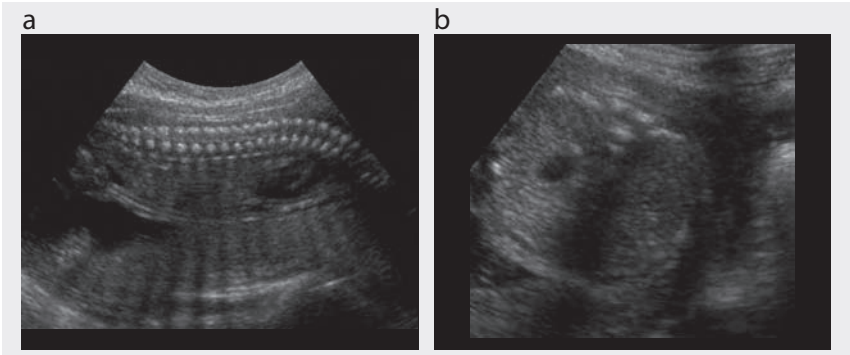

Fig. 2.86. Examples of spina bifida: in the axial view, the laminae are displaced laterally (arrow) (a). In the longitudinal view, the spinal canal shows an enlargement at the level of the vertebral defect (arrows) (b). The meningocoele appears as a cystic structure protruding from the defect (arrow) (c) and (d)

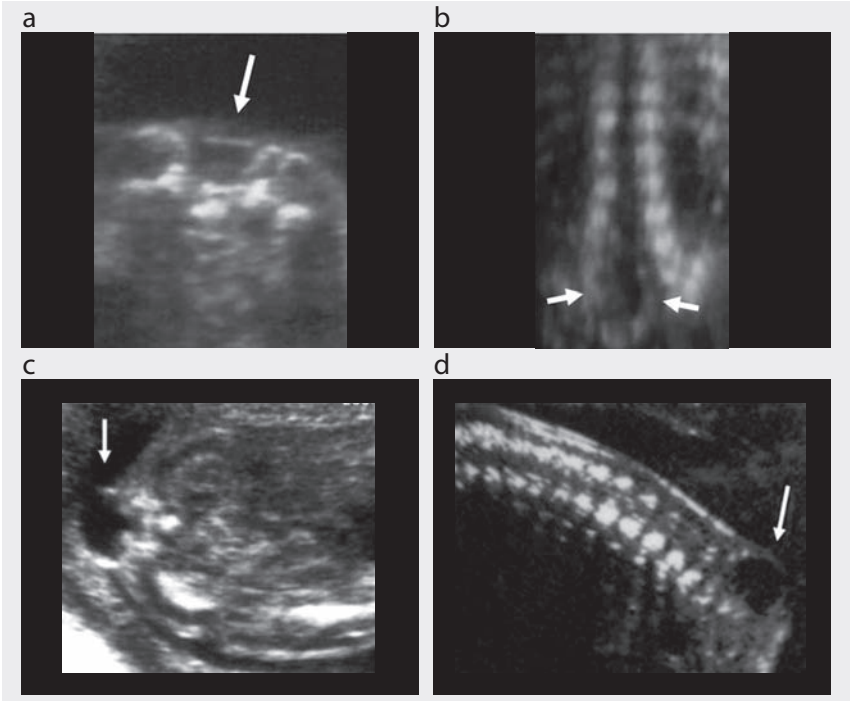

searching for the associated cranial signs typical of the Chiari II malformation, i.e. a small cerebellum with effaced cisterna magna (banana sign) and abnormal shape of the calvaria (lemon sign) (Fig. 2.83).

Fetal lungs

The fetal lungs are usually examined routinely in the axial view of the fetal chest, at the same level at which the four chambers of the fetal heart are visible. They appear as two echogenic wings surrounding the heart (Fig. 2.87).

Fig. 2.87. Axial view of the fetal chest at the level of the four cardiac chambers. The lungs (L) are the echogenic wings surrounding the fetal heart

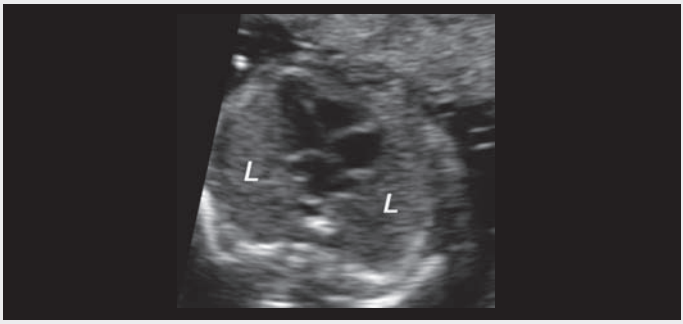

An abnormal appearance of the lungs in this axial view allows detection of several anomalies.

Cystic adenomatoid malformation: The lesion is usually unilateral. Part of the lung is replaced by dysplastic cystic tissue, defined as microcystic or macrocystic depending on the size of the cysts (Fig. 2.88). In the former, the cysts are too small to be visualized by ultrasound, and the lesion appears as an echogenic area of variable size; in the latter, the cystic lesions are clearly recognized. Small lesions may undergo spontaneous regression during pregnancy or after delivery. Large lesions cause mediastinal shift and can be complicated by pleural effusion. Cystic adenomatoid malformation should be differentiated from **pulmonary sequestration**, which is an abnormal solid pulmonary structure that does not communicate with the normal bronchial tree or the pulmonary vessels. Colour Doppler can be used to visualize the feeding vessel of the lesion, which originates directly from the descending aorta.

Pleural effusion: A collection of fluid in the pleural cavity is easily recognizable as an echo-free area compressing the fetal lung. It can be uni- or bilateral (Fig. 2.89). The unilateral lesion is usually a chylothorax; bilateral lesions can be caused by heart malformations, infection or lung malformations, for example, or can be part of generalized hydrops.

Diaphragmatic hernia: In this anomaly, abdominal organs (stomach, gut or even liver) protrude into the mediastinum through a diaphragmatic defect. The commonest site of the defect is in the left posterior area. In the axial view of the fetal chest, the heart is shifted to the right and the lungs are compressed by the herniated abdominal structures (Fig. 2.90). As a consequence of the persisting compression, lung hypoplasia may develop, which is the main cause of neonatal death.

Fig. 2.88. Cystic adenomatoid malformation of the lung: microcystic (a) and macrocystic (b)

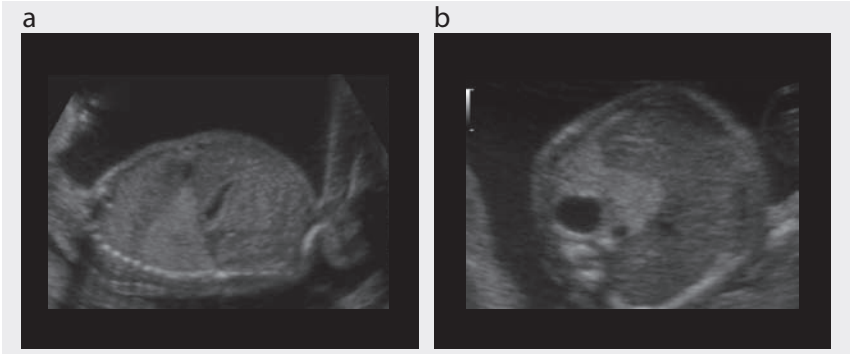

Fig. 2.89. Bilateral pleural effusion in the axial (a) and sagittal (b) view of the chest

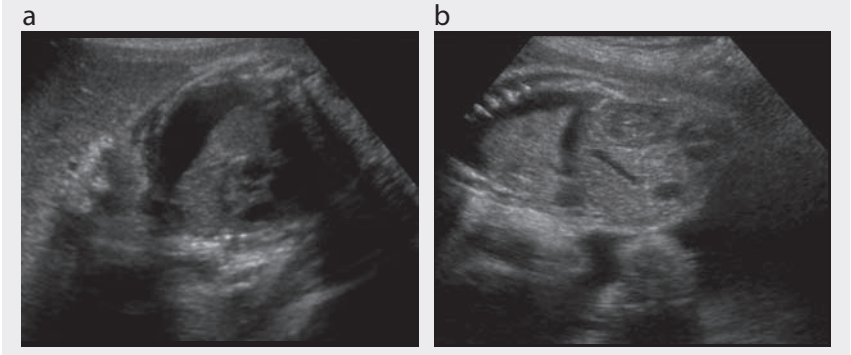

Fig. 2.90. Diaphragmatic hernia: the heart is shifted to the right and the lungs are compressed by the herniated abdominal structures; the herniated stomach is easily recognized as a cystic structure on the left side of the heart

Fetal heart

Sonographic examination of the fetal heart is the most complicated part of the fetal morphological evaluation. The sensitivity of ultrasound in screening for cardiac anomalies depends on the scanning planes used. The simplest screening procedure is based on the four-chamber view of the heart. It can be apical when the apex of the fetal heart points anteriorly towards the transducer (Fig. 2.91) and transverse when the cardiac axis is perpendicular to the ultrasonic beam. Correct acquisition of the four-chamber view requires the following: (i) the situs is normal in relation to the location of the stomach; (ii) two thirds of the heart is in the left half of the thorax; (iii) the apex is pointing to the left (laevocardia); (iv) at least two pulmonary veins can be seen opening into the left atrium; (v) the atria are the same size; (vi) the atrial septum is interrupted by the foramen ovale; (vii) the tricuspid valve is inserted slightly lower than the mitral valve; (viii) the ventricles are almost the same size but have a different shape (the left ventricle is elongated and reaches the apex and the right ventricle is circular due to the presence of the moderator band); (ix) the thickness of the walls is similar in the two ventricles; and (x) the interventricular septum is continuous.

Starting from the four-chamber view and rotating the transducer slightly towards the right fetal shoulder, it is possible to visualize the left outflow tract, with the ascending aorta originating from the left ventricle (Fig. 2.91). With a similar movement towards the left fetal shoulder, the right outflow tract is obtained, with the pulmonary artery emerging from the right ventricle and crossing the aorta (Fig. 2.91).

A further useful section plane is the three-vessel plane, which is obtained simply by starting from the four-chamber view and moving the transducer upwards. It shows the axial section of the superior vena cava, aorta and pulmonary artery located posterior to the thymus (Fig. 2.92).

Fig. 2.91. Apical four-chamber view of the fetal heart (a); visualization of the left (b) and right (c) outflow tracts

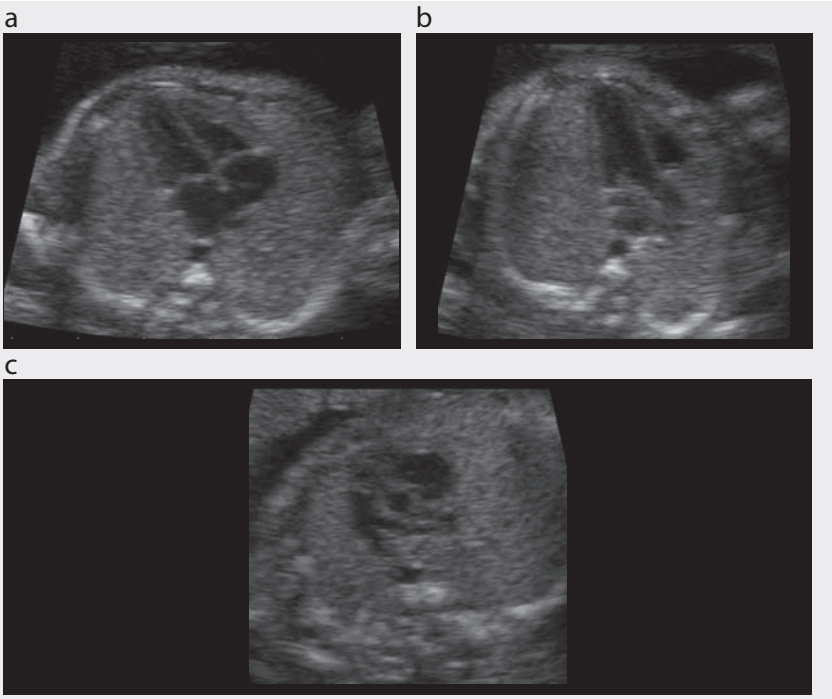

Fig. 2.92. Three-vessel view, showing, from right to left, the superior vena cava, aorta and pulmonary artery

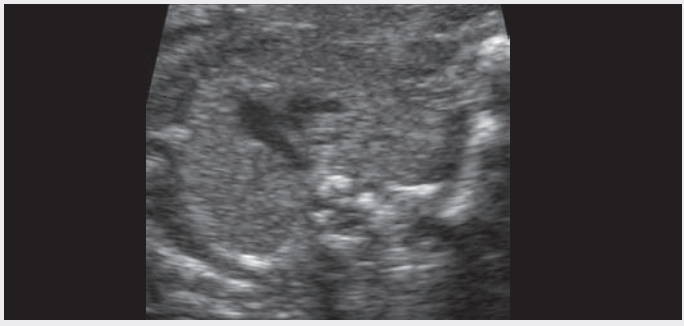

With only the four-chamber view, the sensitivity of ultrasound for detecting fetal cardiac anomalies is less than 50%; this rises to 70% when the outflow tracts are included in the screening procedure.

The number of congenital heart defects is high and their correct diagnosis requires skill and accurate knowledge of the haemodynamic of each disease, so that the mother can be counselled properly. For these reasons, fetal echocardiography is considered a specialized part of antenatal ultrasonography. In this section, we list only the main cardiac malformations that may be suspected during screening.

Anomalies detectable with the four-chamber view

Atrial anomalies: A single atrium is seen in most cases of complete atrioventricular canal (single atrium, single atrioventricular valve, wide ventricular septum defect) (Fig. 2.93). Interatrial defects with normal atrioventricular valves may be missed. An enlarged right atrium may be associated with Ebstein anomaly (low insertion of the tricuspid valve in the right ventricle (Fig. 2.94) or tricuspid valve dysplasia (Fig. 2.95). In both cases, pulsed and colour Doppler demonstrate valvular regurgitation. Dilatation of the left atrium is rarer and is due to mitral insufficiency secondary to critical aortic stenosis.

Septal defects*:* In the four-chamber view, large muscular defects or inlet defects of the perimembranous area can be visualized (Fig. 2.96). Small muscular defects and outlet defects of the perimembranous area cannot be detected.

Ventricular disproportion: A small, sometimes virtual left ventricle associated with mitral atresia is typical of hypoplastic left heart syndrome (Fig. 2.97). A small right ventricle can be seen in association with tricuspid atresia. In this case, a small interventricular septum defect is present. The presence of hypertrophy of the right ventricular walls raises suspicion of coarctation of the aorta (Fig. 2.98), although this finding can be benign and disappear after delivery. Severe dilatation of the left ventricle with increased echogenicity and reduced contractility of the muscular wall is typical of critical aortic stenosis (Fig. 2.99).

Fig. 2.93. Complete atrioventricular canal: the four-chamber view shows a single atrium, a single atrioventricular valve and a wide ventricular septal defect

Fig. 2.94. Ebstein anomaly: the right atrium is extremely enlarged and the tricuspid valve has a low insertion

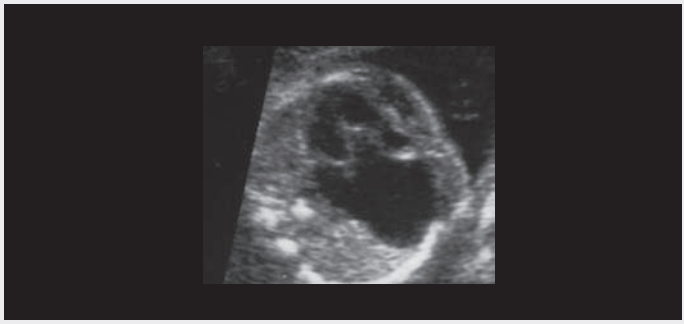

Fig. 2.95. Dilatation of the right atrium in tricuspid valve dysplasia

Fig. 2.96. Inlet interventricular defect of the membranous area

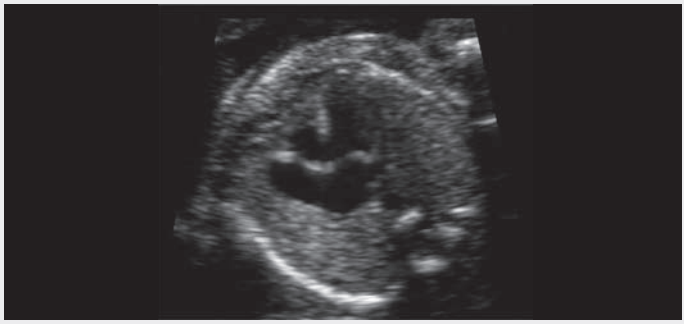

Fig. 2.97. Mitral atresia with small ventricular cavity (hypoplastic left heart syndrome)

Fig. 2.98. Hypertrophy of the right ventricular walls, raising suspicion of coarctation of the aorta

Fig. 2.99. Severe dilatation of the left ventricle with reduced contractility of the ventricular wall, typical of critical aortic stenosis

Anomalies detectable in the outflow tract

Septal anomalies: Interventricular septum defects can be recognized in the left outflow tract. When the emerging aorta overrides the defect, several conotruncal anomalies can be suspected; in these cases, it is important to evaluate the right outflow tract. A small pulmonary artery is typical of the tetralogy of Fallot (Fig. 2.100). When the pulmonary artery rises directly from the aorta, a common arterial truncus is suspected.

Anomalies of vessel crossing: When two parallel vessels are seen on the left outflow tract which do not cross each other, complete transposition of the great arteries is suspected if each vessel originates from separate ventricles (Fig. 2.101); double outlet right ventricle is suspected if both vessels originate from the anterior ventricle.

Fig. 2.100. Interventricular septal defect with overriding aorta in a case of tetralogy of Fallot

Fig. 2.101. Complete transposition of the great vessels: the aorta (ao) and pulmonary artery (p) are parallel and do not cross each other

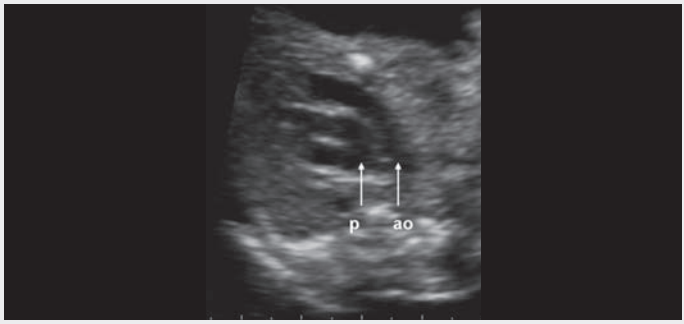

Anomalies of vessel size: A small aortic annulus associated with a dilated left ventricle is typical of critical aortic stenosis. A thin pulmonary artery is typical of pulmonary atresia and is usually associated with a small right ventricle and an interventricular septum defect. A severely dilated pulmonary artery is observed in cases of tetralogy of Fallot, with absent pulmonary valves (Fig. 2.102).

Fig. 2.102. Severe dilatation of the pulmonary artery (P) in tetralogy of Fallot with absent pulmonary valve

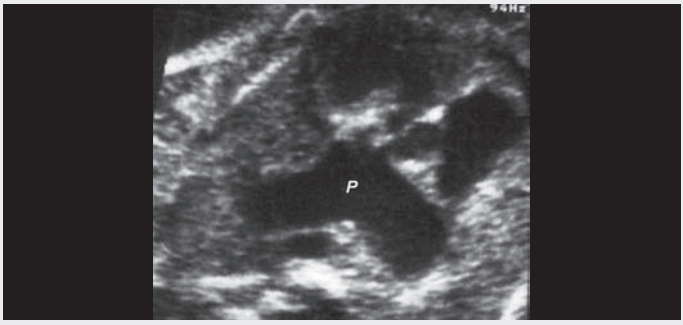

Fetal gastrointestinal tract

Routine examination of the fetal gastrointestinal tract is performed in the axial view of the fetal abdomen. In the upper axial view, the echo-free stomach and the echogenic liver can be visualized with the intrahepatic tract of the umbilical vein (Fig. 2.103a) and the gall bladder (Fig. 2.103b). At a lower level, the echogenic bowel can be seen (Fig. 2.103c).

Bowel obstruction results in different findings depending on the level of obstruction. In **oesophageal atresia**, lack of visualization of the stomach is associated with polyhydramnios secondary to failure of fetal swallowing of amniotic fluid (Fig. 2.104); however, in 90% of cases, oesophageal atresia is associated with tracheo-oesophageal fistula, which allows partial filling of the stomach even in the presence of polyhydramnios. In the longitudinal view, the dilated proximal portion of the oesophagus can be seen during fetal swallowing (Fig. 2.104).

In **duodenal atresia**, dilatation of the stomach and proximal duodenum produces the typical double-bubble sign and polyhydramnios (Fig. 2.105); this condition is frequently associated with trisomy 21.

Dilatation of the intestinal lumen secondary to **ileojejunal obstruction** produces multiple cystic areas in the abdomen below the liver (Fig. 2.106); in this case, polyhydramnios is usually a late occurrence. Severe dilatation may be complicated by bowel perforation and ascites.

Fig. 2.103. Normal gastrointestinal organs. (a) Stomach (S), liver (L) and intrahepatic tract of the umbilical vein (UV). (b) Gall bladder (G). (c) echogenic bowel

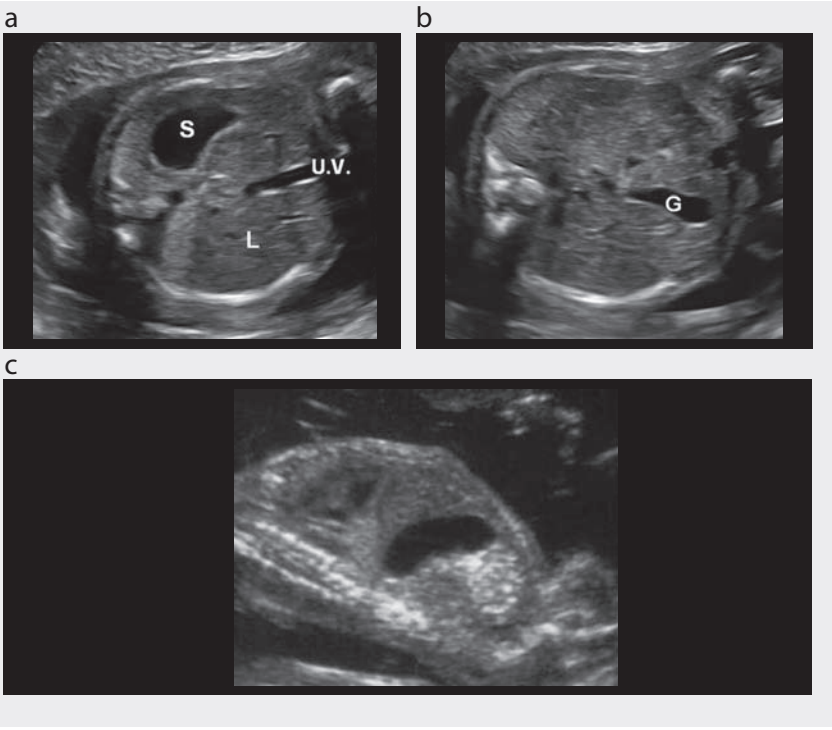

Fig. 2.104. Oesophageal atresia suspected from lack of visualization of the stomach in association with polyhydramnios (a). In the longitudinal view (b), the dilated proximal oesophagus can be seen

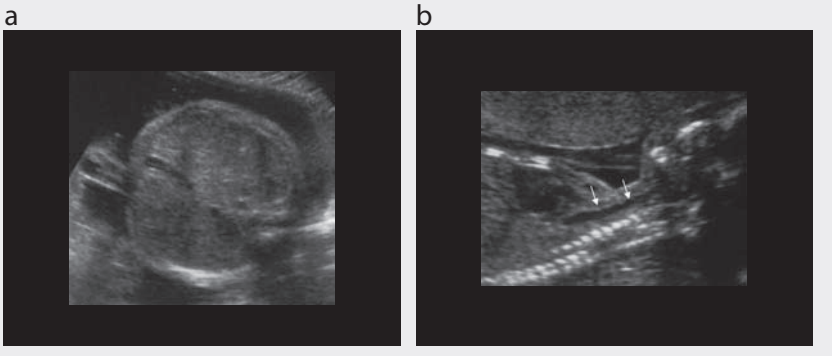

Fig. 2.105. Duodenal atresia: dilatation of the stomach and proximal duodenum produces the typical double-bubble sign

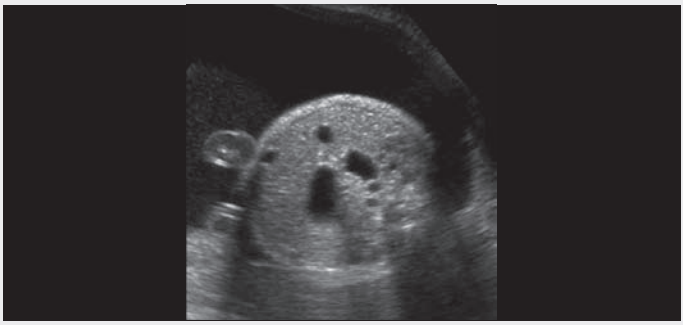

Fig. 2.106. Jejunal obstruction: the dilated bowel produces multiple fluid-filled cystic or tubular areas in the abdomen ((a) sagittal view; (b) axial view)

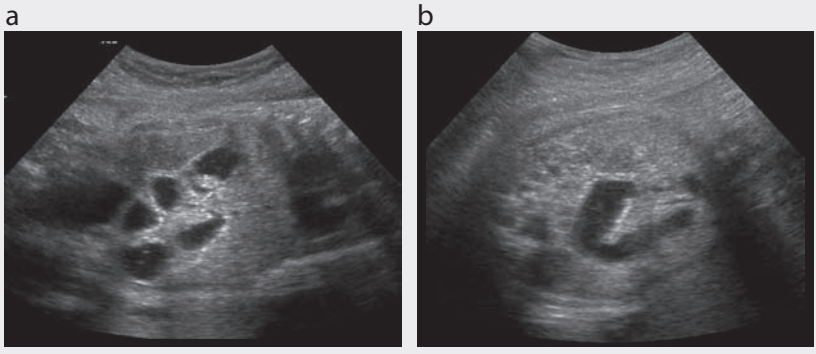

An abnormal shape of the fetal abdomen is produced by **omphalocoele** and **gastroschisis**. In cases of omphalocoele, the abdominal defect is at the level of insertion of the umbilical cord. Intestinal loops or even the stomach and part of the liver (Fig. 2.107) may protrude through the defect and be covered by an amnio-peritoneal membrane. This condition is frequently associated with chromosomopathy.

In cases of gastroschisis, the defect is on the right side of the umbilical cord insertion and is not covered by a membrane; therefore, the herniated bowel loops float freely in the amniotic cavity (Fig. 2.108).

Another anomaly that is easily recognizable on the axial scan of the fetal abdomen is **ascites**, which can have various causes, including cardiac disease, infections, bowel perforation and autoimmune diseases. In these cases, the abdominal circumference is increased and the abdominal cavity is filled with fluid (Fig. 2.109). The ascites can be isolated or be part of general **hydrops** with pleural effusion and soft tissue oedema.

Fig. 2.107. (a) Small and (b) huge omphalocoeles. In the former, only bowel loops are herniated and are covered by a membrane; in the latter, part of the liver may be observed

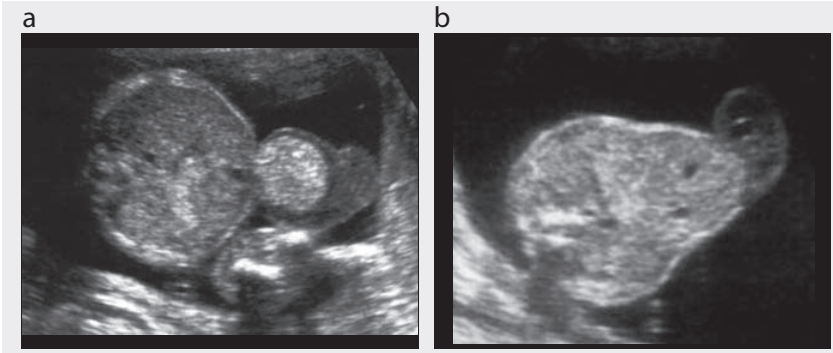

Fig. 2.108. Gastroschisis: herniated bowel loops are floating freely in the amniotic cavity

Fig. 2.109. Fetal ascites. (a) Axial and (b) longitudinal views

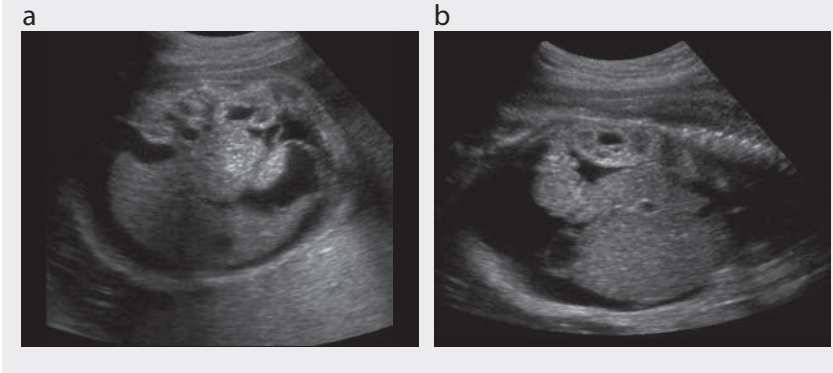

Urinary tract anomalies

Routine evaluation of the fetal urinary tract requires visualization of both kidneys and bladder (Fig. 2.110). The kidneys are usually examined in the axial view of the fetal abdomen, lateral to the spine, sometimes with mild dilatation of the pelvis, which is considered normal up to 5 mm in the second trimester and up to 8 mm in the third trimester.

Fig. 2.110. Normal right kidney in the (a) sagittal and (b) axial views. The renal pelvis (b) (calipers: 3 mm) is not dilated.(c) Normal bladder, axial view, with power Doppler depiction of hypogastric arteries

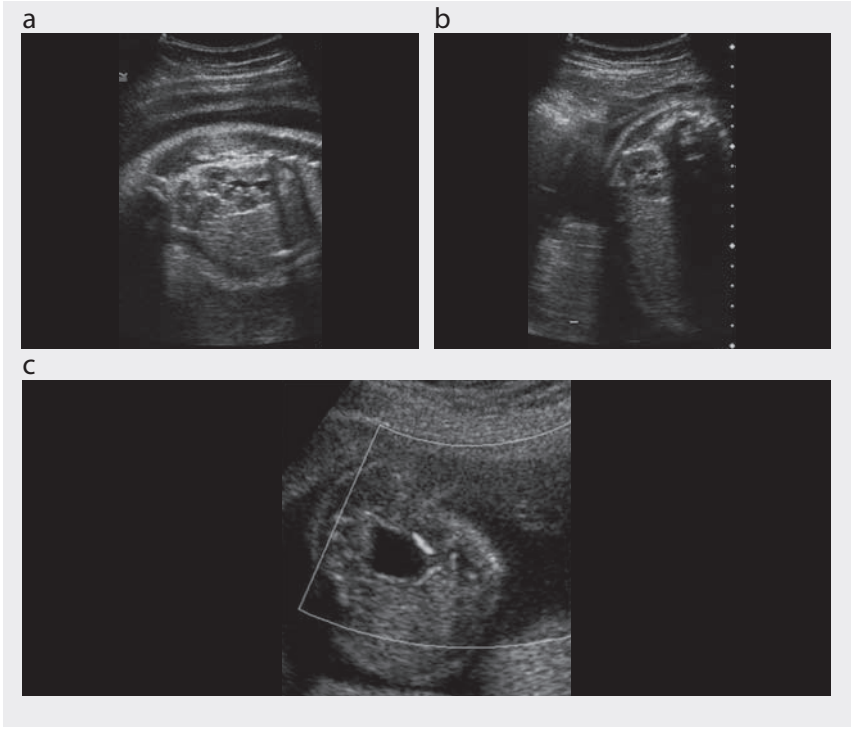

In **bilateral renal agenesis**, the kidneys and bladder cannot be visualized and severe oligohydramnios is present due to lack of fetal urine production (Fig. 2.111). The diagnosis is not easy as the oligohydramnios affects image quality; furthermore, the adrenal glands may mimic the presence of the kidneys. The inability to visualize the renal arteries with colour Doppler may be a helpful sign. This technique also helps to confirm a diagnosis of **unilateral renal agenesis** or **ectopic kidney** (Fig. 2.112).

In **polycystic kidney disease**, both kidneys are enlarged and uniformly hyperechoic; the bladder is absent, and severe oligohydramnios is present (Fig. 2.113). This condition may be part of the Meckel-Gruber syndrome in association with cephalocoele and polydactyly.

Fig. 2.111. Bilateral renal agenesis. The kidneys cannot be visualized; severe oligohydramnios is present

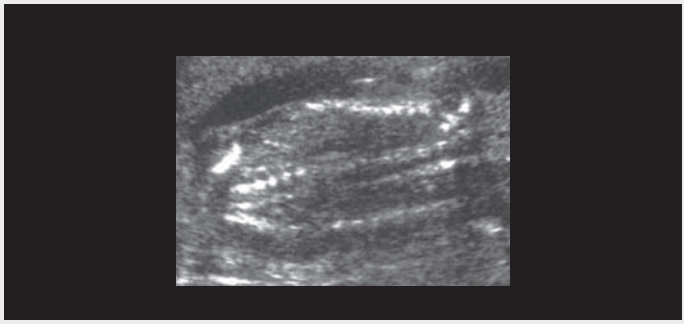

Fig. 2.112. Colour Doppler visualization of the aorta and renal arteries in a normal fetus (a), bilateral renal agenesis (b) and unilateral renal agenesis (c)

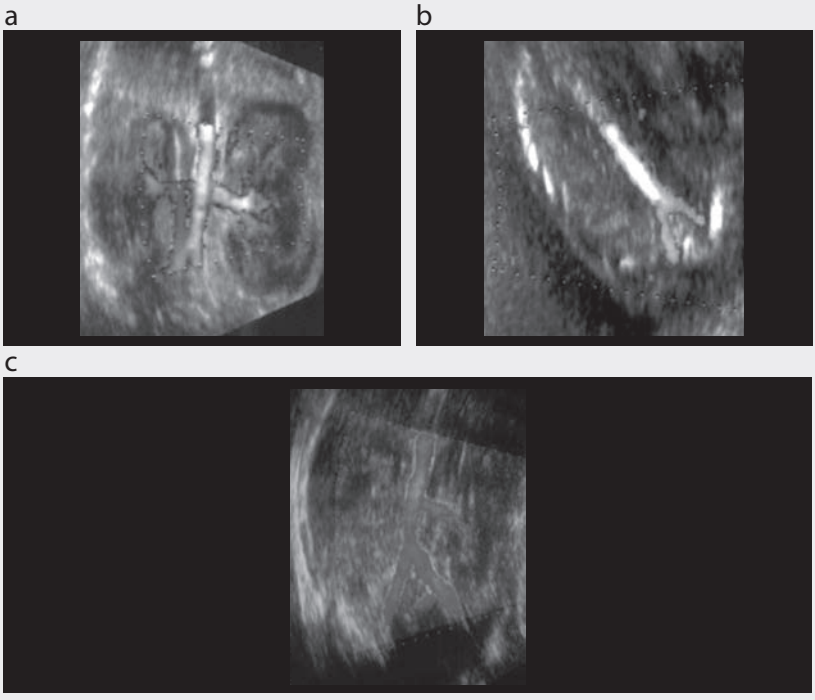

Fig. 2.113. Polycystic kidney disease. Both kidneys are symmetrically enlarged and uniformly echo-rich; severe oligohydramnios is present

Fig. 2.114. Unilateral multicystic kidney disease. The affected kidney (arrows: (a) transverse view; (b) sagittal view) is enlarged compared with the normal contralateral kidney due to the presence of multiple cysts of variable size

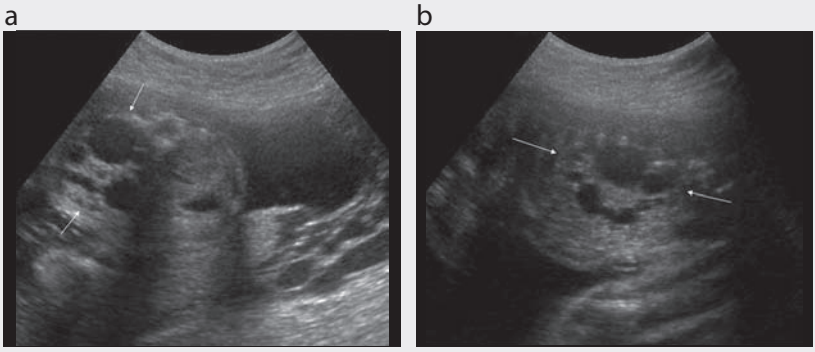

In **multicystic kidney disease**, which is usually unilateral, the affected kidney is enlarged due to the presence of multiple cysts of variable size (Fig. 2.114) as a consequence of early-onset dysplasia of the developing kidney.

Urinary tract obstruction causes different sonographic findings depending on the level of the obstruction. **High-level obstruction**, such as ureteropelvic stenosis, causes dilatation of the renal pelvis and calyces of variable degrees, leading to thinning of the kidney parenchyma (Fig. 2.115).

In **middle-level obstruction**, such as uretero-vesical stenosis, vesico-ureteral reflux and primitive megaureter, the dilated ureter appears as an irregular cystic tubular structure with associated pyelectasis of variable degrees (Fig. 2.116).

Lower urinary tract obstruction can include posterior urethral valves and urethral atresia. In these conditions, the prominent sonographic sign is severe bladder

Fig. 2.115. Moderate (a) and severe (b) unilateral hydronephrosis (calipers: renal pelvis). The renal parenchyma is normal

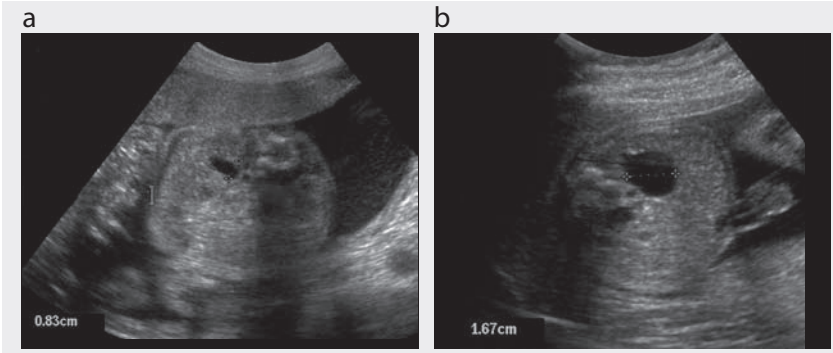

Fig. 2.116. Vesico-ureteral obstruction leading to dilatation of the ureter (U) and pelvis (P). B, bladder

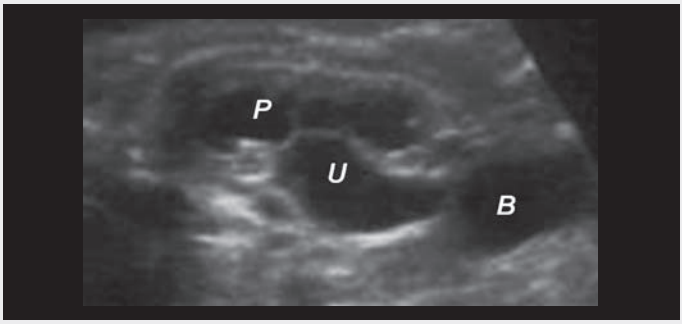

dilatation. In cases of posterior urethral valves, the proximal dilated urethra can also be visualized, forming the typical key-hole appearance of the bladder (Fig. 2.117). As a consequence of the obstruction, bilateral hydronephrosis and subsequent renal dysplasia occur; renal dysplasia should be suspected in the presence of uniformly hyperechoic kidneys (Fig. 2.118) or multiple small cortical cysts. In the most severe forms, the dilated bladder may occupy the entire fetal abdomen, with compression of the diaphragm and lungs.

Fig. 2.117. Severe bladder dilatation in posterior urethral valves. The dilated proximal urethra causes the typical key-hole appearance of the bladder

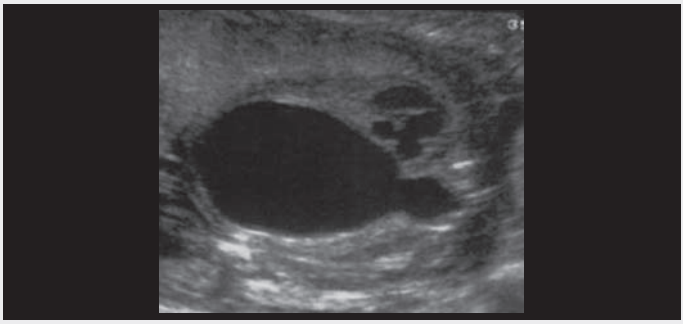

Fig. 2.118. Hyperechoic dysplastic kidney

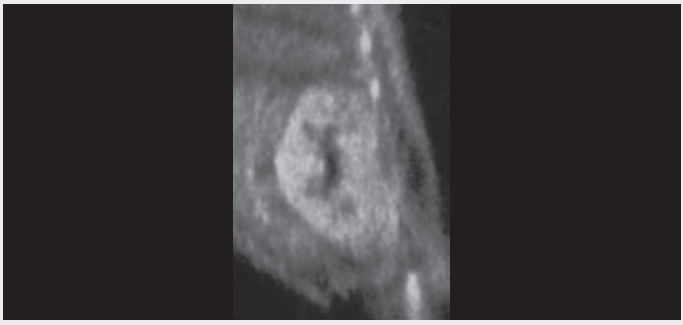

Fetal skeletal system

Sonographic evaluation of the fetal skeleton includes examination of the long bones and extremities, the spine and chest, the head, the degree of mineralization and abnormal contractures.

Long bones and extremities*:* In evaluating the long bones and extremities, the ratio between the rhizomelic (femur:humerus), mesomelic (tibia:fibula, radius:ulna) and acromelic (hand:foot) portions of the limbs must be considered (Fig. 2.119).

Hypoplasia of a single segment is defined as rhizomelia, mesomelia or micromelia, depending on the segment. If the limb is totally hypoplastic, the term 'micromelia' is used (Fig. 2.120).

Fig. 2.119. Normal upper and lower limbs: visualization of the shoulder, arm, forearm, and hand (a) and of the thigh, calf, and feet (b) at 21 weeks' gestational age; hands (c) and foot (d) at 25 weeks' gestational age

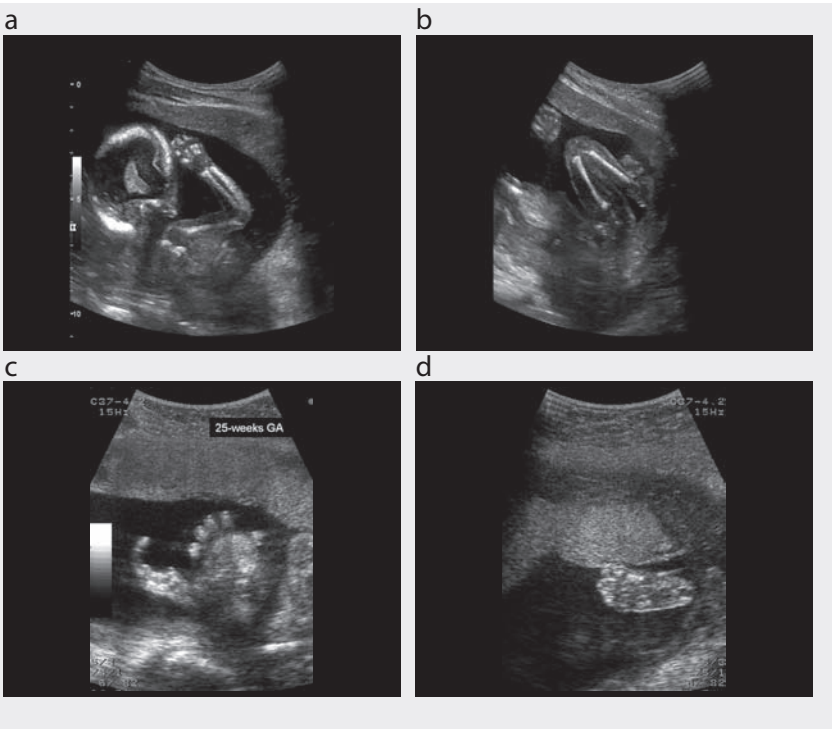

Fig. 2.120. Micromelia of the lower limbs, short and abnormal in shape

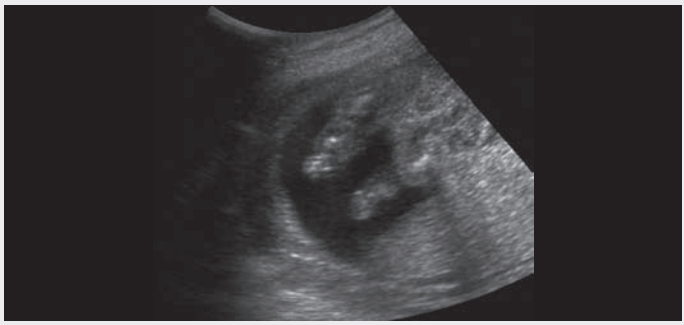

Abnormal shape and fractures of the long bones can also be seen (Fig. 2.121). Abnormal positions of the extremities include club foot (Fig. 2.122) and ulnar deviation of the hand.

Fig. 2.121. Abnormally curved, hypoplastic femur

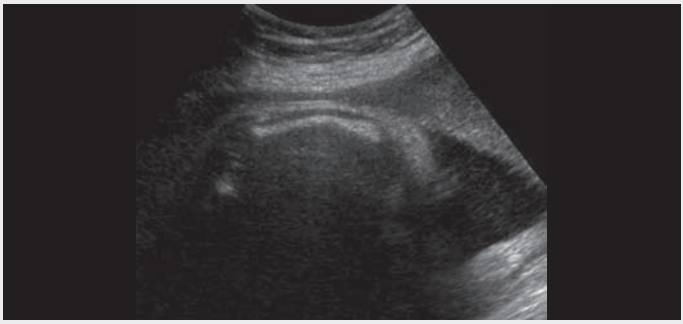

Fig. 2.122. Club foot

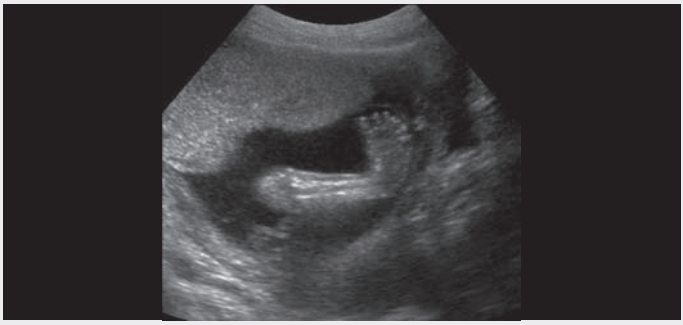

Spine and chest: An abnormally shaped spine can be due to scoliosis or hemivertebra. A hypoplastic chest is common to various skeletal dysplasias and can cause neonatal death as a consequence of the associated lung hypoplasia (Fig. 2.123).

Head: An abnormally shaped head is most commonly due to synostosis. The characteristic sign is the cloverleaf skull, which is typical of thanatophoric dysplasia (Fig. 2.124). Other abnormalities include frontal bossing (Fig. 2.125) and micrognathia.

Degree of mineralization: Thin and transparent skull bones are signs of hypomineralization, which is commonly observed in association with osteogenesis imperfecta (Fig. 2.126) and hypophosphatasia.

Fig. 2.123. Severe hypoplasia of the chest and achondrogenesis in a 22-week fetus

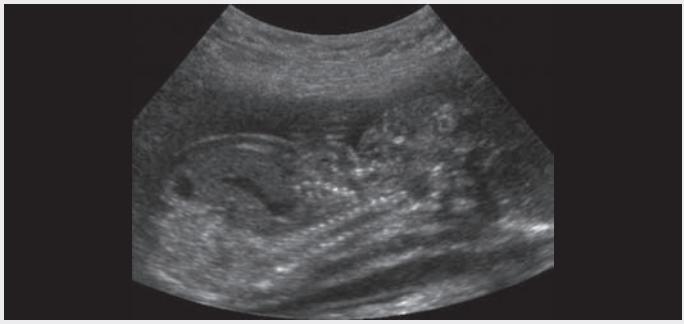

Fig. 2.124. Cloverleaf skull typical of thanatophoric dysplasia

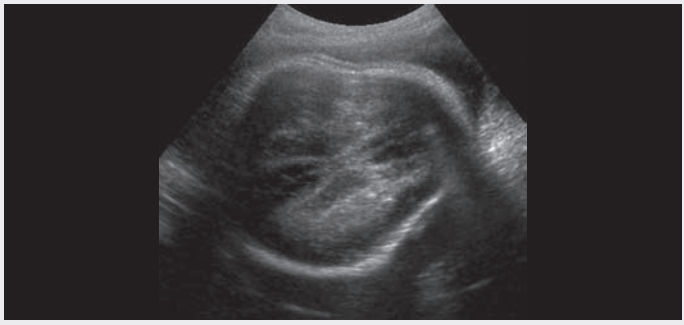

Fig. 2.125. Frontal bossing

Fig. 2.126. Thin and transparent skull bones (arrowheads): a sign of hypomineralization in osteogenesis imperfecta

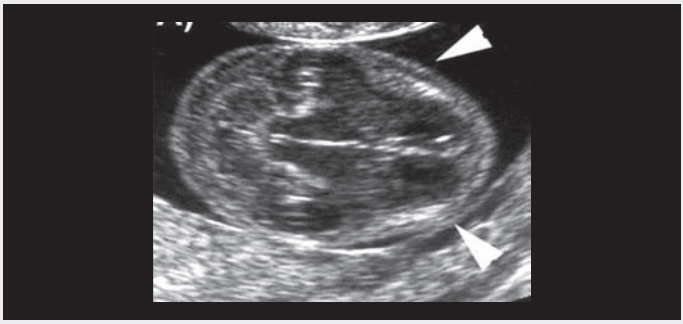

Abnormal contractions: Abnormal contractions of the limbs are typical of arthrogryposis, akinesia deformation syndrome, multiple pterygium syndrome and trisomy 18.

The abnormal sonographic findings described are typical of various skeletal dysplasias, and the antenatal diagnosis is not specific in most cases. By combining the different signs, however, it is possible to make a differential diagnosis or limit the number of possible diagnoses (Table 2.5).

Table 2.5. Differential diagnoses on the basis of main and associated signs

Main sign	Associated signs	Diagnosis
Micromelia	Hypoplastic chest, cloverleaf skull	Thanatophoric dysplasia
	Multiple fractures, hypomineralization	Osteogenesis imperfecta
	Severe diffuse hypomineralization	Hypophosphatasia
	Hypoplastic chest, cardiac defect, polydactyly	Short rib polydactyly syndrome
Rhizomelia	Frontal bossing, macrocrania	Achondroplasia
	Hypoplastic chest, renal anomalies	Jeune syndrome
	Exadactyly, cardiac defect	Chondroectodermal dysplasia
Hypoplastic chest	Micromelia, cloverleaf skull	Thanatophoric dysplasia
	Rhizomelia, renal anomalies	Jeune syndrome
	Micromelia, hypomineralization	Achondrogenesis
	Micromelia, cardiac defect, polydactyly	Short rib polydactyly syndrome

Use of Doppler in obstetrics

Assessment of fetal circulation is essential for better understanding of the pathophysiology of a wide spectrum of pathological pregnancies and their clinical management. This section is intended as a brief description on how to use Doppler application in obstetrical clinical practice. The first part describes the basic concepts of Doppler

sonography, which are essential for understanding its diagnostic uses. The second focuses on the primary clinical applications of Doppler techniques in obstetrics and in assessing fetal health status in pregnancies complicated by placental insufficiency.

Doppler ultrasound: principles and practice

Doppler principles

Competent use of Doppler ultrasound techniques requires an understanding of three components: the capacity and limitations of Doppler ultrasound, the parameters that contribute to a flow assessment and the features of blood flow in arteries and veins.

Ultrasound images of flow are obtained by measuring moving fluids. In ultrasound scanners, a series of pulses is transmitted to detect the movement of blood; echoes from moving scatterers determine slight differences in the time for return of the signal to the receiver. These differences can be measured as direct time differences or, more often, in terms of a phase shift from which the Doppler frequency is obtained (Fig. 2.127). They are then processed to produce a colour flow display or a Doppler sonogram.

Fig. 2.127. Doppler effect

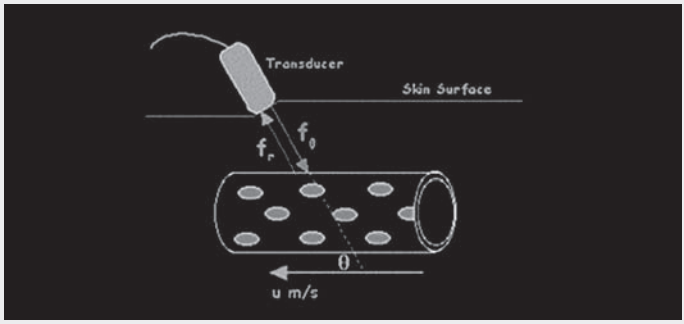

Fig. 2.127 shows the Doppler transducer scanning at an angle θ to a blood vessel, in which blood flows at a velocity of u m/s. The ultrasound waves are emitted by the transducer at a frequency f_o and are directed back to the transducer by moving reflectors in the blood (red blood cells) at a different frequency f_r. The difference between the transmitted and received frequencies, Δf, is related to the velocity of the flowing blood, u, and the speed of sound in tissue, v, according to the equation:

$$\Delta f = f_o - f_r = \frac{2 f_o u \cos \theta}{v}$$

There has to be motion in the direction of the beam to obtain Doppler signals; this does not happen if the flow is perpendicular to the beam.

The magnitude of the Doppler signal depends on:

- blood velocity;
- ultrasound frequency: the higher the ultrasound frequency, the higher the Doppler frequency. As in B-mode, lower ultrasound frequencies have better penetration; the choice of frequency is therefore a compromise between better sensitivity and better penetration;
- the angle of insonation: the Doppler frequency increases as the angle between the beam and the direction of flow becomes smaller.

The two main types of Doppler systems in common use today are **continuous wave** and **pulsed wave**. They differ in transducer design, operating features, signal processing procedures, and the types of information provided.

Doppler practice

Continuous-wave Doppler requires continuous generation of ultrasound waves with continuous ultrasound reception. A two-crystal transducer has this dual function, with one crystal for each function. The main advantage of continuous-wave Doppler is for measuring high blood velocities accurately; its main disadvantage is the lack of selectivity and depth discrimination. As continuous-wave Doppler is constantly transmitting and receiving from two different transducer heads (crystals), there is no provision for imaging or range gating to allow selective placing of a given Doppler sample volume in space.

Pulsed-wave Doppler systems have a transducer that alternates transmission and reception of ultrasound in a way similar to the M-mode transducer. The main advantage of pulsed Doppler is that Doppler shift data are produced selectively from a small segment along the ultrasound beam, referred to as the sample volume, the location of which is controlled by the operator. An ultrasound pulse is transmitted into tissues and travels for a given time (time X) until it is reflected back by a moving red cell. It then returns to the transducer over the same interval but at a shifted frequency. The total transit time to and from the area is 2X. This process is repeated alternately through many transmit–receive cycles each second. The range gating therefore depends on a timing mechanism that samples the returning Doppler shift data from only a given region. All other returning ultrasound information is essentially ignored. The main disadvantage of pulsed-wave Doppler is that high blood flow velocities cannot be measured accurately.

Aliasing effect: Pulsed-wave systems have a fundamental limitation. When pulses are transmitted at a given sampling frequency (pulse repetition frequency), the maximum Doppler frequency that can be measured is half of that frequency. Therefore, if the Doppler frequency is greater than half the pulse repetition frequency,

the Doppler signal is ambiguous. This condition is known as *aliasing*. The interval between sampling pulses must be sufficient for a pulse to go away and come back to the transducer. If a second pulse is sent before the first is received, the receiver cannot correctly discriminate between the two. The deeper the sample volume, the longer the pulse's journey, so that the pulse repetition frequency must be reduced for unambiguous ranging. The result is that the maximum measurable Doppler frequency decreases with depth.

Ultrasound Doppler modes: colour flow imaging and spectral Doppler

Colour flow imaging produces a picture of a blood vessel by converting the Doppler data into colours, which are overlaid onto the B-mode image of the blood vessel and represent the speed and direction of blood flow through the vessel. It is useful for identifying the vessels under examination, verifying the presence and direction of flow and finding the correct angle of insonation for velocity measurements.

Power Doppler is a newer ultrasound technique that is up to five times more sensitive in detecting low blood flow than standard colour Doppler. The magnitude of the flow output rather than the Doppler frequency signal is shown. Power Doppler can obtain some images that are difficult or impossible to obtain with standard colour Doppler.

Spectral Doppler (pulsed-wave Doppler) is used to provide a sonogram of a vessel in order to measure the distribution of flow velocities in the sample volume. The Doppler signal is processed in a Fourier spectrum analyser. The amplitudes of the resulting spectra are encoded as brightness, and these are plotted as a function of time (horizontal axis) and frequency shift (vertical axis) to give a two-dimensional spectral display. With this technique, a range of blood velocities in a sample volume will produce a corresponding range of frequency shifts on the spectral display.

To obtain proper images and measures, the operator should:

- identify the vessel (possibly by colour flow imaging);
- adjust the gain so that the sonogram is clear and free of noise;
- place the Doppler cursor on the vessel to be investigated (sample volume) and set the correct size;
- obtain a proper angle of insonation (60° or less);
- adjust the pulse repetition frequency to suit flow conditions and avoid aliasing.

Flow waveform analysis: Doppler waveform analysis is often used for diagnosis in the clinical assessment of disease. The complex shapes of Doppler waveforms can be described by relatively simple indices, which have been used to evaluate fetal health and organ blood flow. Common indices are the pulsatility index (PI), resistance index (RI) and the ratio of systolic to diastolic (S/D or A/B).

$$\mathrm{PI} = \frac{f_{\max} - f_{\min}}{f_{\mathrm{mean}}}$$

$$RI = \frac{f_{max} - f_{min}}{f_{max}}$$

$$S/D = \frac{f_{max}}{f_{min}}$$

where f_{max} is the maximum systolic frequency, f_{min} is the minimum diastolic frequency, and f_{mean} is the time-averaged frequency (Fig. 2.128).

An advantage of these waveform indices is that they consist of ratios of Doppler shift frequencies and are thus independent of transmission frequency and Doppler angle. Generally, low- and high-pulsatility waveforms occur in low- and high-resistance vascular beds, respectively. In addition to these indices, the flow waveform can be described or categorized by the presence or absence of a particular feature, for example the absence of end-diastolic flow and the presence of a post-systolic notch.

Fig. 2.128. Doppler waveform indices (for abbreviations, see text)

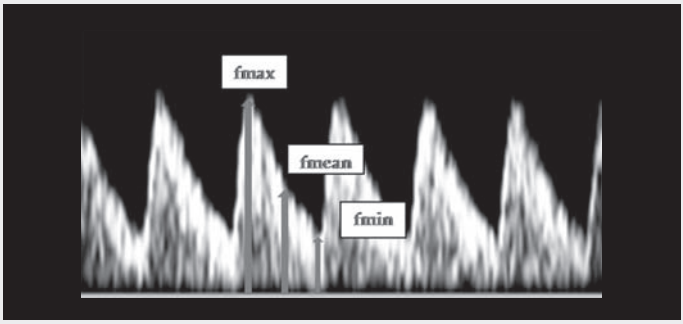

Doppler assessment of placental and fetal circulation

Placental insufficiency is the primary cause of intrauterine growth restriction in normal fetuses. The use of Doppler during antenatal fetal surveillance involves assessment of umbilical arterial and venous flow velocity waveforms, the fetal cerebral circulation and the fetal venous circulation, in particular the ductus venosus.

Assessment of placental function with umbilical artery Doppler velocimetry

The yolk sac develops 7–16 days after conception, and early development of the primary chorionic villi takes place. Thereafter, the chorioallantoic placenta develops in stages, consisting of invasion of the spiral arteries by an endovascular cytotrophoblast,

followed by a second wave of invasion that extends into the myometrium. Spiral arteries invaded by cytotrophoblastic cells are converted into uteroplacental arteries characterized by a dilated and tortuous lumen, with complete absence of muscular and elastic tissue and no continuous endothelial lining. The placental villi development leads to a progressive increase in the vessel diameter lumen and to the growth of a complex capillary network: the terminal villi will have small calibre (40–100 μm) but reach an extensive surface area (>10 m^2), thus reducing impedance to flow and optimizing feto-maternal exchange in the intervillous space.

The basic organization of the human placenta is present by approximately day 20 of pregnancy. Further refinement of the basic structure continues until term, at which time there are approximately 50–60 primary fetal stem villi branching into several terminal or tertiary villi. The branching of the stem villi is responsible for the low vascular resistance, the increased placental blood flow and the increased transplacental gas exchange that characterize human placentation. The low umbilical-placental vascular resistance also allows increased end-diastolic blood flow velocity in the umbilical artery during the third trimester of a normal pregnancy. Impaired placentation results in abnormally high umbilical-placental vascular resistance, reduced umbilical blood flow and chronic fetal hypoxaemia.

With increased downstream placental vascular resistance, the velocity of the end-diastolic flow in the umbilical cord artery is reduced, while the peak-systolic component is not significantly affected (Fig. 2.49).

To obtain umbilical artery Doppler waveforms with a pulsed-wave Doppler system, an ultrasound scan is first made, a free-floating portion of the cord is identified and the Doppler sample volume is placed over an artery and the vein. The angle of the fetal Doppler insonation should be kept at < 45° for optimal recording.

Several factors affect the umbilical artery Doppler waveform, independently of changes in placental vascular resistance:

- **Gestational age**: With advancing gestation, umbilical arterial Doppler waveforms show a progressive rise in end-diastolic velocity and decreased impedance indices. Gestational age-dependent nomograms are necessary for accurate interpretation of umbilical cord artery velocimetry.
- **Fetal heart rate**: When the heart rate drops, the diastolic phase of the cardiac cycle is prolonged and the end-diastolic frequency shift declines. The change is of no clinical significance when the heart rate is within the normal range.
- **Fetal breathing movements**: During fetal breathing, the shape of the flow velocity waveforms varies. Therefore, Doppler examinations should be conducted only during fetal apnoea and in the absence of excessive fetal movement.
- **Location of sample volume**: The impedance indices are significantly higher at the fetal end of the cord than at the placental end. It is recommended that umbilical artery Doppler waveforms be measured within 5 cm of the umbilical cord insertion.

Table 2.6. Umbilical artery pulsatility index at the fetal end of the umbilical cord based on 513 observations in 130 low-risk pregnancies

Gestational age (weeks)	Percentile				
	5th	25th	50th	75th	95th
24	0.94	1.11	1.24	1.38	1.59
25	0.91	1.08	1.21	1.34	1.55
26	0.87	1.04	1.17	1.31	1.51
27	0.84	1.01	1.14	1.27	1.48
28	0.81	0.98	1.11	1.24	1.45
29	0.78	0.95	1.08	1.21	1.42
30	0.75	0.92	1.05	1.18	1.39
31	0.73	0.89	1.02	1.16	1.36
32	0.70	0.87	0.99	1.13	1.34
33	0.67	0.84	0.97	1.11	1.32
34	0.65	0.82	0.95	1.08	1.30
35	0.62	0.79	0.92	1.06	1.28
36	0.60	0.77	0.90	1.04	1.26
37	0.58	0.75	0.88	1.02	1.24
38	0.56	0.73	0.86	1.00	1.23
39	0.54	0.71	0.84	0.98	1.21
40	0.52	0.69	0.82	0.97	1.20
41	0.50	0.67	0.80	0.95	1.18

Modified from Acharya et al. (2005)

In high-risk pregnancies complicated by maternal hypertension, intrauterine growth restriction or multiple pregnancy, umbilical artery Doppler studies should be part of antenatal assessment (Table 2.6). Placental insufficiency can be classified on the basis of the reduction in end-diastolic Doppler flow velocity into reduced, absent and reversed end-diastolic flow velocity. The risk for perinatal mortality increases up to 60% with increasing severity of reduced to reversed end-diastolic flow velocity. As there is no evidence that use of umbilical artery Doppler is of value in low-risk pregnancies, it should not be used for routine screening.

Prediction of fetal hypoxaemia from the fetal middle cerebral artery

With increased downstream placental vascular resistance, the velocity of the end-diastolic flow in the umbilical cord artery is reduced. In fetal hypoxaemia, there is an increased blood supply to the brain, myocardium and adrenal glands and reduced perfusion of the kidneys, gastrointestinal tract and lower extremities. This mechanism allows a preferential supply of nutrients and oxygen to vital organs. The phenomenon has been described as brain sparing. Chronic hypoxia with increased pCO_2 or reduced pO_2 will increase the fetal cerebral arterial Doppler end-diastolic flow velocity, probably related to cerebral vasodilatation (Fig. 2.50 and Table 2.7).

Compensation through cerebral vasodilatation is limited. In a series of intrauterine growth-restricted fetuses, longitudinally examined, a curvilinear relationship

Table 2.7. Longitudinal reference ranges for the middle cerebral artery pulsatility index based on 566 observations in 161 low-risk pregnancies

Gestational age (weeks)	Percentile				
	5th	25th	50th	75th	95th
24	1.38	1.64	1.86	2.10	2.52
25	1.44	1.71	1.94	2.19	2.62
26	1.50	1.78	2.01	2.26	2.71
27	1.55	1.83	2.06	2.33	2.78
28	1.58	1.88	2.11	2.38	2.84
29	1.61	1.91	2.15	2.42	2.88
30	1.62	1.92	2.16	2.44	2.90
31	1.62	1.92	2.16	2.43	2.90
32	1.61	1.90	2.14	2.41	2.87
33	1.58	1.87	2.10	2.37	2.82
34	1.53	1.81	2.04	2.30	2.74
35	1.47	1.74	1.96	2.21	2.64
36	1.39	1.65	1.86	2.11	2.52
37	1.30	1.55	1.75	1.98	2.38
38	1.20	1.44	1.63	1.85	2.22
39	1.10	1.32	1.49	1.70	2.05

Modified from Ebbing C et al. (2007)

was found between impedance in cerebral vessels and the status of fetal oxygenation; the progressive fall in impedance reached a nadir 2 weeks before the onset of late fetal heart rate decelerations. Middle cerebral artery Doppler velocimetry is thus unsuitable for longitudinal monitoring of growth-restricted fetuses. Venous velocity waveforms give more information regarding fetal status.

The middle cerebral artery parameters that are mainly taken into account are pulsatility index and cerebroplacental ratio (middle cerebral artery pulsatility index/umbilical artery pulsatility index). A low cerebroplacental ratio reflects redistribution of the cardiac output to the cerebral circulation and has been shown to improve accuracy in predicting adverse outcomes over that obtained with the middle cerebral artery or umbilical artery Doppler alone.

To conduct appropriate scanning of the middle cerebral artery, a transverse section of the fetal brain is obtained at the level of the biparietal diameter and the transducer is slightly moved towards the base of the skull. With colour flow imaging, the middle cerebral artery can be seen as a major lateral branch of the circle of Willis, dividing the anterior and the middle cerebral fossae (Fig. 2.50). The pulsed Doppler sample volume is obtained from the middle part of the vessel. During the examination, care should be taken to avoid high pressure on the maternal abdomen, as fetal head compression is associated with alterations of intracranial arterial waveforms.

The same factors that affect umbilical artery Doppler waveforms can also affect fetal cerebral artery Doppler waveforms.

Prediction of fetal hypoxaemia with fetal venous Doppler

The fetal liver with its venous vasculature (umbilical and portal veins, ductus venosus and hepatic veins) and the inferior vena cava are the main areas of interest in investigating venous blood return to the fetal heart. The ductus venosus originates from the umbilical vein before it turns to the right, and it enters the inferior vena cava in a venous vestibulum just below the diaphragm. The diameter of the ductus venosus is approximately one third that of the umbilical vein. With colour Doppler, the ductus venosus is identified in a midsagittal or oblique transection as a vessel connecting the umbilical vein with the inferior vena cava and exhibiting the typical aliasing of high velocities when compared with the umbilical vein (Fig. 2.51).

In severe hypoxaemia, the umbilical venous blood is redistributed to the ductus venosus at the expense of the hepatic blood flow. Consequently, the proportion of umbilical venous blood contributing to the fetal cardiac output is increased to ensure an increase in umbilical venous-derived oxygen delivery to the myocardium and increased oxygen delivery to the fetal brain. Increased placental resistance and peripheral vasoconstriction, seen in fetal arterial redistribution, cause an increase in the right ventricular afterload, and thus ventricular end-diastolic pressure increases. This may result in highly pulsatile venous blood flow waveforms and umbilical venous pulsations due to transmission of atrial pressure waves through the ductus venosus. In the inferior vena cava, reverse flow during atrial contraction increases with progressive fetal deterioration, suggesting a higher pressure gradient in the right atrium.

The next step in the disease is extension of the abnormal reversal of blood velocities in the inferior vena cava to the ductus venosus, inducing an increase in the ratio of peak systolic velocity to end-diastolic velocity, mainly due to a reduction in the latter component of the velocity waveforms (Fig. 2.51). The main ductus venosus Doppler parameter that is taken into account is the pulsatility index for veins, PI, which is calculated as:

$$\mathrm{PI} = \frac{v_s - v_d}{v_m}$$

where v_s is peak systolic velocity, v_d is end-diastolic velocity and v_m is time-averaged maximum velocity.

The high venous pressure induces a reduction in velocity at end-diastole in the umbilical vein, causing typical end-diastolic pulsations. Umbilical venous pulsations, particularly double pulsations, have been associated with perinatal mortality rates of up to 16% with absent umbilical artery end-diastolic flow velocity and 60% with reversed umbilical artery end-diastolic flow velocity.

The ductus venosus pulsatility index and short-term variations in fetal heart rate are important indicators for the optimal timing of delivery before 32 weeks of gestation (Table 2.8). Delivery should be considered if one of these parameters is persistently abnormal. The interval may be as short as a few hours in late gestation

Table 2.8. Longitudinal reference ranges for the pulsatility index of veins of the ductus venosus based on 547 observations in 160 low-risk pregnancies

Gestational age (weeks)	Percentile				
	5th	25th	50th	75th	95th
24	0.27	0.38	0.47	0.68	0.83
25	0.27	0.37	0.47	0.67	0.83
26	0.27	0.37	0.46	0.67	0.82
27	0.26	0.36	0.46	0.67	0.82
28	0.26	0.36	0.45	0.66	0.81
29	0.25	0.35	0.45	0.65	0.81
30	0.25	0.35	0.44	0.65	0.80
31	0.24	0.34	0.43	0.64	0.79
32	0.23	0.33	0.42	0.63	0.78
33	0.22	0.32	0.41	0.62	0.77
34	0.21	0.31	0.40	0.61	0.76
35	0.20	0.30	0.39	0.60	0.75
36	0.19	0.29	0.38	0.59	0.74
37	0.18	0.28	0.37	0.58	0.73
38	0.17	0.27	0.36	0.57	0.72
39	0.16	0.26	0.35	0.56	0.71

Modified from Kessler et al. (2006)

and in women with pre-eclampsia; in contrast, during the second trimester, severely abnormal venous waveforms can be present several days before intrauterine death.

Clinical recommendations

- Umbilical artery Doppler should not be used for screening in healthy pregnancies.
- Doppler assessment of the placental circulation is important in screening for impaired placentation and its complications of pre-eclampsia, intrauterine growth restriction and perinatal death.
- In these conditions, abnormal umbilical artery Doppler velocimetry is an indication for accurate evaluation of fetal health status. Doppler investigation of fetal middle cerebral artery and ductus venosus is recommended.
- Measurements must be taken and interpreted by expert operators with appropriate instruments and technique to avoid inappropriate clinical decisions.

Recommendations on reporting of obstetrical ultrasound examinations

A report should be written at the end of every sonographic examination.

First trimester

In the first trimester of pregnancy, the report must contain:

- the reason for the examination;
- the position and number of gestational sacs;
- the number of embryos and fetuses;
- the presence or absence of cardiac activity;
- chorionicity and amnionicity in cases of multiple pregnancy;
- the mean diameter of the gestational sac;
- craniocaudal length (crown–rump length) or biparietal diameter of the embryo or fetus.

The measurements of all parameters must be compared to reference curves in order to assess whether the sonographic age coincides with the anamnestic (i.e. menstrual) gestational age. The report should mention whether the pregnancy is to be re-dated.

The report should also include:

- possible uterine or adnexal anomalies;
- suggestions on the need and timing of further sonographic examinations (between 20 and 22 weeks and 30 and 34 weeks or, on particular indications, at other times);
- any limitations of the examination (maternal obesity, unfavourable position of the fetus);
- the device used: 3.5-MHz transabdominal probe or 7.5-MHz endovaginal probe;
- images;
- the date and signature of the operator.

Second trimester

In the second trimester of the pregnancy, the report must contain:

- number of fetuses and presence or absence of cardiac activity
- results of the anatomical evaluation
- results of the biometric evaluation
- chorionicity and amnionicity in cases of multiple pregnancy
- the position of the placenta.

The measurements of all parameters and morphological aspects must be compared to reference curves in order to assess whether the sonographic age coincides with the anamnestic gestational age. The report should mention whether the pregnancy is to be re-dated.

The report should also include:

- any limitations of the examination (maternal obesity, unfavourable position of the fetus, oligoamnios) that hindered or limited morphological study of the fetus;
- suspect or pathological features requiring further diagnostic investigations;
- suggestions on the need and timing of further sonographic examinations (between 30 and 34 weeks or, on particular indications, at other times);
- images;
- the date and signature of the operator.

Third trimester

In the third trimester of the pregnancy, the report must contain:

- the number of fetuses and the presence or absence of cardiac activity;
- the situation and presentation of the fetus;
- the position of the placenta;
- the quantity of amniotic fluid;
- the estimated fetal weight;
- all biometric parameters and morphological aspects, particularly the thickness of the atrium (atrial width) of the cerebral ventricles, fetal cardiac activity, both kidneys and the bladder; and the curve of fetal growth, reported on a reference curve;
- suggestions about the need and timing of further sonographic examinations;
- any limitations of the examination (maternal obesity, unfavourable position of the fetus, oligoamnios);
- images;
- the date and signature of the operator.